Politecnico di Torino

Master Degree in Aerospace Engineering

Master Degree Thesis

Design and Development of a High Fidelity Electromechanical Actuator Numerical Model Based on the Simscape Environment(PMSM-sinusoidal triphase electrical motor)

Supervisors:
Prof. Paolo Maggiore
Eng. Matteo D. L. Dalla Vedova
Eng. Gaetano Quattrocchi

Candidate:
Alexandru Sabin Jianu

July 2022

To my Mother, Ivonne, Attila, Asia and to all those that made this possible.....

Contents

1 Introduction

1.1 Overview

The main purpose of this thesis is the development of a High Fidelity numerical model of an PMSM electromechanical actuator using the Simscape environment. It will be focused on the mechanical side of the actuator, with emphasis on the various non linearities that characterize this system.
In the last years the aerospace industry has taken big steps toward creating greener, safer and cheaper air transport. To do this the existing concept of 'More Electric Aircraft' is being pushed toward an 'All Electric Aicraft'. In order to achive this the use of electrical power networks for electrically supplied power is being used as a replacement of conventional hydraulical, pneumatic and mechanical power networls.
At the moment EHAs are being used as backup actuators on aircrafts like the A380 and the A350. Although they remove central hydraulic power distribution, EHAs still use hydraulics locally to maintain the major advantages of conventional actuators.
EMAs, however, remove both the central and local hydraulic circuits by transmitting motor power to the load through mechanical reducers. Unfortunately, EMAs are not yet sufficiently mature to replace conventional hydraulic servo actuators in safety critical functions as flight controls.
Some technical challenges have to be overcome: voltage spikes and current transients affecting the pollution and stability of electrical networks and reduced inertia which affects the dynamic performance.
A model based and simulation approach can provide engineers with efficient means to address the critical issues in order to develop an Electromechanical actuator that can have an extremely low failure rate.
The purpose of this work is to develop the mechanical side of High Fidelity EMA actuator and compare it to the one built in the Simulink environment. The various non linearities which are involved in the function of the system are going to be modeled and the results will be compared to the ones obtained from the Simulink model.

1.2 Flight controls

Flight control surfaces serve the purpose of confering an aircraft stability, controllability and maneuvrability. Flight stability is defined as the inherent tendency of an aircraft to oppose any input and return to the original trim condition if disturbed.
When the summation of all forces along each of the three axes, and the summation of all the moments about each of the three axes are zero, an aircraft is said to be in trim. Control is the process of changing the aircraft flight condition from an initial trim point to a final or new trim point. This is performed by the pilot or the autopilot, through moving the control surfaces.

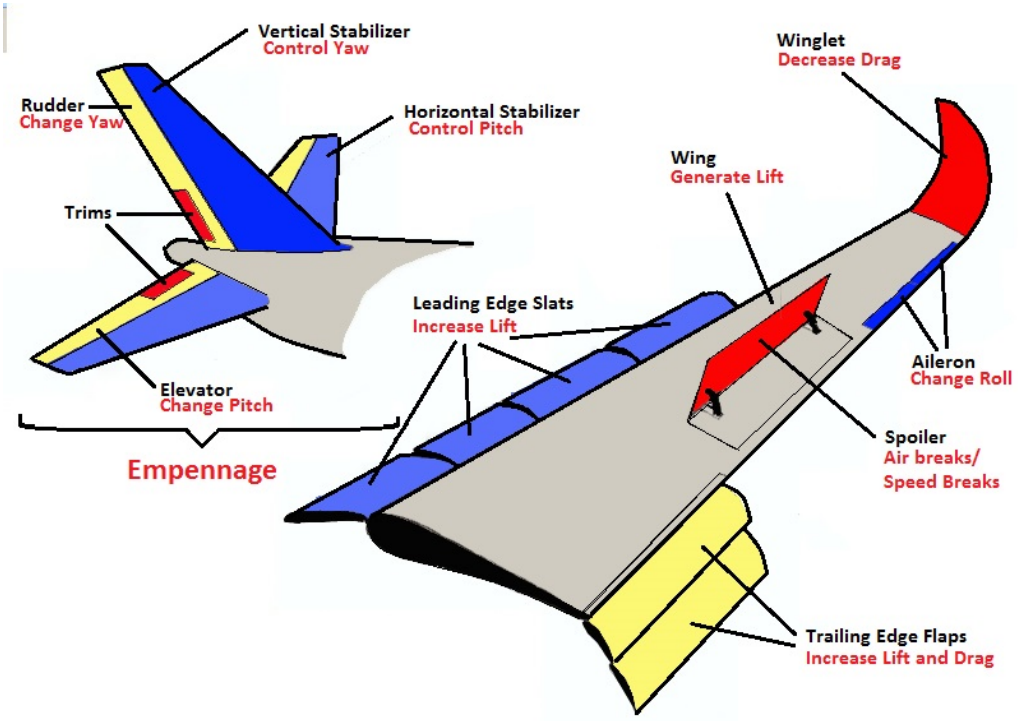

Figure 1: Flight control surfaces

Control surfaces can be classified into two main groups: primary and secondary control surfaces.

1.2.1 Primary flight controls

The primary control surfaces, which are ailerons, elevator and rudder, are respectively used for lateral control, longitudinal control and directional control. However, they also contribute largely to lateral trim, longitudinal trim and directional trim of the aircraft. In the majority of aircraft configurations, lateral and directional motions are coupled; hence the aileron also affects the directional motion and the rudder affects the lateral motion.

The continous operation of these surfaces during flight implies that the loss of primary flight controls often results in the loss of the aircraft. This means that a very high level of reliability is required, which is achieved through the use of various redundancies. Other primary control surface requirements are sensitiviy, stability and instinctivity. The quick variation in a short time results in an additional requirement which is that of a high cut-off frequency. When control surfaces are deflected, the cambers of their related lifting surfaces are changed. This varies the aerodynamic forces and consequently a resultant moment will influence the aircraft motion. An aircraft is capable of performing various maneuvers and motions. These may be classified in three main groups: longitudinal, lateral and directional motion. The definition of the motions is as follows:

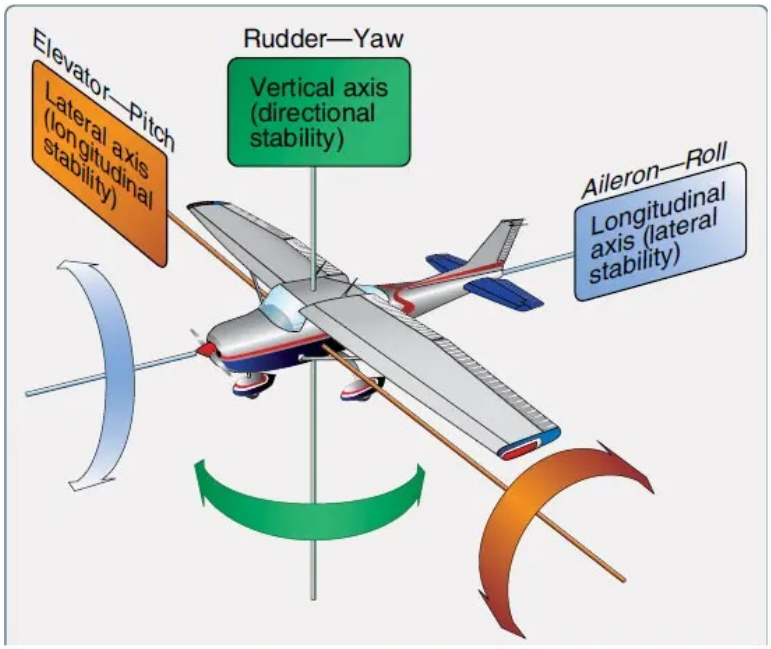

Figure 2: Primary flight controls

- **Longitudinal motion:** Any aicraft motion in the xz plane is called longitudinal motion. Lift, drag and pitching moment have the major influence on this motion. This is achieved through the elevator.
- **Lateral motion:** The aircraft rotation about the x-axis is called lateral motion. Lift force and rolling moment have the major influence on this motion. This is achieved through the ailerons.
- **Directional motion:** The aircraft rotation about the z-axis and any motion along the y-axis is called directional motion. Side-force and yawing moment have the major influence on this motion. This motion is achieved through the rudder.

Primary flight controls can be reversible or powered. The first used was the reversible type which consist of a direct mechanical linkage: it uses a collection of mechanical parts such as rods, tension cables, pulleys, counterweights, and sometimes chains to transmit the forces applied from the cockpit controls directly to the control surfaces

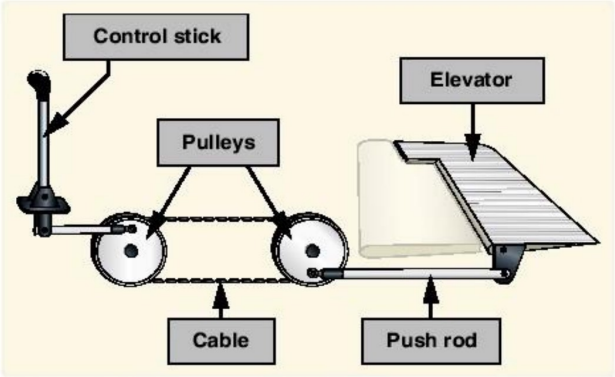

Figure 3: Mechanical flight control system

Increases in the control surface area required by large aircraft or higher loads caused by high airspeeds in small aicraft lead to a large increase in the forces needed to move them.

Consequently complicated mechanical gearing arrangements were developed to extract maximum mechanical advantage in order to reduce the forces required from the pilots.

In large aircrafts the control surfaces are operated by power operated hydraulic actuator controlled by valves moved by control yoke and rudder pedals. An artificial feel system gives the pilot the feedback that is proportional to the flight loads on the surfaces. In the event of hydraulic failure, the control surfaces are controlled by the servo tabs in a process known as manual reversion.

1.2.2 Secondary flight controls

Secondary flight control surfaces are in fact auxiliary control surfaces and are applied in special cases. These surfaces mainly include: high-lift devices (flaps), tabs and spoilers.

Usually a flap is used to increase the wing lift coefficient when the speed is low, typically during take off and landing. High lift devices may be employed at the leading edge and trailing edge of the wing. The trailing edge high lift device is called flap, while two groups of leading edge high lift devices are slots and slats.

Spoilers are flat sheets on top of the wing. The spoiler essentially has two functions: brake during landing and as an auxiliary device during roll. They are used to decrease lift when deflected up. They are sometimes used as aileron substitutes, for roll control, especially when torsional aeroelasticity is critical.

The third type of secondary control surface, the tab, has different types such as trim tab, balance tab, geared tab and flying tab. Its main role is to reduce the force necessary for control by the pilot when a mechanical actuation system is used.

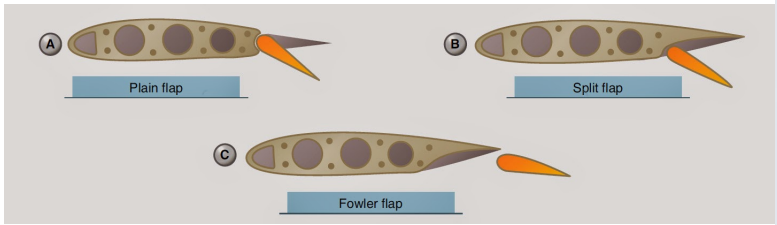

(a) Flaps

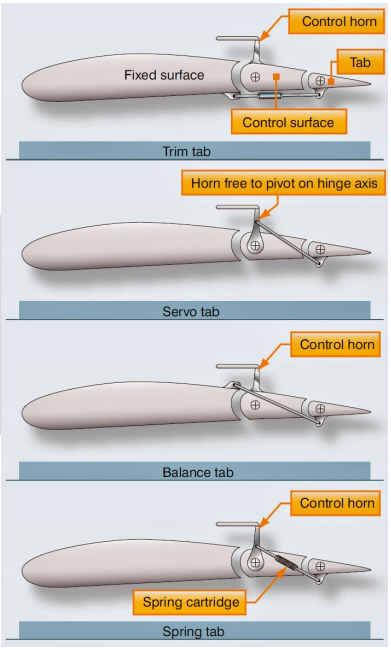

(b) Tabs

Figure 4: Secondary flight surfaces.

1.3 Actuation systems

The complexity and weight of the mechanical system increases with size and performance of the aircraft. When the pilot's action is not directly sufficient for the control, the main option is powered system that assists the pilot. Tipically, hydro-mechanical or electro-mechanical actuation systems are used to comand the flight control surfaces.

Primary flight control surfaces usually use hydraulic actuation systems comprising of linear motors with piston-cylinder or, more rarely, rotatory motors. Secondary control surfaces are generally made of hydraulic or electric rotatory motors. In the last decades, as a result of the development of more reliable electric motors, which have a high power to weight ratio, electromechanical secondary controls have begun to be used for military and sometimes commercial aircrafts. Also, this type of actuation system is now starting to be applied to the primary flight control surfaces of small unmanned air vehicles.

In order to provide a precise control of the aircraft, closed loop system are used: that is the input to the actuator and the output are compared, then the error signal is sent to the actuator. The main types of servomechanism systems are now going to be described.

1.3.1 Hydromechanical

Hydraulically powered actuators were introduced in the 1950s and were the preferred solution for high force/low speed high power density actuation.
In a hydromechanical actuation system the input to the servovalve spool is transmitted through mechanical signalling. Therfore, the spool moves generating a pressure gradient and a flow rate in the chambers of a hydraulic jack. This allows the jack to move the control surface. The three centers lever provides both the input, to the spool, and the feedback. In doing so, when the actuator reaches the desired position the servo-valve will automatically close itself. In this way the three centers lever behaves like a proportional controller because it associates the opening of the valve, through the movement of the spool, with the input of the pilot and the position of the controlled surface.

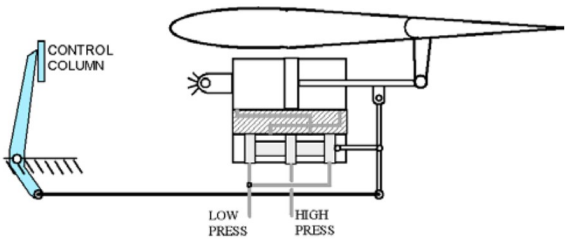

Figure 5: Hydromechanical

There are a numbers of disadvantages in a hydromehcanical system:

- they are heavy and require careful routing of flight control cables through the aircraft using pulleys, cranks, tension cables and hydraulic pipes;
- they require redundant backup to deal with failures, which increases weight;
- they have a limited ability to compensate for changing aerodynamic conditions;
- dangerous characteristics such as stalling, spinning and pilot-induced oscillation, which depend mainly on the stability and structure of the aircraft rather than the control system itself, can still occur with these systems;

1.3.2 Electrohydraulic

By using electrical control circuits combined with computers, designers can save weight, improve reliability, and use the computers to mitigate the undesirable characteristics mentioned above. Modern advanced fly-by-wire systems are also used to control unstable fighter aircrafts.

This type of servomechanism is the most used actuation system on modern airliner and fighter aircraft. The pilot's input is transmitted as an electrical signal that commands the servovalve. As for the hydromechanical system, the servovalve regulates the hydraulic oil that moves the jack, through the spool. In this case the position of the jack is measured by a Linear Variable Differential Transducer that transmits the signal to the electronics control.
There are mainly three types of Electrohydraulic servo valves:

1. **Flapper-nozzle :** it is also called two stages because the first stage is made of an electric torque motor which moves the flapper. This clogs one of the two nozzles of the second stage causing a difference of pressure. The second stage is made of the hydraulic circuit and the spool. The pressure difference moves the spool allowing the movement of the jack. The first and second stage are connected through a feedback spring.

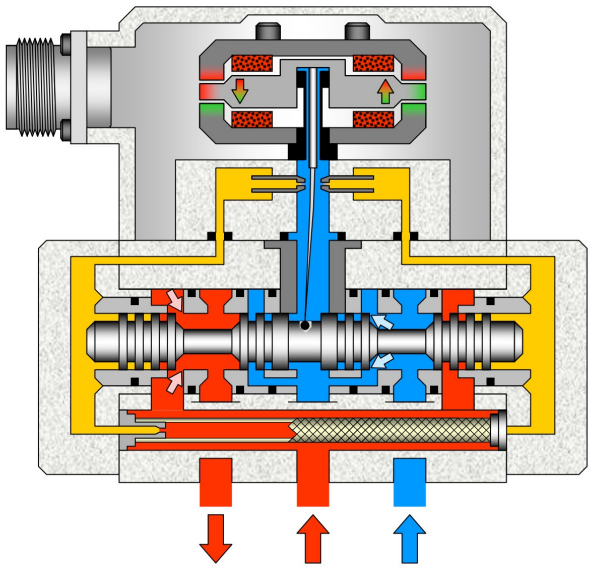

Figure 6: Flapper-nozzle

2. **Jet pipe :** in this case the torque motor deflects a pipe from which oil flows in one of the two circuits, generating a pressure difference that moves the spool. This type of servovalve is more rigid so it's less proned to vibrational disturbances than the flapper nozzle. Also, the jet pipe nozzle is bigger than the flapper nozzles so debris and dirty particles cause less harm.

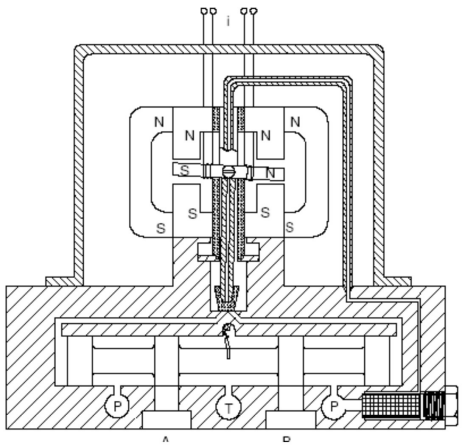

Figure 7: Jet pipe

3. **Direct Drive valve :** this is a modern type of servovalve which allows to eliminate the system based on torque motor or jet pipe. In this case the spool is directly moved by a linear electric motor. This allows bigger forces and bigger pressure compared to the other servovalves. The drawback are that this servovalves are bigger, they are very sensitive to electromagnetic disturbances and are prone to problems at high frequencies.

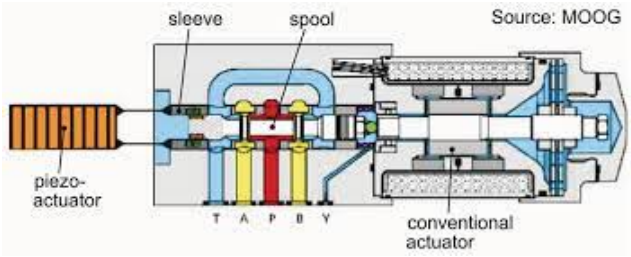

Figure 8: DDV

1.3.3 Electrohydrostatic (EHA)

The electrohydraulic actuator relies on an external hydraulic circuit. A failure of this circuit makes it impossible for the electrohydraulic actuator to work. Hence to avoid this consequence the centralized hydraulic system is replaced by a localized compact actuator system.

Electro hydrostatic actuator is a self contained, modular and compact actuactor system. It mainly consists of controller, servo motor, pump, control elements and actuator. The servo motor drives bi-directional pump which in turn supplies oil to the actuator. The speed and direction of the actuator is controlled by the speed and direction of the servo motor. This way the need of servo valve is eliminated. The controller gives output signal based on error between desired displacement and measured displacement

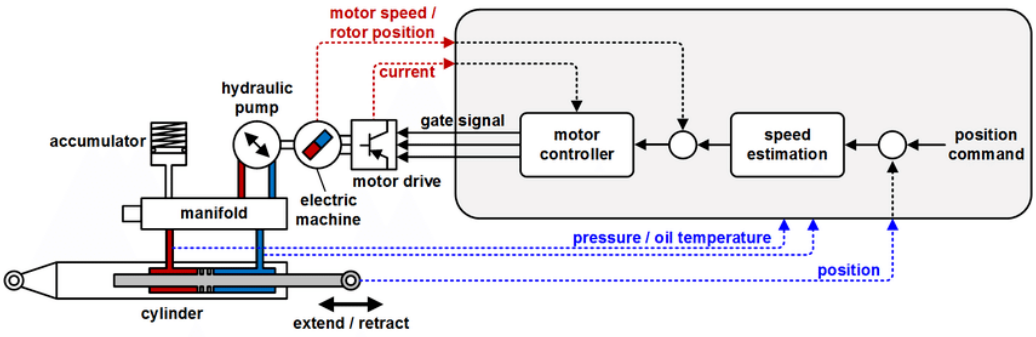

Figure 9: EHA

1.3.4 Electromechanical (EMA)

By reducing or eliminating the hydraulic an pneumatic secondary power systems, the aicrafts benefits from improved maintainability, reduced life costs, improved flight readiness and efficient energy use. This led to the development of the electromechanical actuator system.

With advances in rare earth magnetic materials, solid-state power switching devices and high voltage dc power control, it was possible for electromechanical actuator system to be used for flight control surfaces. However, concerns over the safety of flight mission reliability and combat survivability will have a major impact on the flight control hardware and architecture chosen for present and future aircrafts. Electromechanical actuators have advantages over hydraulic actuators, not because they are better in a conventional comparison sense, but because of the changes they allow in the total secondary power system of the aircraft, which means less weight, no hydraulic leakage, less complexity, cheaper installation and maintenance costs. However, the fact that their reliability is lower than that of hydraulic actuators and many fault modes are not yet entirely known kept the electromechanical actuators from being used for primary control surfaces in commercial and military aircrafts. At the moment they are used for non safety critical functions like secondary flight controls, landing gear retraction and cargo bay doors and for primary controls on small UAVs.

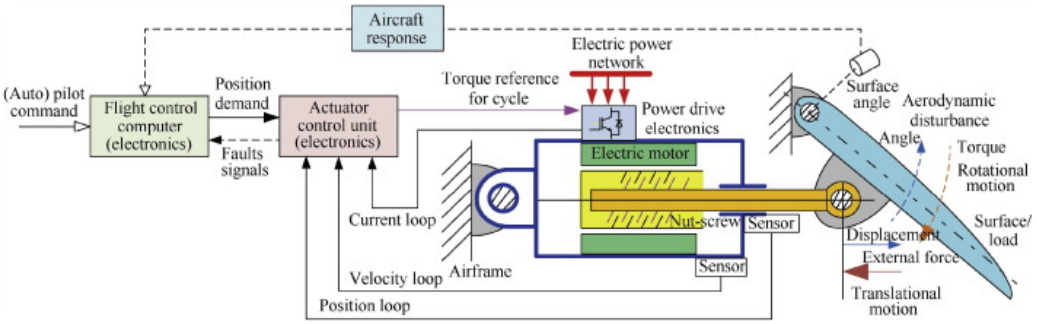

Figure 10: EMA actuation system

The EMA actuation system consists of the following components:

- actuactor control electronics (ACE), which receives the fly by wire comand in the form of electric signal. This signal is then compared with the feedback signal in order to generate the comand to the PDE;
- power drive electronics (PDE), which controls the amount of power flowing between the electrical supply and the motor in order to reach the reference position. It is usually made of a three phase inverter H-bridge;
- an electric motor (DC or three phase BLDC/PMSM) that transforms power between the electrical and the mechanical rotational domains;
- a nut-screw mechanical transmission that transforms power between the high speed low torque rotational and low velocity high force translational domains;
- sensors of current, speed, position and force if necessary. A RVDT is the primary mean of angular position acquisition that is usually used with LVDTs to ensure redundancies.

The transmission ratio, which is the ratio between motor and user angular speed or the ratio between user and motor torque, is defined as:

$$\tau = \frac{\dot{\theta_{\mathrm{m}}}}{\dot{\theta_{\mathrm{u}}}} = \frac{1}{\eta}\frac{T_{\mathrm{u}}}{T_{\mathrm{m}}}$$

where η is the transmission efficiency.
The electric motor produces low torques at a very high angular speeds so in order for the user to receive very high torque and low angular speed, the transmission ratio must be high. Appropriate reducers that can achieve such high ratio with a good efficiency and small dimensions include planetary gears or more exotic devices like harmonic drivers.

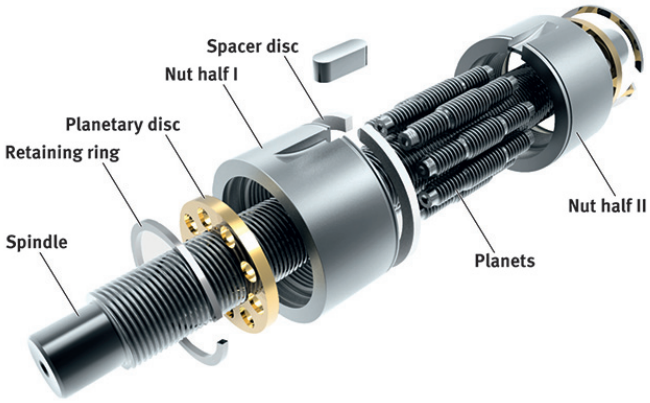

Figure 11: Roller screw actuator

Rotary to linear motion is done by a ball screw or a roller screw. They allow a higher efficieny compared to lead screws since the elements are mainly rolling and this type of resistance is much lower than friction resistance. This also implies other advantages like higher maximum loads and better wear resistance.

The main disadvantage of using an electric motor for driving the transimission is their difficuly to hold a commanded position when an external load is applied. In order to keep that position the same phase is powered leading to the overheating of the windings through joule effect.

This problems can be overcome by using in irreversible transmission, which, however has many disadvantages like transmission lock in case of motor failure. A hybrid stepper motor could be a solution to this problem .

2 Brushless motors

To overcome the problems of DC motors, a motor called brushless direct current (BLDC) motor was developed. This motor has similar electrical characteristics to a DC motor, but it has an enhanced reliability by replacing mechanical commutation with electronic commutation. Hence, the function of brushes and commutators is replaced with semiconductor switches operating based on the information from the rotor position using Hall sensors or by measuring the CEMF on non active coils. As a result of this replacement the configuration of a BLDC motor is similar to the configuration of a permanent magnet synchronous motor (PMSM).

The BLDC motor has a configuration in which the windings are placed on the stator side and the magnets on the rotor side. Such configuration has the following advantages over DC motors. Compared to the heavy rotor of DC motors consisting of many conductors, BLDC motors have a low inertia rotor. Thus this motor can provide a rapid speed response. Moreover, windings placed on the stator side can easily dissipate heat, allowing BLDC motors to have a better attainable peak torque capability compared to DC motors whoes maximum current is limited to avoid the demagnetization of magnets. In addition, BLDC motors can operate at a higher speed because of nonmechanical commutation devices. This long list of positive characteristics makes the BLDC a perfect candidate where reliability, weight saving and high performance are required, like in aerospace.

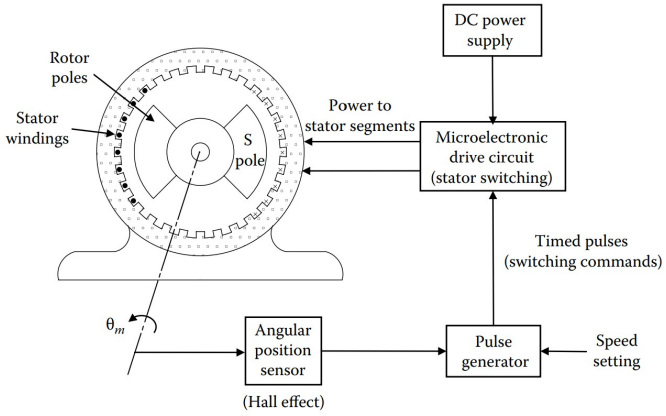

Figure 12: Brushless DC motor

BLDC motors can be categorized according to their number of stato windings: single-phase, two-phase, three-phase, and multi-phase.

2.1 Stator

It's function is to hold the copper windings which make up the excitation coils. The stator is usually made of soft iron in order to have small losses of energy since polarity is continuosly varying. This soft iron comes in the form of laminated steel which are stacked up to carry the windings. Generally there are two types of phase windings architecture, Y connection (also called star) and delta connection, but since a phase must be left unpowered the Δ pattern cannot be used. In a star connection phase voltage is $1/\sqrt{3}$ of line voltage. This means that ,compared to the delta connection, lower current flows through the coils therfore a lower torque is delivered.

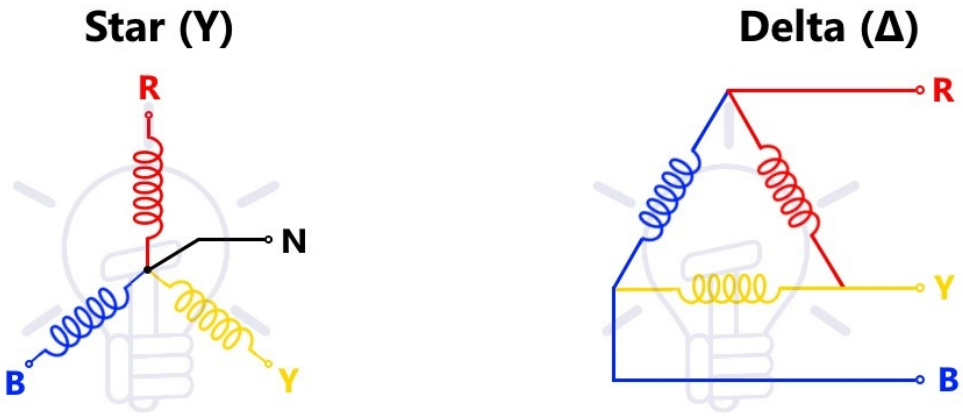

Figure 13: Y and Delta connection

The steel laminations can be slotless or slotted. In the slotted design the coils are wound within slots around the stator. With a sloteless design the coil is wound in a separate external operation and is then inserted directly into the air gap during motor assembly. In this way slotless BLDC motors can be made smaller in size while in in slotted motors the presence of stator teeth prevents the overall size motor from being minimized.

Slotted can offer higher torque than the slotless design as it can handle higher temperatures, allowing more torque generation. The advantages of the slotless configuration are that of a lower inductance hence a higher maximum speed, and also a more regular torque output.

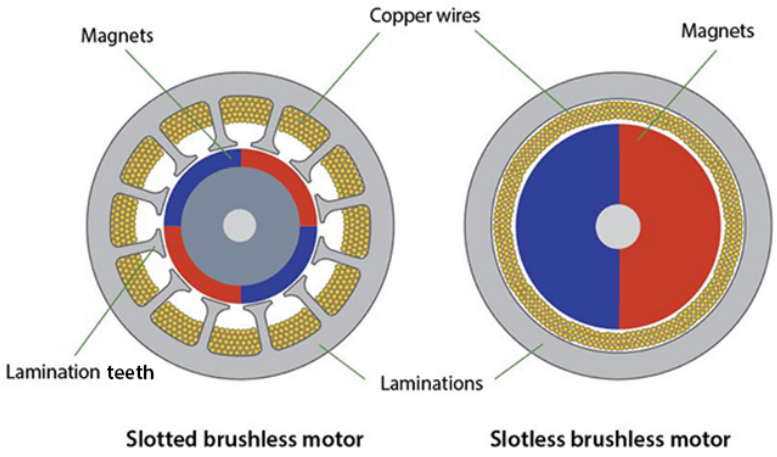

Figure 14: Stator

2.2 Rotor

The rotor is the component which produces the torque that can be than used to control the actuator. It is usually made of a permanent magnet. Initially the permanet magnet was made of cheap Ferrite materials. Since better performance and a reduced risk of demagnetization were desired hard iron is now being used. The most common material that is used is a Neodymium-Iron-Boron alloy since it can generate a magnetic flux which is greater than 1 Tesla. Such high value makes it possible to increase stator-rotor magnetic coupling constant and consequently the maximum torque output.

Another characteristic of the rotor is the number of poles. A greater number of poles allows a smoother torque output at the expense of the maximum speed which is going to be lower due to increased commutation frecquency of power transistors in the controller

2.3 Principles of operation

The basic driving principle of the BLDC motor is to change the phase windings, which should be excited according to the position of permanent magnet on the rotor for producing continuous torque. To implement this function, information on the rotor magnet position is indispensable. The position sensing is commonly achieved with Hall effect sensors.

A two pole three-phase Y-connected BLDC motor drive system is shown in FIG 15 . Three Hall effect sensors are displaced from each other by 120 electrical degrees on the stator to detect the magnetic field flux produced from the rotor magnets. Three output signals of Hall effect sensors enable us to recognize the rotor position divided into six different sections.

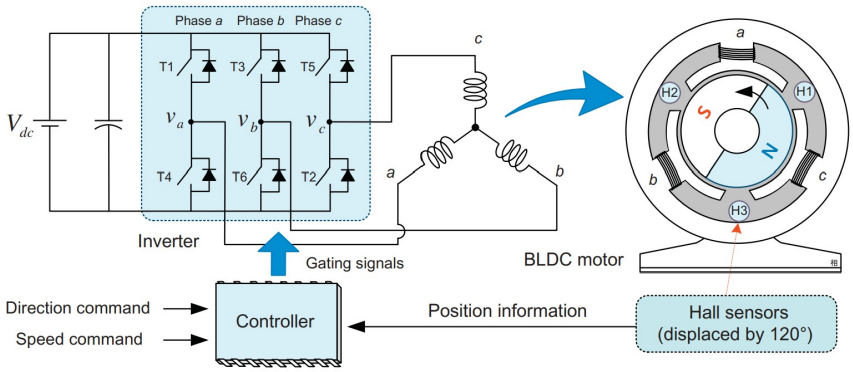

Figure 15: Principle of operation

The switching sequence for the six-step drive is shown in FIG 16 . In the BLDC motor drive, only two of the three phase windings are excited, while the other winding is left unexcited. Rotor position feedback singals can be used to determine which two of the three-phase windings should be excited to produce the continuos torque at each istant. As a driving circuit, a three phase inverter is used to flow the current into the required two-phase windings. In the inverter for a BLDC motor drive as shown in FIG 15, switching devices of only two phases work at any given instant. Accordingly, each switching device has a 120 deg conduction interval. In the six step drive, a changeover of an active switch is done to the switching of the other phase, and thus a dead time is not required for short circuit protection in the inverter.

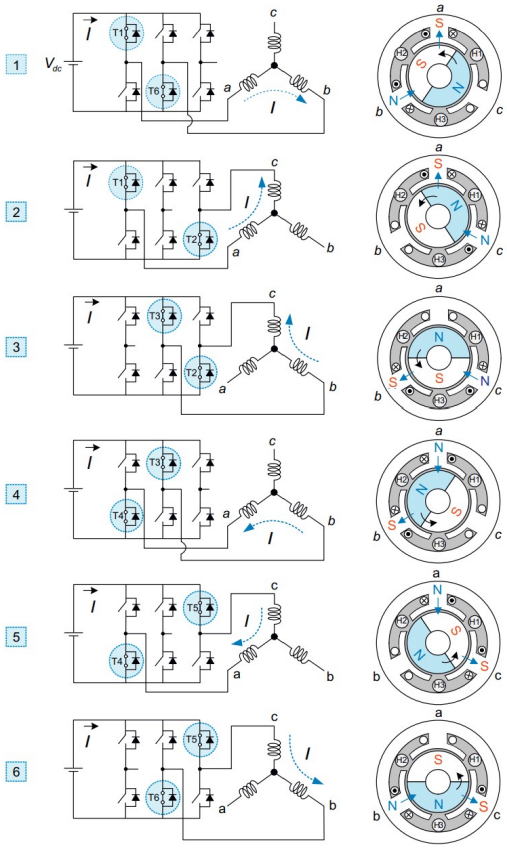

Figure 16: Principle of operation

FIG 17 illustrates Hall effect sensor signals (H1, H2, H3) with respect to the counter EMFs of stator windings in the six-step drive, and the relationship between the sensor signals and the phase currents. Here, assume that each sensor outputs a digital high level for the north pole, whereas it outputs a low level for the south pole. From the sensor signals, the excited phase windings should be changed every 60 electrical degrees of rotation for producing a continuous torque.

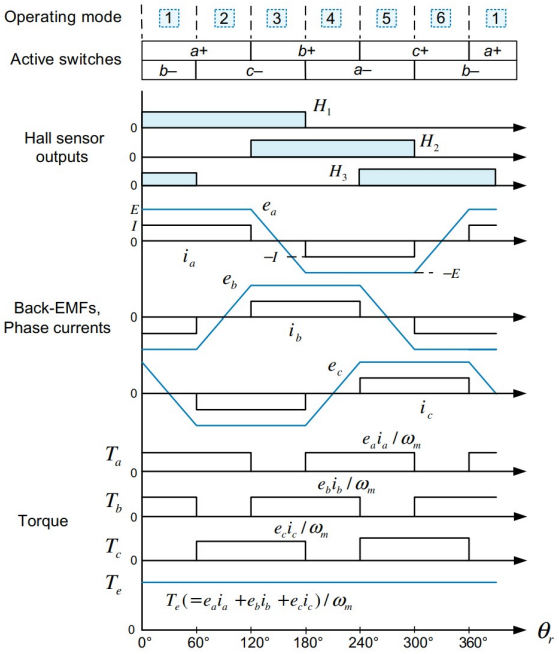

Figure 17: Principle of operation

2.4 Torque and speed characteristics

The generation of torque in BLDC motors is possible due to the interaction between rotor permanent magnets and stator windings. The current flowing through stator coils makes the stator to behave like a magnetic dipole, which dipole moment is:

$$\vec{m} = NAi\vec{n}$$

where n is the normal versor to the coil plane, i is the current intensity, A is the area of the coil and N is the number of windings in the coil.
This magnetic dipole is situated in the magnetic field generated by the rotor of intensity **B** . Therfore, the torque produced is then:

$$\vec{T} = \vec{m} \times \vec{B}$$

Consequently we can see that the output torque of the motor is directly proportional to the current, permanent magnets flux density, area and number of coil windings. Usually the number and area of windings are not increased over certain values to avoid bigger and heavier motors. The maximum current intensity is also limited because of heating problems due to Joule effect in the coils which can result in damage to the motor. Finally, the flux density of permanent magnets depends on the physical properties of the material that is being used. Among these materials, Neodymium-Iron-Boron alloys have the best performance.

The *motor torque costant* ,k_{T}, allows us to express torque proportionaly to applied current. Each phase contributes to total torque by adding them in a vectorial way. As known from algebra, the maximum magnitude of two vectors in cross product will be when the angle between them is 90 deg. Hence, the commutation logic activates the phases to keep the stator magnetic field as near as possible to 90 deg in respect to the rotor magnetic field.

If a coil is immersed in a variable magnetic flux, an electromotive force is generated. The rotation of the rotor can be seen as a variable magnetic flux from the point of view of the coils, so a counter electromotive force is induced on each phase. This cEMF is proportional to the angular speed of the rotor and the counter electromotive constant k_{fcem}. This cEMF opposes current and consequently reduces torque output. The voltage in each coil is:

$$V = Ri + k_{\mathrm{T}}\omega$$

then:

$$T = k_{\mathrm{T}}i = \frac{Vk_{\mathrm{T}}}{R} - \frac{{k_{\mathrm{T}}}^2}{R}\omega$$

The output power is :

$$P_{\mathrm{out}} = T\omega = \frac{Vk_{\mathrm{T}}}{R}\omega - \frac{{k_{\mathrm{T}}}^2}{R}\omega$$

which trends can be seen in FIG 18 . The maximum torque output occurs at null velocity and decreases linearly with speed. Maximum power is rated approximately to half the maximum no load angular velocity.

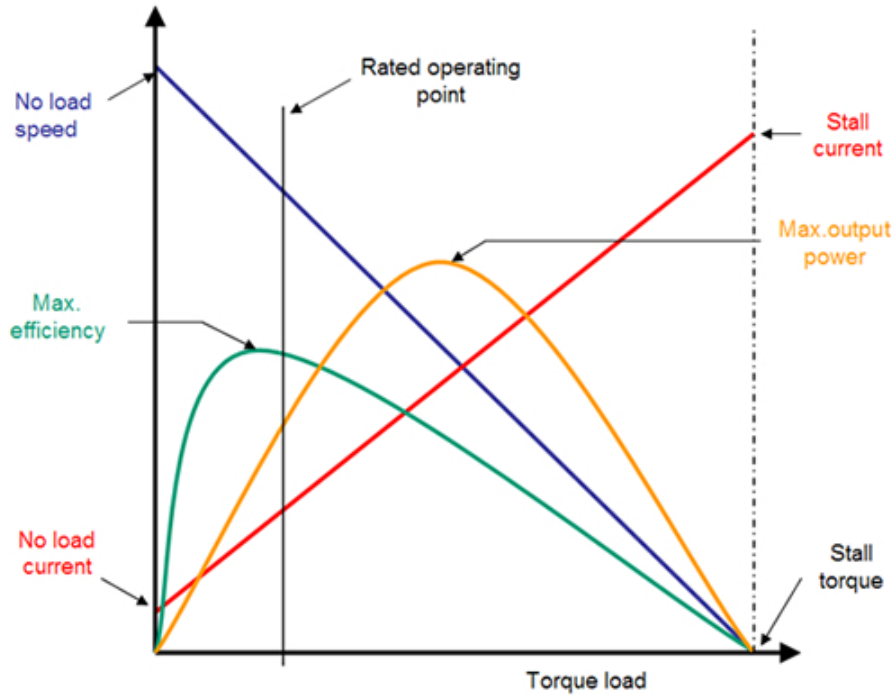

Figure 18: Torque and Speed Characteristics

There are two torque parameters used to define a BLDC motor, peak torque and rated torque. During continuous operations, the motor can be loaded up to rated torque. This requirement comes for brief period, especially when the motor starts from stand still and during acceleration. During this period, extra torque is required to overcome the inertia of load and the rotor itself. The motor can deliver a higher torque up to maximum peak torque, as long as it follows the speed torque curve. As the speed increases to maximum value of the torque of the motor, continous torque zone is maintained up to the rated speed after exceeding the rated speed the torque decreases. The stall torque represents the point on the graph at which the torque is maximum, but the shaft is still. The no load speed is essentially controlled by the voltage, and may be varied by varying the supply voltage. This is usually controlled by PWM and gives rise to a series of torque/speed characteristics in the boundaries of continuos and intermittend operation.

Figure below shows the speed torque characteristics of BLDC motor. The continous limit is usually determined by heat transfer and temperature rise. The intermittent limit may be determined by the maximum ratings of semiconductor devices in the controller, or by temperature rise.

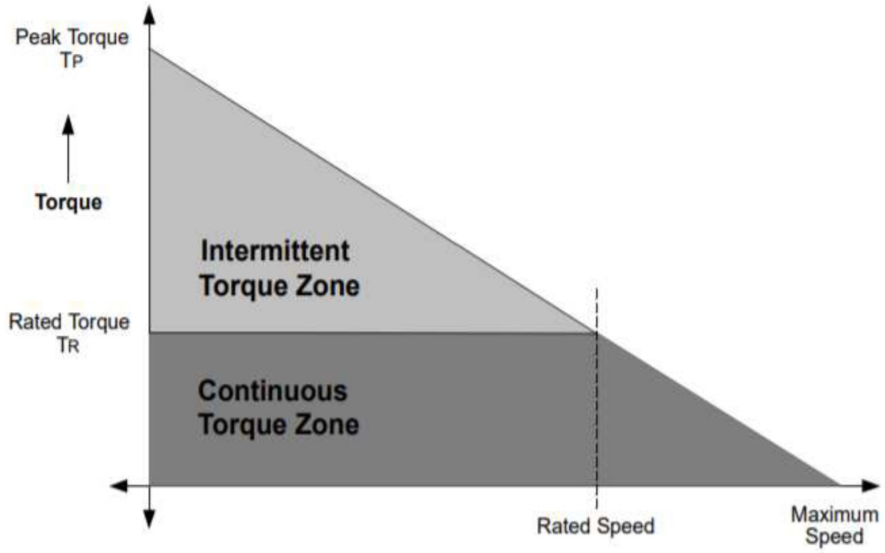

Figure 19: Torque and Speed Characteristics

Finally, efficieny is defined as the ratio between output and input powers as follows:

$$\eta = \frac{P_{\text{out}}}{P_{\text{in}}}$$

and since $P_{\text{in}} = Vi$, then:

$$\eta = \frac{k_{\text{t}}\omega}{V}$$

Since the losses due to friction and viscous effects are much smaller than the Joule effect losses, they have been neglected.

2.5 Motor control

A BLDC motor can be easily operated by a proper commutation of phase current based on the information of the rotor position. There are various ways to control a BLDC motor using different control parameters.

The simplest speed control system to control the speed of a BLDC motor uses a proportional-integral controller. This PI speed controller outputs the motor voltage reference as a function of the motors angular position and the K_{P} and K_{I} which are the proportional and integral gains of the PI speed controller.

This reference voltage is generated by a PWM (Pulse Width Modulation) technique and then applied to the BLDC motor. This speed control system is simple but has a big problem: in this method, the motor current is hard to control within a proper range. This is because when speed command is changed, the voltage reference may be largely changed. Thus it cannot be expected to obtain a good dynamic response of the speed control. Moreover, this may incur a large transient current more than the rated current, which may lead to the shutdown of the drive system.

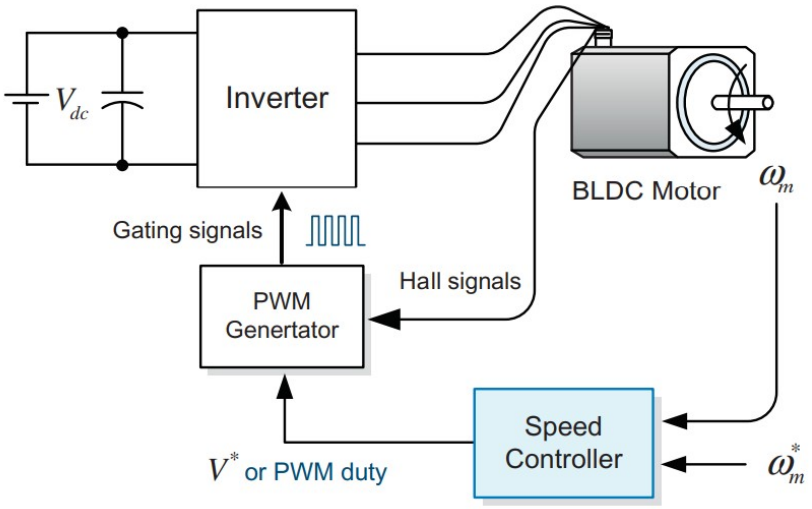

Figure 20: Speed Control

PWM is a method of reducing the average power deliverd by an electrical signal by effectively chopping it up into discrete parts. The average value of voltage and current fed to the motor is controlled by turning the switch between supply and load on and off at a fast rate. This is done through duty cycle which describes the portion of 'on' time to the regular interval 'period' of time: a low duty cycle corresponds to low power, because the power is off for the most of the time. By using this type control instead of a linear control, the power dissipation is much smaller. When a switch is off there is practically no current, and when it's on and power is being transferred to the load, there is almost no voltage drop across the switch. Power loss, which is the product of voltage and current, is thus in both cases close to zero.

PWM is particularly suited for running inertial loads such as motors which are not as easily affected by this discrete switching, because their inertia causes them to react slowly.

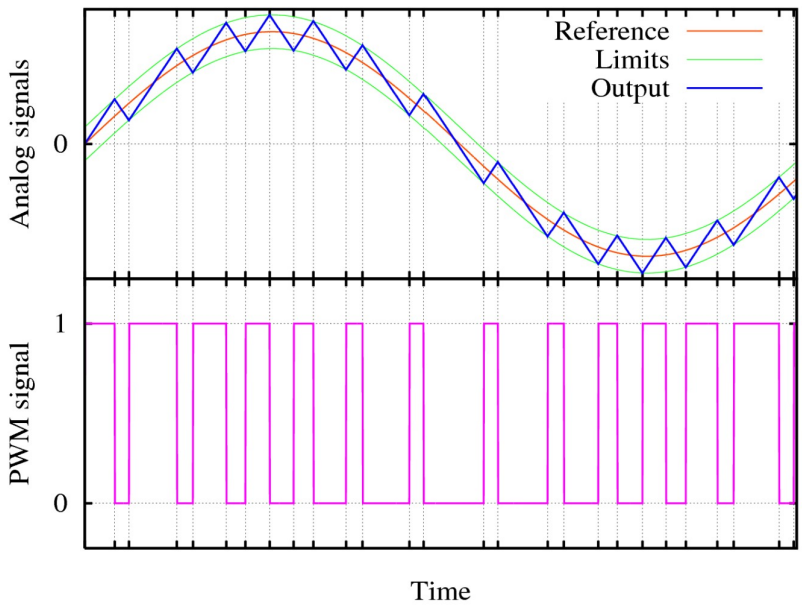

Figure 21: Speed Control

To obtain a better dynamic response it is necessary to control the speed by controlling the torque or current of the BLDC motor. Compared to the previous system, this type includes a

current controller to control the speed by regulating the current, thus torque. In this case, the output of the PI speed controller becomes the motor current reference.

In this case the motor is forced to deliver a constant torque regardless of speed and external load. Since motor torque output depends on magnetic flux in the stator coils, and advanced analysis is required in order to achieve a realistic implementation. However, by recalling the direct proportionality between torque and current through the motor torque coefficient k_{T}, a simplified model can be implemented.

In this case the total current can be obtained through the measurement of the voltage drop caused by the resistance of the ground line. This voltage drop is then multiplied by k_{T} and then compared to the required torque command signal. This error signal goes to the PID controller which creates a signal that modifies the PWM duty cycle, and by doing so regulating phase voltages and phase currents.

There are some conditions that can lead to the damage of the motor. A series of safes must be implemented. In the case of rotor locking, the counter EMF will drop causing the rise of phase currents to a very high level. This results in the overheating and then the damage of the coil insulation, which can lead to the permanent magnet rotor demagnetization due to the exceedence of Curie temperature, or to the damage of the power electronics. Also, a sudden velocity reversal can lead to the demagnetization of the rotor. In order to avoid such matters, a motor protection control mode is needed in order to override the normal control.

A series of limits must be imposed on the current: there is the **peak current** which is the maximum current allowed during transients. A saturation is applied for higher values than this in order to protect the motor. **Maximum working current** is the maximum value which can be used during normal operations. Like for the peak current, a motor protection logic doesn't allow this value to be exceeded.

Another type of limit is the undervoltage protection which makes it possible to avoid damaging lithium-polymer batteries when the system is battery operated, and to also identify a faulty Hall sensor.

3 Simulink electromechanical actuator reference model

The purpose of this reference model, which level of detail is very high, is to enable us to perform various analysis instead of using a real and expensive test bench. This reference model simulates a F-16 combat flap that has a dynamic response time which is halfway between primary and secondary flight control system.

Consequently, this model is complex and requires a very high computational capacity. In order to avoid numerical errors, a time step of at least two orders of magnitude less than the smallest characteristic time of the system has to be chosen. An adequate time step for the simulation is $1 \cdot 10^{-6} s$. The simulation time interval used for the analysis is 2 s.

A Runge-Kutta first order fixed step integrator, namely Euler's method, is used for the simulation of the EMA's operation. Higher order integrator are not recommended because the solver might use a longer step size which would lead to convergence problems.

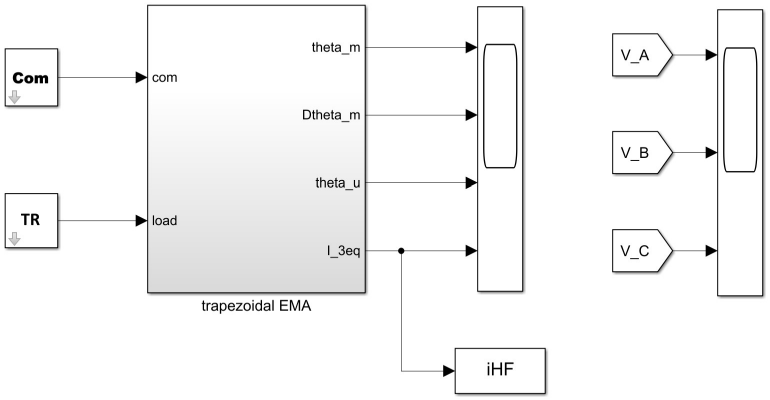

Figure 22: EMA model

The high fidelity model consists of different subsystems which represent the physical components of the EMA. A brief description of the main blocks is shown now.
Firstly we have the Com block which allows us to give the command that the system has to reach.
The TR block represents the external load that acts on the system.
The Trapezoidal EMA block consists of the main block components that allow to correctly simulate the functioning of the EMA.
There are also some scope blocks that enable to evaluate the main electrical and mechanical variables.
Below all the main blocks are described in detail.

3.1 Com subsystem

The Com subsystem block provides the command type that the system has to pursue. There are different commands that can be activated individually or can be combined together to form peculiar commands. The parameters of each command can be modified from the mask.

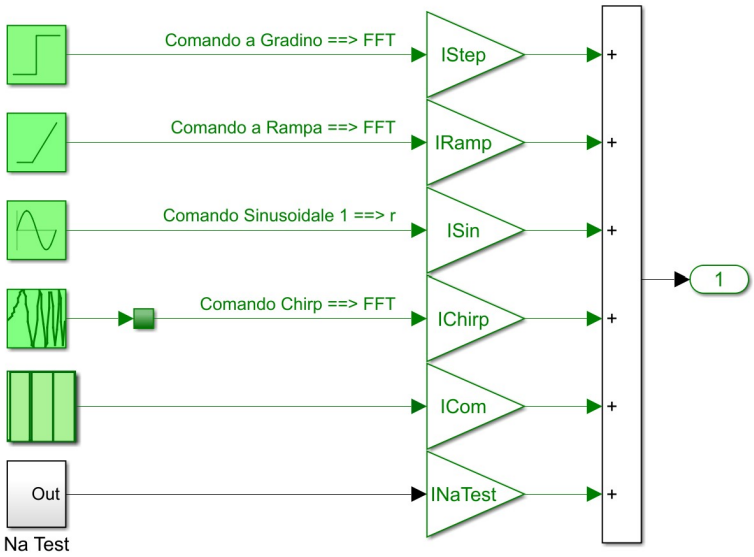

Figure 23: Com block

3.2 External load subsystem

The external load block permits to define the external load that opposes the actuator. It is very similar to the Com block in the way that the external load can be composed of a singular type of load or by a combination of multiple type of loads. These can be step, ramp or sinusoidal type of loads. The parameters of each load can be modified from the mask.

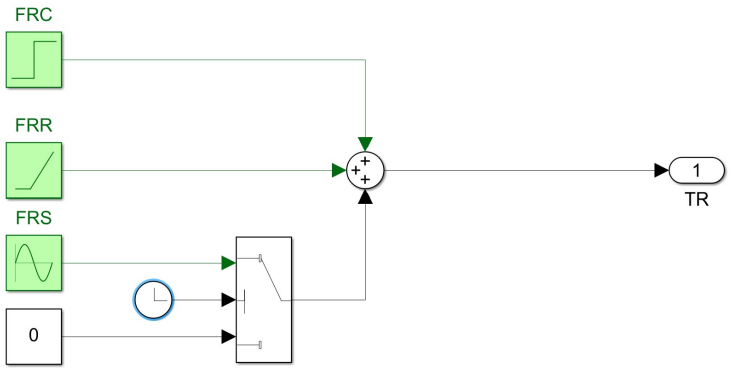

Figure 24: External load block

3.3 Trapezoidal EMA block

This block is the most complex one and is composed of multiple subsystems that allow for a high fidelity simulation of an F-16 trapezoidal EMA. The system comprise of mechanical, electric and electronics subsystems.

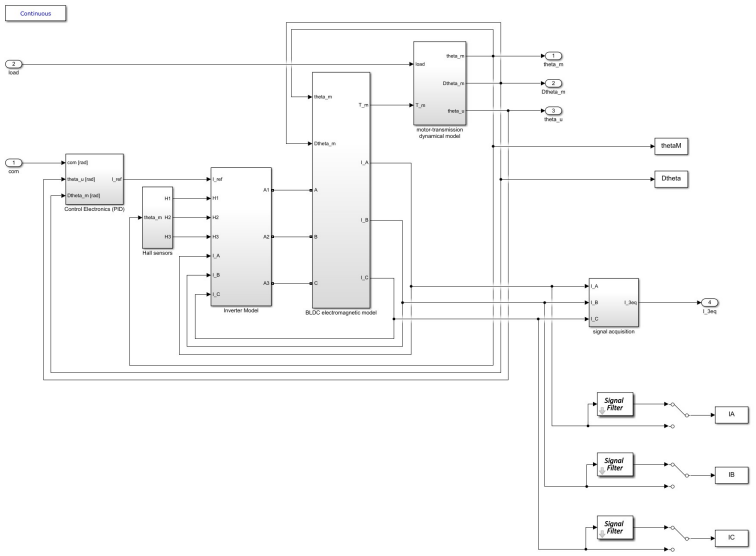

Figure 25: Trapezoidal EMA subsystems

It can be seen that the command signal is acquired by the Control Electronics block, while the load is applied to the motor-transimission dynamic model.
There are multiple outputs such as the user and motor angular position and velocity and the currents of the three coils. These currents are passed through a low-pass filter.

3.3.1 Control Electronics (PID) block

This block is tasked with determining the error signal, which is the difference between the commanded value (com input) and the user position (θ_u). This error signal is then multiplied by a gain that allows it to be subtracted by the third input which is the angular speed ($\dot{\theta}_m$).

The PID controller is made of three branches: the proportional one, which gives a proportional gain to the error through a coefficient; the integral branch, that has a correction action when the steady state error is not zero; lastly the derivative branch, it has a corrective action during the transient augmenting the system response time but simultaneously deteriorating the steady state error.

The Integral and Derivative gains are set to zero, since the dynamic performances are satisfied with only the Proportional gain which is equal to 0.05.

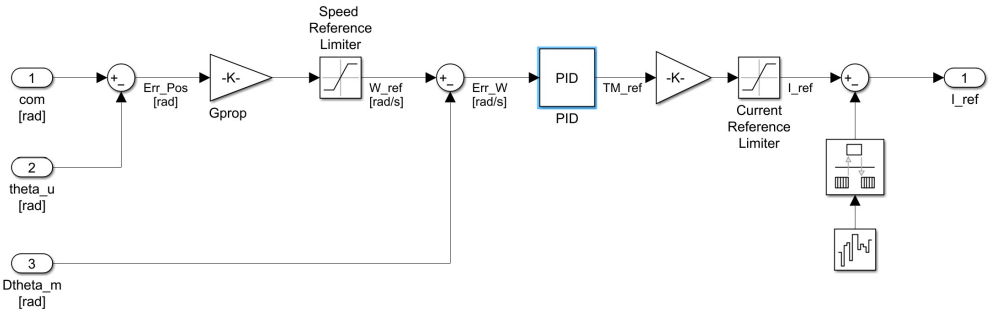

Figure 26: Control Electronics block

After the gains are applied to the signal, it is divided by the cEMF of the motor in order to have a current signal.

There are two saturations blocks: one which limits the angular speed error between two values (±8000 rpm) and the second which limits current error between a maximum and a minimum value (±22.5 A). These are needed in order to avoid the damaging of the motor assembly. Electrical noise is added in the end with the aim of including realistic disturbance to the main signal.

3.3.2 Hall sensor block

The input of the Hall sensor block, which comes from the motor-transmision dynamical model, is the mechanical angular position of the motor. The three outputs, H1, H2 and H3, are the signals that go to the inverter allowing to determine the rotor's position

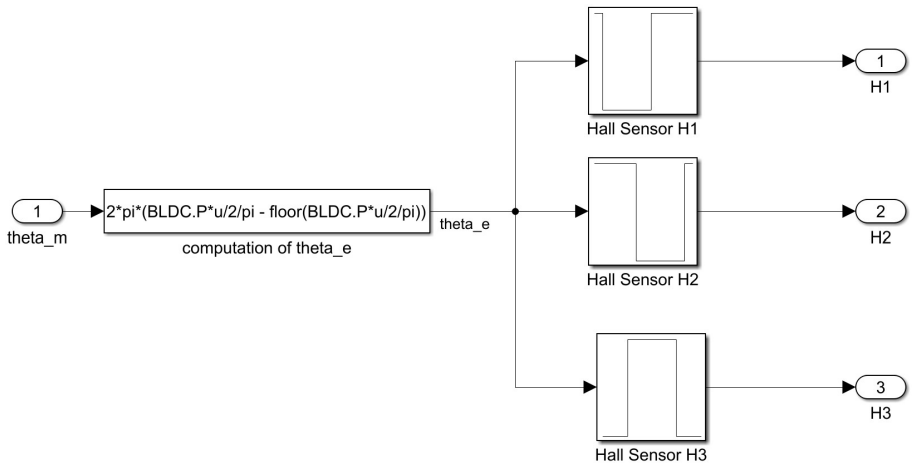

Figure 27: Hall sensor block

Firstly, the electrical angle must be determined through the following formula:

$$\theta_{\mathrm{e}} = 2\pi \left[\frac{p\theta_{\mathrm{m}}}{2\pi} - floor\left(\frac{p\theta_{\mathrm{m}}}{2\pi} \right) \right]$$

, where θ_{m} is the mechanical position and p is the number of motor pole pairs.
Then, three lookup table, which perform a 1D linear interpolation of the input values using the specified table data are used in order to determine the low/high signal of each Hall sensor.

3.3.3 Inverter block

The inverter block simulates the behaviour of the power electronics which feeds the trapezoidal motor. It is used to model a digital PWM inverter. It is composed of multiple blocks that are now described in depth:

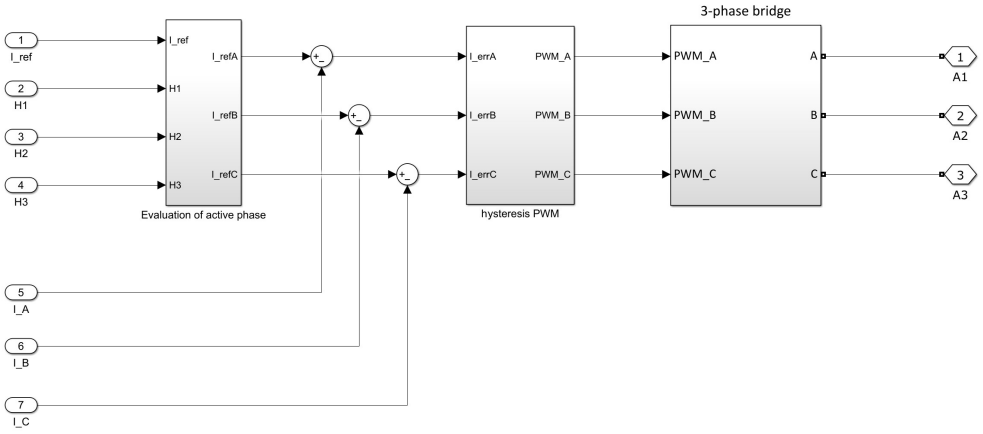

Figure 28: Inverter block

- **Evaluation of active phase**: The three signals from the Hall sensors and the signal from the PID controller are here evaluated and then multplied by each other in order to generate three reference current signals (I refA, I refB, I refC). This block allows us to simulate the switching logic of a three phase trapezoidal BLDC motor.

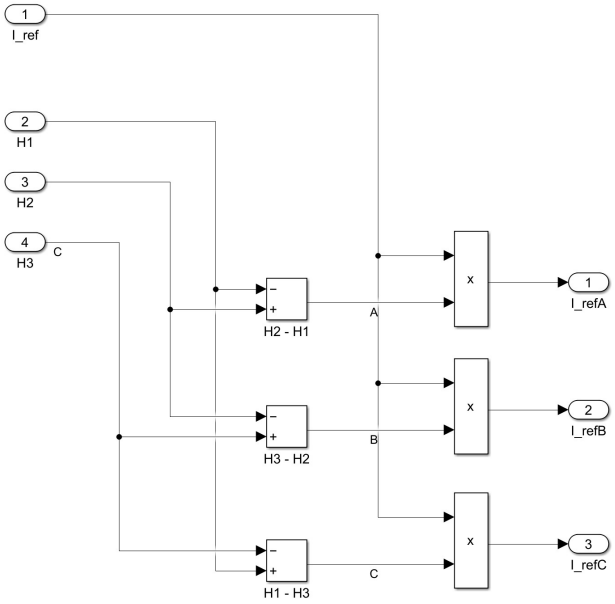

Figure 29: Evaluation of active phase block

- **Hysteresys PWM**: These reference current are then substracted by the three coil current which arrive from the BLDC electromagnetic model, generating three error signals which are fed to the hysteresys PWM block. This uses three hysteresys blocks in order to generate the PWM signals that drive the 3 phase H-bridge. The hysteresys block returns 1 if the input is greater than +hb, which is half the deadband, or 0 if it's less than -hb. Therfore, it is the width of the deadband that determines the PWM carrier frequency.

  This way, the integration step has to be smaller than the phase switching frequency by at least one order of magnitude, as stated by the Nyquist-Shannon Sampling Theorem. This must be done in order to avoid aliasing problems.

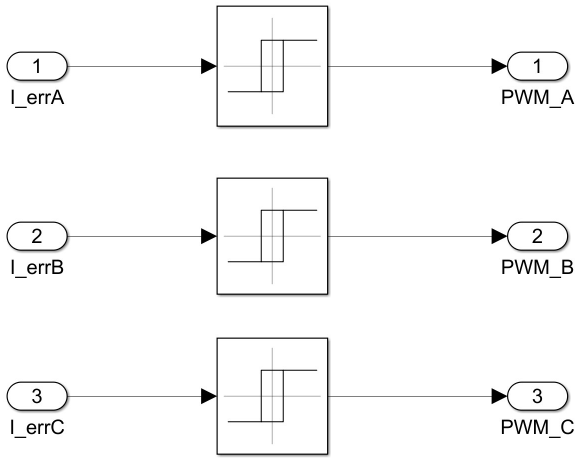

Figure 30: Hysteresys PWM block

- **3-phase bridge**: The three PWM signals are transformed in their boolean and negation signals which activate one of the six MOSFET power transistor of the three phase H-bridge.

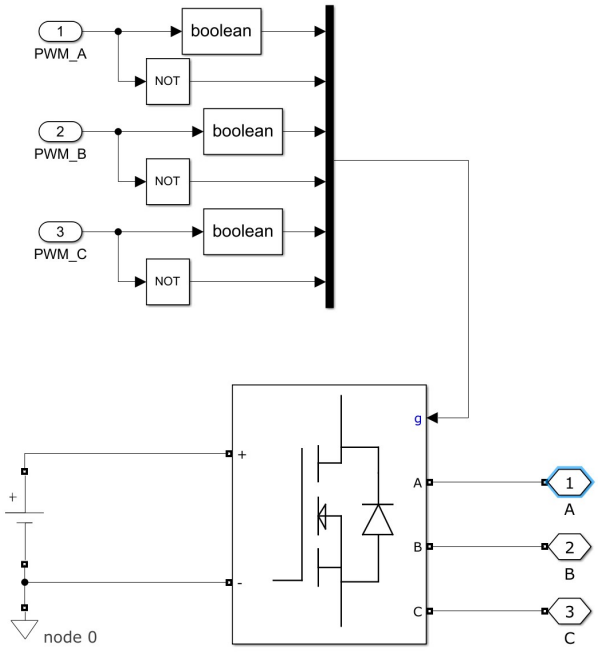

Figure 31: Hysteresys PWM block

This last component is modeled through an Universal Bridge Simulink block, which is part of the Simscape library. This component allows for the simulations of complex electrical systems. The DC power source is connected to the Universal Bridge in order to supply the inverter with voltage.

In order to avoid the occurrance of short circuit between supply and ground the following occurs: when the transistor which connects the phase with the supply is on, the same phase transistor that connects the same phase to ground is off.

The three outputs (A1, A2, A3) from the H-bridge are fed to the BLDC electromagnetic model

3.3.4 BLDC electromagnetic model block

As it can be seen from FIG 32 the inputs to this block are the motor's angular position and speed. These are used to compute the counter EMF, , the torque, the voltages and the current of each coil.

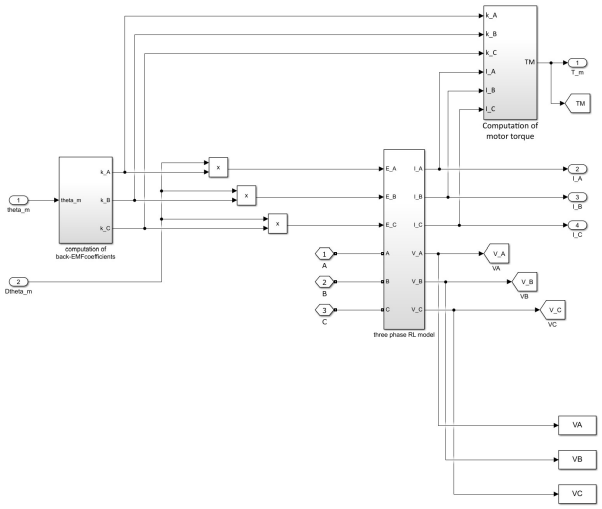

Figure 32: BLDC electromagnetic model

- **Computation of back-EMF coefficients**: This block takes as input the rotor angular position and uses the same formula used in 3.3.2 to calculate the electrical angle. Then it uses three lookup tables and three mux blocks in order to calculate the back EMF of each phase.
  The value that is meant to be calculated is the normalized CEMF, which is defined as the ratio between the actual CEFM and the rotor angular speed:

$$CEMF_{\text{norm}} = \frac{CEMF}{\omega_{\text{m}}} = k_{\text{cemf}}$$

  For each pole-pair of the motor the effect of rotor eccentrity is used in order to account for the electromagnetic coupling costant value which depend of the rotor angular position (θ_{m}):

$$k^i_{\text{cemf}} = k^i_{\text{e}}(\theta_{\text{m}}) \left[1 + \zeta cos\left(\theta_{\text{m}} + \frac{2\,(i-1)}{3}\pi\right)\right]$$

  where $\zeta = \frac{x_0}{g_0}$ takes account for eccentricity effects, k^i_{e} is the trapezoidal wave-shaped normalized CEMF relative to the i-th phase.

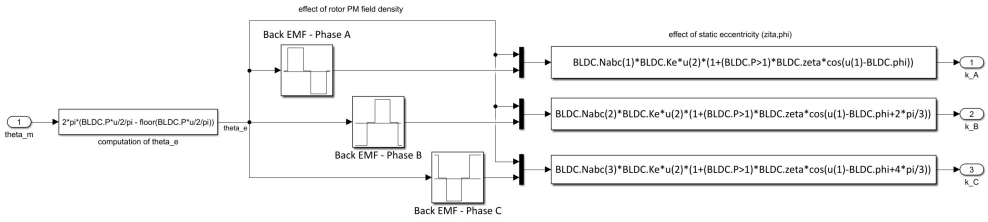

Figure 33: CEMF coefficient calculation block

- **3-phase RL model**: The three CEMF coefficients are then multiplied by the rotor angular speed and the value is passed to the 3-phase RL model block.
  This block uses 3 series RLC blocks that are part of the Simscape library. These are used to model the three stator coils. There are also three current measurment blocks, which are going to be used as a feedback signal for the PWM logic, and three voltage measurment blocks, that are used for post-processing and visualisation.

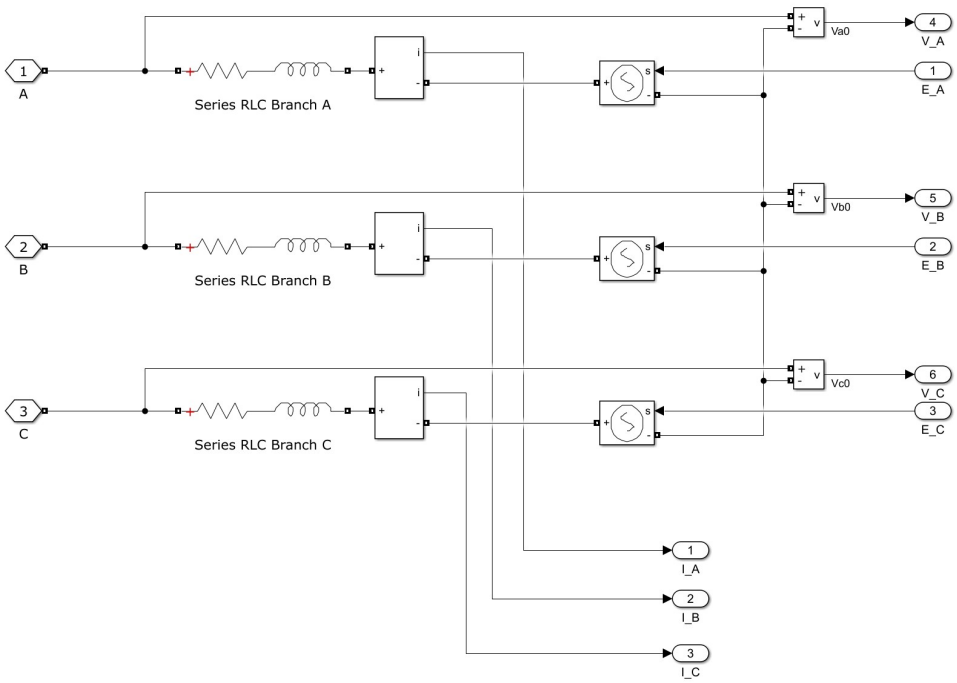

Figure 34: 3-phase RL model block

- **Motor Torque Computation**: this block uses the three phase currents and normalized counter electromotive forces to compute the torque delivered by the motor. Each phase contribution is summed in order to obtain the total torque of the motor. This is then limited through a saturation block in order to account for the saturation of the magnetic flux in the stator core.

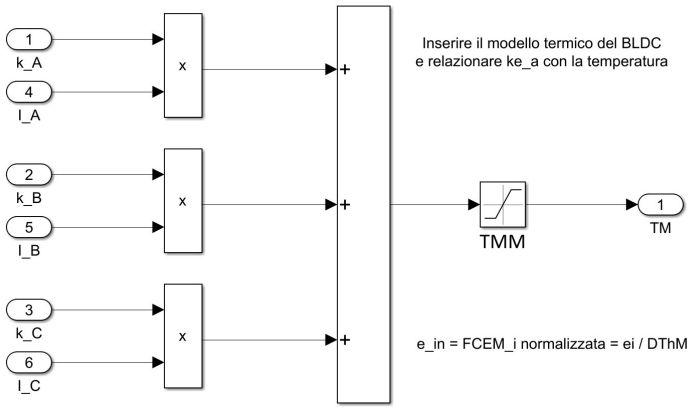

Figure 35: Motor Torque Computation block

3.3.5 Motor-transimission dynamical model block

This last block is the most important one with regard to this study, as it aims to properly model the transmission between motor and final user. The same thing will be done using the Simscape toolbox.
The inputs to this block are the external load and the motor torque. The system's outputs are the angular speed and user position.

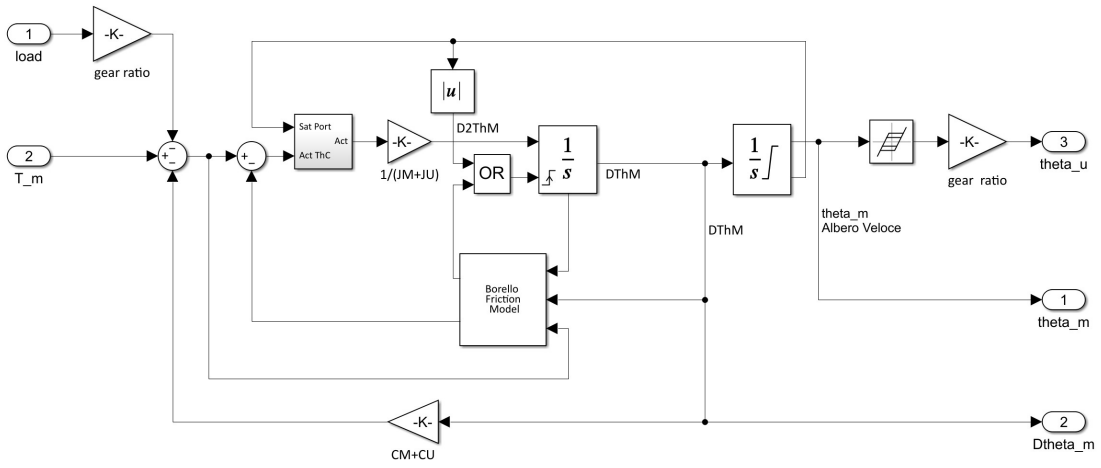

Figure 36: Motor-transimission dynamical model block

The transmission between motor and user is modelled as a second order system with a single degree of freedom. Viscous and inertial effects are included and also non linearities, such as dry friction, end-stops and backlash.

The friction model that is used is the Borello one. This is an innovative mathematical model which allows for the correct friction simulation. This model is easily integrable in complex computational programs and it has a high robustness toward the simulated conditions.

This model overcomes the problems and limits that models like Karnopp and Quinn introduced. This model has the following distinctive features:

- the sign of the friction couple is now function of the direction of the speed vector;
- it sets apart stick condition from slip condition;
- it evaluates the stopping of a moving element;
- it correctly maintains a standstill element in stick conditions, or a moving element in slipping conditions;
- it correctly evaluates the departure of a standstill element;
- it can be used for correctly modelling of end-stops;

The friction force computed by this model is function of the active force applied on the element and of it's speed. The mathematical model can be formulated in the following way:

$$FF = \begin{cases} F_{\text{act}} \quad if \quad v = 0 \quad or \quad |F_{\text{act}}| \leq FSJ \\ sign(F_{\text{act}}) \cdot FSJ \quad if \quad v = 0 \quad or \quad |F_{\text{act}}| > FSJ \\ FDJ \quad if \quad v \neq 0 \end{cases}$$

, where FF is the computed friction force, FSJ is the static friction force, FDJ is the dynamic friction force and F_{act} is the force acting on the element.

To avoid numerical instability phenomenons, like those occuring in the Karnopp model, the following condition is imposed:

$$v(t_{\text{i}+1}) = 0 \quad if \quad v(t_{\text{i}+1}) \cdot v(t_{\text{i}}) \leq 0$$

, meaning that if there is a change in sign between integration steps the element is stopped and the direction of speed is changed. If the stopping of the element should result not correct, beacause of the active force being greater than the passive ones, the element would start to move in the next step. This last condition is what makes this model very robust and not subject to instability phenomenons.

A backlash and transmission ratio block are introduced between fast and slow shaft with the aim to have a model that is as realistic as possible. In order to evaluate the cEMF and the operating phase switching logic, the rotor electric position is also evaluated by using the number of pole-pairs that are to be fed to the electromechanical model.

3.3.6 Signal acquisition block

Lastly, the signal acquisition block takes in the three coil currents and gives as an output one equivalent current signal. This is going to be then used as a cross-reference with the monitor model, which is a simplified model of the EMA that simulates only one equivalent coil.

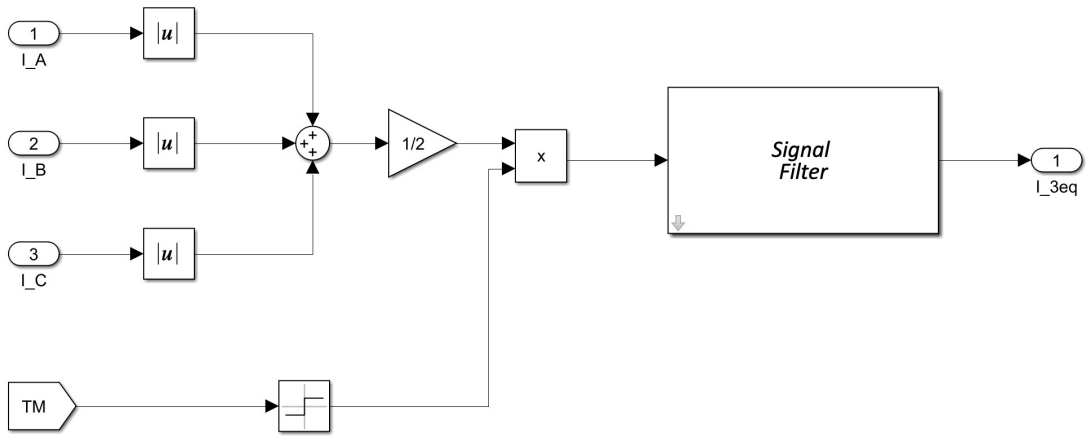

Figure 37: Signal acquisition block

The following values are being used for the simulation of the Electromechanical Actuator in the Simulink evironment:

```
run('F16data.m')

%% parametri simulazione

simulation.TiBr      = 2.0;            % [s]          durata simulazione
simulation.DT        = 1e-4;           % [s]          passo di integrazione
simulation.initPos   = F16.x0(5);      % [rad]        posizione iniziale (albero lento)

simulation.tauFilter = 5*10e-5;        % [s]          tempo caratteristico filtro I_3eq

simulation.timeCom   = [0 0.1 0.1+simulation.DT simulation.TiBr];   % parametri comando 'Com'
simulation.com       = [0 0 0.1 0.1];

%% controller

controller.Gprop    = 1e5;             % [1/s]        guadagno proporzionale controller     % 5e2/tau
controller.W_refMax = 8000*pi/30;      % [rad/s]      saturazione errore posizione          % 6060*pi/30%;
controller.I_Max    = 22.5;            % [A]          saturazione I_ref
controller.Knoise   = 0;               % []           coefficiente moltiplicativo Rumore (0 - 1 - 10 - 100)

controller.PID.GAP  = 0.05;            % [Nms/rad]    guadagno proporzionale PID            % 0.05;%0.1;%0.75
controller.PID.GAI  = 0;               % [Nm/rad]     guadagno integrativo PID              % 10
controller.PID.GAD  = 0;               % [Nms/rad]    guadagno derivativo PID               % 5e-5
controller.PID.ErIM = 100;             % [Nm]         Max Errore Integrativo

%% inverter

inverter.PWM.hb           = 0.5;       % [A]          ampiezza banda di isteresi
inverter.Hbridge.Vdc      = 48;        % [V]          tensione alimentazione
inverter.Hbridge.RSnubber = 1e5;       % [ohm]        resistenza snubber
inverter.Hbridge.CSnubber = inf;       % [F]          capacità snubber
inverter.Hbridge.Ron      = 1e-2;      % [ohm]        Ron (in Universal Bridge)

%% motore

BLDC.P    = 2;                         % []           numero paia poli
BLDC.Nabc = [1 1 1];                   % []           frazione spire attive (fasi A, B, C)

BLDC.Rs   = 2.130;                     % [ohm]        resistenza nominale fase-fase (es. Rab)
BLDC.Ls   = 720*1e-6;                  % [H]          induttanza nominale fase-fase (es. Lab)
BLDC.Ke   = 0.0752/2;                  % [Nm/A]       costante di fcem del motore

BLDC.TMM = 1.689;                     % [Nm]         saturazione coppia

BLDC.zeta = 0;                         % []           modulo eccentricità statica
BLDC.phi  = 0;                         % []           fase eccentricità statica

%% dinamica motore-trasmissione

dynamics.tau = 1/500;                  % rapporto di trasmissione

dynamics.JM            = 130e-007;     % [kg*m^2]     Momento d'inerzia del DC Motor (AV=albero veloce)
dynamics.CM            = 30/pi*1e-6;   % [N*m*s/rad]  Coefficiente di smorzamento viscoso dimensionale DC Motor (AV)
dynamics.JU            = 12e-6;        % [kg*m^2]     Momento d'inerzia utilizzatore ridotto all'albero veloce
dynamics.CU            = 4.5070e-7;    % [N*m*s/rad]  Coefficiente di smorzamento viscoso dimensionale utilizz.(AV)

dynamics.friction.FSTm = 0.06;         % []           attrito statico  motore       (albero veloce - espresso in percentuale di BLDC.TMM)
dynamics.friction.FDTm = 0.03;         % []           attrito dinamico motore       (albero veloce - espresso in percentuale di BLDC.TMM)
dynamics.friction.FSTu = 0.04;         % []           attrito statico  utilizzatore (albero veloce - espresso in percentuale di BLDC.TMM)
dynamics.friction.FDTu = 0.02;         % []           attrito dinamico utilizzatore (albero veloce - espresso in percentuale di BLDC.TMM)

dynamics.BLK           = 1e-5;         % [rad]        Backlash Width (albero lento)

dynamics.ThUmin        = -1;           % [rad]        finecorsa inferiore
dynamics.ThUmax        = 1;            % [rad]        finecorsa superiore
```

Figure 38: Matlab HF Values

The simulation was carried with a step of unitary input. It can be seen from the diagrams below that the motor and user have identical trends but reach different values. This is due to the different inertia of the two.
The motor reaches a speed of 600 rad/sec, which is kept until the user reaches it's desired value. When this happens the motor stops.

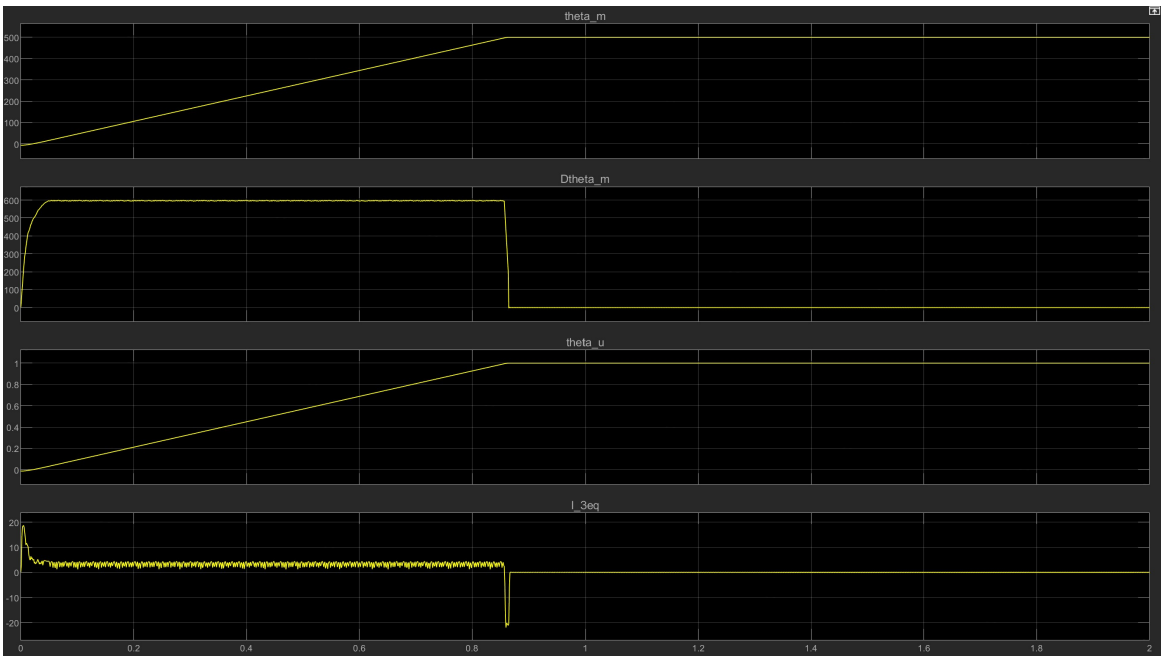

Figure 39: postion, speed and current trends

4 Mechanical Nonlinearities

In order to correctly model a complex system such as an electrmechanical actuator, all the present nonlinearities have to be taken in account.

Nonlinearity is the behavior of a system, in which the output quantity does not vary in direct proportion to the input quantity. These systems do not follow superposition property. Nonlinearity can be classified on the basis of the magnitude: which can be an incidental nonlinearity that is present inherently in the system or an intentional nonlinearity that is inserted in the system to modify the system characteristics; else it can be classified on the basis of frequency. In the figure below it can be seen the main types of nonlinearities:

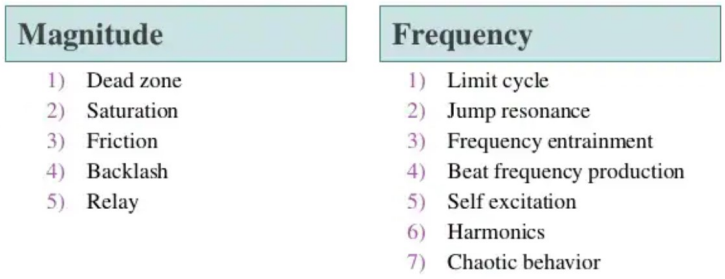

Figure 40: Nonlinearity types

A brief description of the most important types of nonlinearities is now done:

- **Saturation**: All systems have some maximum output capability, regardeless of the input. The output of the system is proportional to input in limited range of input signal. On exceeding the range, output tends to become nearly constant. For example, when we are in the saturation range the input command can be doubled and yet non double or even significantly change the output.
  All actuators present saturation for some values of input command. A significant problem that can be caused by saturation is the integral wind-up which can degrade the dynamic response of the system.
  Saturation can also limit the maximum achievable magnetic field in systems containing electromagnetic components. It can also cause harmonics and intermodulation distortion when applying AC signal in electronic circuits ferromagnetic core inductor.

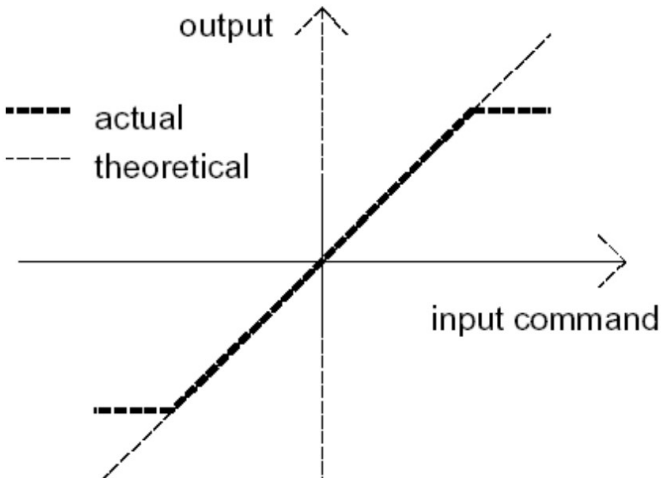

Figure 41: Saturation

- **Dead zone**: This is a nonlinearity in which the system doesn't respond to the given input until the input reaches a particular level or it can be also seen as when the output becomes zero when input crosses certain limiting value. This nonlinearity can lead to performance degradation of the system, reduced positioning accuracy and destabilization.
  For example, dead zone in actuators can give rise to limit cycle and instability.

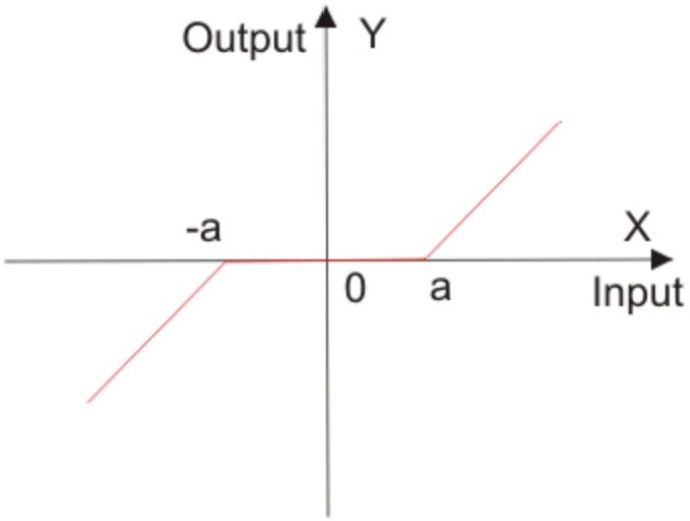

Figure 42: Dead zone

- **Static and Coulomb Friction**: This phenomenon leads to a nonlinearity especially when the velocity is next to zero. If we have a motor velocity of zero we should have no friction but in reality a small amount of static (Coulomb) friction is almost always present.
  This can lead to stick and slip phenomenon which can degrade the system performance. The actuator will come to slightly different final resting position each time. This position will depend on the final value of the static friction. Some motor torque is wasted overcoming friction forces which leads to inefficiency from an energy viewpoint.
  Initially the surfaces are in the static friction regime. In order for movement to begin a force greater than the static friction is required. As the system starts moving the friction decreases passing from static do dynamic friction. This results in a jerky actuator motion, making positional control and repeatability difficult.

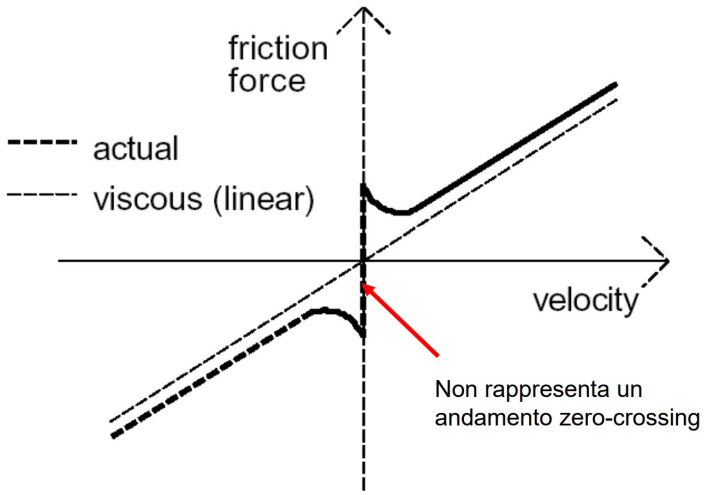

Figure 43: Static and Coulomb friction

- **Backlash**: Gear backlash is the play between teeth, which is critical in preventing binding. Measured at the pitch circle, it is the distance between the involutes of the mating gear teeth as seen in FIG 44

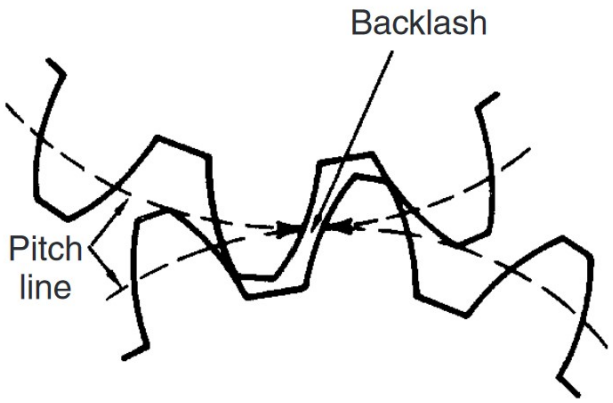

Figure 44: Backlash

Backlash is necessary to provide the running clearance needed to prevent binding of the mating gears, which can result in heat generation, noise, abnormal wear, overload and failure of the drive. Some backlash is to be expected because of the dimensional tolerances needed for cost-effective manufacturing.
The increase in backlash does not adversely affect operation with non-reversing drives or drives with continous load in one direction. However, for reversing drives where timing is critical, excesive backlash that results from wear usually cannot be tolerated.
In this case when the input gear reverses direction, a small rotation is required before the output gear begin to move. This phenomenon is very important because it can couple with control law, causing a performance degradation and in some cases dynamic instability which can lead to a limit cycle(Hysteresis).
In order not to use an oversized motor, on EMA actuator a high transmission ratio is needed. Usually, the motor speed rating is from about thousands to ten of thousand of RPM. Meanwhile the typical required speed by the shaft moving the flight control

surface is about tens of degrees per second. This requirement is usually called the null actuation speed, which is the speed the motor can give when no load is applied to the flight surface. This is usually expressed in angular terms. For example, 50-60 deg/sec for primary flight control surfaces, and 5-6 deg/sec for secondary flight control surfaces. For auxiliary seocondary flight control surfaces (flight spoiler or combat flap) the angular velocity can reach up to 15 deg/sec.

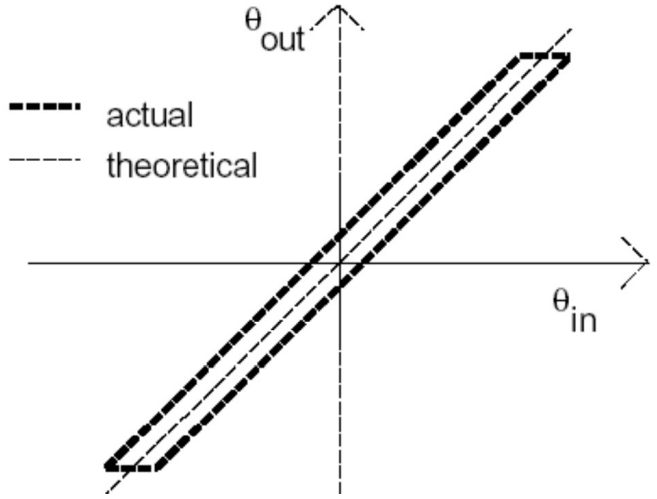

Figure 45: Backlash

- **End Stops**: all mechanical systems, like linear/rotary actuators, valves and dampers have and end stop. This is defined as the maximum range of distance that the mechanism can move. It is restricted by an lower and higher limit within which the actuator can perform its defined purpose. This is a non linearity that depends on the asumption that are being made while the model of the mechanism is being defined. The more close to reality the model aims the higher the non linearity will be.

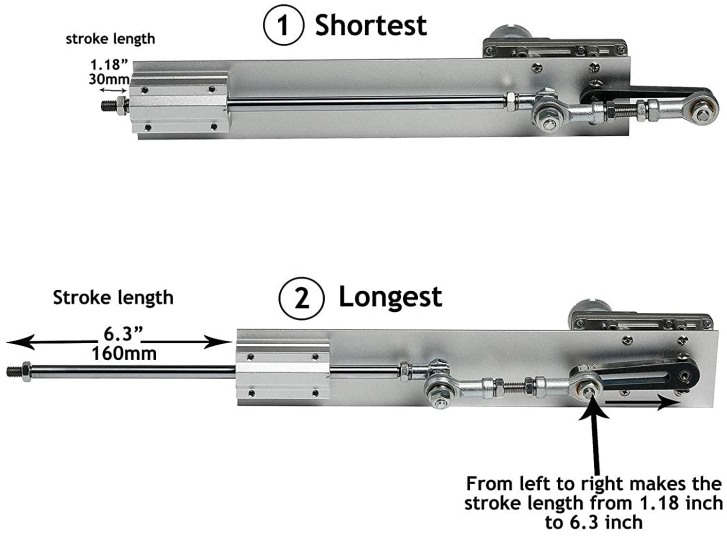

Figure 46: Actuator End Stop

For example, if the impact is considered perfectly inelastic, this will simplify the model and the non linearity will be lower than if a not perfectly inelastic impact would be considered. The same stands if the dynamic vibration of the impact are being neglected. This will have to be correctly modeled in order to have a model that behaves as closely as the real mechanism.

- **Limit cycle**: It's a non linearity that is classified based on the frequency. It corresponds to an oscillation of fixed amplitude and period. The limit cycle is usually a closed trajectory but other trajectories about the limit cycle can be spirals from various points of the phase plane. It can be divided in three types of limit cycles:
  A stable limit cycle which means that the system will approach an oscillatory state regardless of the initial condition;
  A semi-stable limit cycle which means that in this case maintenance of oscillation depends on the initial condition;
  Finally, we have the unstable limit cycle that means the system will move away from the stable condition.
  Limit cycles are usually less sensitive to the system parameter variation.

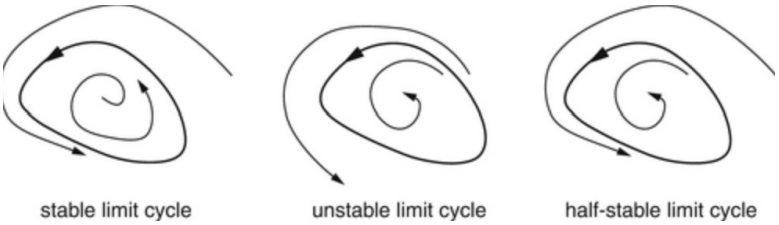

Figure 47: Limit cycle types

5 Simscape toolbox

Simscape is a toolbox available within the Simulink evironment. It consists of a set of block libraries and simulation features for modeling physical systems. Simscape is based on the Physical Network approach, which differs from the standard Simulink modeling approach and is particularly suited for simulating systems that consist of real physical components.
In Simulink models mathematical relationships are modeled using blocks connected by signal carrying links. The blocks perform specific mathematical functions.

Simscape uses blocks that represent physical objects and these blocks replicate the constitutive relations that govern the behavior of the physical object represented by the block. Most often the network resembles typical schematics of the system that the user is familiar with. Thus, an electric circuit or mechanical system looks like the circuit/system seen in texts. The exchange currency of these networks is power, or energy flow over time. The elements transmit power amongst each other through their points of entry or exit which are also known as ports. These connections ports are non directional and they are similar to physical connections between elements.

Connecting Simscape blocks together is analogous to connecting real components, such as mass, spring ,etc. Just like real systems, flow direction need not to be specified when connecting Simscape blocks. In this physical network approach the two variables that make up power are known as the *Through Variable* and *Across Variable*.

The number of connection ports for each element is determined by the number of energy flows it exchanges with other elements in the system or the number of points through which power may enter or leave the element.

The Through and Across are the variables whose product is the energy flow in watts, they are the basic variables. For example, the basic variables for mechanical translational systems are force and velocity, for mechanical rotational systems are torque and angular velocity. This variables are characterized by their magnitude and sign.

A brief description of the main blocks is now done:

- **Inertia block**: It represents an ideal mechanical translational inertia that is described with the following equation:

$$T = J\frac{d\omega}{dt}$$

  , where T is the inertia torque, J is inertia, ω the angular velocity and t is time.

  By default, the block has one mechanical translational conserving port. The block positive direction is from its port to the reference point. This means that the inertia torque is positive is inertia is accelerated in the positive direction. This block can have one or two ports. The two-port variant is purely graphical: the two ports have the same angular velocity.

Figure 48: One and two port inertia block

- **Mechanical Rotational Reference**: This block represents a reference point, or frame, for all mechanical rotational ports. All rotational ports that are rigidly clamped to the frame (ground) must be connected to this block.

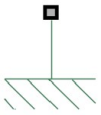

Figure 49: Mechanical rotational reference block

- **Rotational damper block**: It represents an ideal mechanical rotational viscous damper described with the following equations:

$$T = D \cdot \omega$$

$$\omega = \omega_{\mathrm{R}} - \omega_{\mathrm{C}}$$

,where T is the torque transmitted through the damper, D is the damping coefficient, ω the relative angular velocity and ω_{R} and ω_{C} are the absolute angular velocities of terminals R and C.

The block positive direction is from port R to port C. Connections R and C are mechanical translational conserving ports, with R representing the damper rod while C is associated with the damper case.

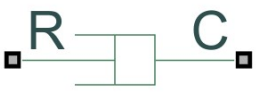

Figure 50: Rotational damper block

- **Rotational free end block**: The rotational free end block represents a mechanical rotational port that rotates freely, without torque. It can be used to terminate mechanical rotational ports on other blocks that are unconnected. This block can be also used to set the initial rotational velocity at a node.

Figure 51: Rotational free end block

- **Rotational friction block**: It represents friction in contact between rotating bodies. The friction torque is simulated as a function of relative velocity and is assumed to be the sum of Stribeck, Coulomb, and viscous components, as shown in the following figure.

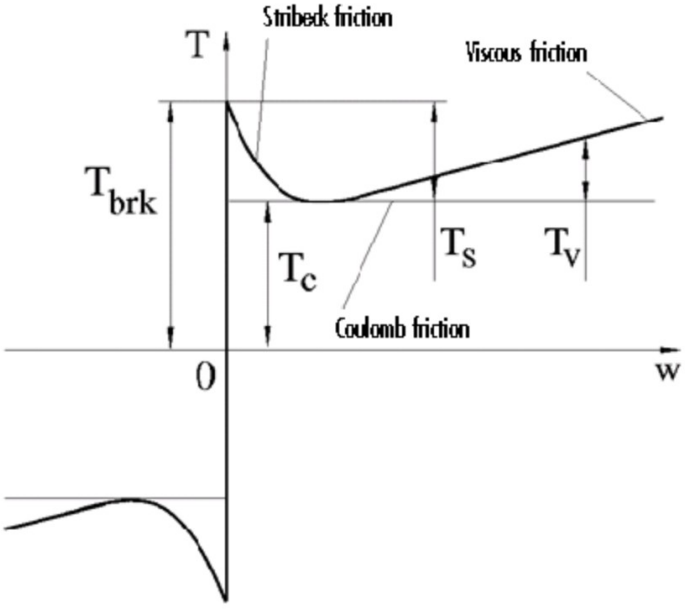

Figure 52: Stribeck plus Coulomb and Viscous friction

The Stribeck friction (T_S) is the negatively sloped characteristics taking place at low velocities. The Coulomb friction (T_C) results in a costant torque at any velocity. The viscous friction (T_V) opposes motion with the torque directly proportional to the relative velocity. The sum of the Coulomb and Stribeck frictions at the vicinity of zero velocity is

often referred to as the breakaway friction (T_{brk}). The friction is approximated with the following equations:

$$T = \sqrt{2e}\,(T_{\mathrm{brk}} - T_{\mathrm{C}}) \cdot e^{-\left(\frac{\omega}{\omega_{\mathrm{St}}}\right)^2} \cdot \frac{\omega}{\omega_{\mathrm{St}}} + T_{\mathrm{C}} \cdot tanh\left(\frac{\omega}{\omega_{\mathrm{Coul}}}\right) + f\omega$$

$$\omega_{\mathrm{St}} = \omega_{\mathrm{brk}}\sqrt{2}$$

$$\omega_{\mathrm{Coul}} = \omega_{\mathrm{brk}}/10$$

$$\omega = \omega_{\mathrm{R}} - \omega_{\mathrm{C}}$$

,where ω_{brk} is the breakaway friction velocity, ω_{St} the breakaway velocity threshold, ω_{Coul} the Coulomb velocity threshold and f is the viscous friction coefficient.
The exponential function used in the Stribeck portion of the force equation is continuous and decays at velocity magnitudes greater than the breakaway friction velocity.
The hyperbolic tangent function used in the Coulomb portion of the force equation ensures that the equation is smooth and continuous through $\omega = 0$, but quickly reaches its full value at nonzero velocities.
The block positive direction is from port R to port C. This means that if the port R velocity is greater than that of port C, the block transmits torque from R to C.

Figure 53: Rotational friction block

- **Backlash block**: This block represents a double-sided mechanical rotational hard stop that restricts motion of a body between upper and lower bound. Both ports of the block are of mechanical rotational type. The impact interaction between the slider and the stops is assumed to be elastic. The stop is implemented as a spring that comes into contact with the slider as the gap is cleared. The spring opposes slider penetration into the stop with the torque linearly proportional to this penetration. To account for the energy dissipation and nonelastic effects, the damping is introduced as a block parameter, thus making it possible to account for energy loss.

The basic hard stop model, full stiffness and damping applied at bound, damped rebound, is described with the following equations:

$$T = \begin{cases} K_{\mathrm{p}} \cdot (\phi - g_{\mathrm{p}}) + D_{\mathrm{p}} \cdot \omega & for \quad \phi \geq g_{\mathrm{p}} \\ 0 & \\ K_{\mathrm{n}} \cdot (\phi - g_{\mathrm{n}}) + D_{\mathrm{n}} \cdot \omega & for \quad \phi \geq g_{\mathrm{n}} \end{cases}$$

$$\omega = \frac{d\phi}{dt}$$

,where T is the interaction torque between the slider and the case; g_{p} is the initial gap between the slider and upper bound; g_{n} is the initial gap between the slider and lower bound; ϕ is the slider angular position; K_{p} is the contact stiffness at upper bound; K_{n} is the contact stiffness at lower bound; D_{p} is the damping coefficient at upper bound; D_{p} is the damping coefficient at lower bound; ω is the slider angular velocity.

Figure 54: Backlash block

- **Rotational Spring block**: This block represents and ideal mechanical rotational linear spring which is described with the following equations:

$$T = K \cdot \phi$$

$$\phi = \phi_{\mathrm{init}} + \phi_{\mathrm{R}} - \phi_{\mathrm{C}}$$

$$\omega = \frac{d\phi}{dt}$$

, where T is the torque transmitted through the spring; K is the spring rate; ϕ is the relative displacement angle; ϕ_{init} is the spring preliminary winding or spring offset; ϕ_{R} and ϕ_{C} are the absolute angular displacements of terminals R and C.

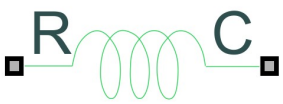

Figure 55: Rotational spring block

- **Translational Spring block**: This block represents an ideal mechanical linear spring, described with the following equations:

$$F = Kx$$

$$x = x_{\mathrm{init}} + x_{\mathrm{R}} - x_{\mathrm{C}}$$

$$v = \frac{dx}{dt}$$

, where F is the force transmitted through the spring; K is the spring rate; x is the relative displacement or spring deformation; x_{init} is the spring initial displacement which can be less than zero if the spring is streched or more than zero is the spring is compressed; x_{R} and x_{C} are the absolute displacements of terminals R and C; v is the relative velocity.

Figure 56: Translational spring block

- **Ideal force source**: This block represents an ideal source of mechanical energy that generates force proportional to the input physical signal. The source is ideal in a sense that it is assumed to be powerful enough to maintain specified force at its output regardeless of the velocity at source terminals.

  Connections R and C are mechanical translational conserving ports. Port S is a physical signal port, through which the control signal that drives the source is applied. You can use the entire variety of Simulink signal sources to generate the desired force variation profile. Positive signal at port S generates force acting from C to R. The force generated by the source is directly proportional to the signal at the control port S.

  The block positive direction is from port C to port R. This means that the force is positive if it acts in the direction from C to R. The relative velocity is determined as $v = v_C - v_R$, where v_R and v_C are the absolute velocities at ports R and C, respectively, and it is negative if velocity at port R is greater than that at port C. The power generated by the source is negative if the source delivers energy to port R.

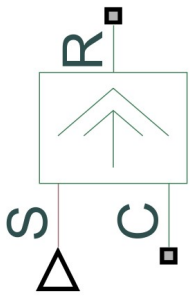

Figure 57: Ideal force source

- **Ideal Torque Source**: The ideal source block represents an ideal source of mechanical energy that generates torque proportional to the input physical signal. The source is ideal in a sense that it is assumed to be powerful enough to maintain specified torque regardless of the angular velocity at source terminals.

  Connections R and C are mechanical rotational conserving ports. Port S is a physical signal port, through which the control signal that drives the source is applied. You can use the entire variety of Simulink signal sources to generate the desired torque variation profile. Positive signal at port S generates torque acting from C to R. The torque generated by the source is directly proportional to the signal at the control port S.

  The block positive direction is from port C to port R. This means that the torque is positive if it acts in the direction from C to port R. This means that the torque is positive

if it acts in the direction from C to R. The relative velocity is determined as $\omega = \omega_C - \omega_R$ where ω_R and ω_C are the absolute angular velocities at ports R and C, respectively, and it is negative if velocity at port R is greater than that at port C. The power generated by the source is negative if the source delivers energy to port R.

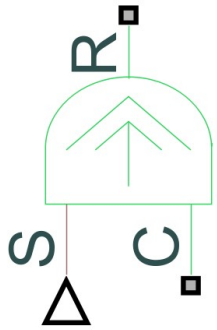

Figure 58: Ideal torque source

- **Ideal Translational Motion Sensor**: This block represents a device that converts an across variable measured between two mechanical translational nodes into a control signal proportional to velocity or position. You can specify the initial position (offset) as a block parameter.
  The sensor is ideal since it does not account for inertia, friction, delays, energy consumption, and so on.
  Connections R and C are mechanical translational conserving ports that connect the block to the nodes whose motion is being monitored. Connections V and P are physical signal output ports for velocity and position, respectively.
  The block positive direction is from port R to port C. This means that the velocity is measured as $v = v_R - v_C$.

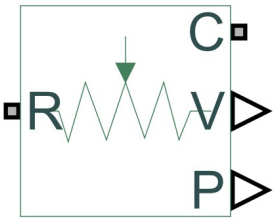

Figure 59: Ideal translational motion sensor block

- **Ideal Rotational Motion Sensor**: The ideal rotational motion sensor block represents an ideal mechanical rotational motion sensor, that is, a device that converts an across variable measured between two mechanical rotational nodes into a control signal proportional to angular velocity or angle. You can specify the initial angular position (offset) as a block parameter.

  The sensor is ideal since it does not account for inertia, friction, delays, energy consumption, and so on.
  Connections R and C are mechanical rotational conserving ports that connect the block

to the nodes whose motion is being monitored. Connections W and A are physical signal output ports for velocity and angular displacement, respectively.

The block positive direction is from port R to port C. This means that the velocity is measured as $\omega = \omega_R - \omega_C$.
The Wrap angle to [0, 2*pi] parameter lets you control the angular displacement output range. When set to On, it keeps angular displacement within the range from 0 to 2*pi radians, regardless of the number of revolutions performed by the object and the direction of rotation. When set to Off, the output range is unrestricted.

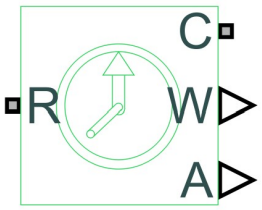

Figure 60: Ideal rotational motion sensor block

- **Gear Box**: The gear box block represents an ideal, nonplanetary, fixed gear ratio gear box. The gear ratio is determined as the ratio of the input shaft angular velocity to that of the output shaft. the gear box is described with the following equations:

$$\omega_S = N \cdot \omega_O$$

$$T_O = N \cdot T_S$$

$$P_S = \omega_S \cdot T_S$$

$$P_O = -\omega_O \cdot T_O$$

, where ω_S is the input shaft angular velocity; ω_O is the output shaft angular velocity; N is the gear ratio; T_S is the torque on the input shaft; T_O is the torque on the output shaft; P_S is the power on the input shaft; P_O is the power on the output shaft. The minus sign in computing P_O is because of the network rules that is the power flowing through a conserving port is positive if it is removed (dissipated) from the circuit, and is negative if the component generates power into the system.

Connection S and O are mechanical rotational conserving ports associated with the box input and output shaft, respectively. The block positive directions are from S to the reference point and from reference point to O.

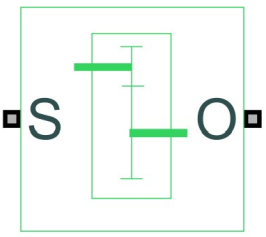

Figure 61: Gear box block

- **PS-Simulink Converter**: This block converts a physical signal into a Simulink output signal. It is used to connect outputs of a Simscape physical network to Simulink scopes or other Simulink blocks.

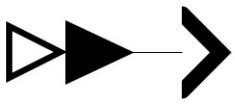

Figure 62: PS-Simulink converter block

- **Simulink-PS Converter**: This block converts the Simulink input signal into a physical signal. It is used to connect Simulink sources or other Simulink blocks to the input of a Simscape physical network.

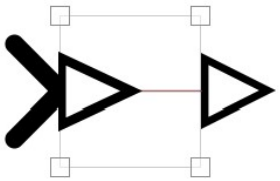

Figure 63: Simulink-PS converter block

- **Solver Configuration**: Each physical network represented by a connected Simscape block diagram requires solver settings information for simulation. The Solver configuration block specifies the solver parameters that your model needs before you can begine simulation. Each topologically distinct Simscape block diagram requires exactly one Solver Configuration block to be connected to it.

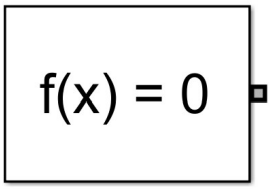

Figure 64: Solver configuration block

5.1 Linear MCK model: Simulink vs Simscape

The mass-spring-damper is the simplest second order mechanical system. Any mechanical vibrational system can be modeled using a MCK.
The system is made of a mass (M) which can move on an horizontal, frictionless plane. This mass is subject to an external force (F), to the elastic force (K) of the spring and to the damped force (C) of the viscous damper.

To model this system in Simulink it is necessary to first define the mathematical model. This is, initially, made of a differential equation which can be tranformed in an algebric equation using the Laplace transform. This can be made given that this is a linear system.

Therfore, there are two ways of modelling this system using the Simulink blocks: the first way consist of using the second order differential equation and highlighting the highest order term and then arrange the blocks in order to recreate the equation;

$$M \cdot \ddot{x} + C \cdot \dot{x} + K \cdot x = F$$

$$\ddot{x} = \frac{F - C \cdot \dot{x} - K \cdot x}{M}$$

The second way consist in using the Laplace transform which introduces the complex variable s. In this case the dynamic characteristic of the system can be represented through a tranfer function G(s).

$$M \cdot s^2 \cdot \overline{x} + C \cdot s \cdot \overline{x} + K \cdot \overline{x} = \overline{F}$$

$$G(s) = \frac{\overline{x}}{\overline{F}} = \frac{1}{M \cdot s^2 + C \cdot s + K}$$

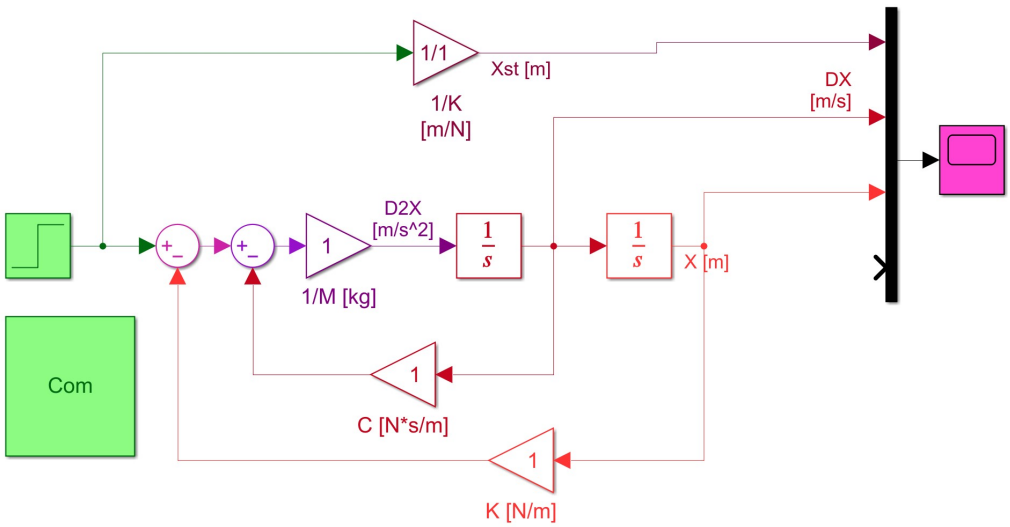

Figure 65: MCK modelled with Simulink

On the other hand, when using Simscape the MCK system is modelled using a physical approach. The input force is the same used for the Simulink model. It can be seen that this type of modelling seems much more simple and intuitive.

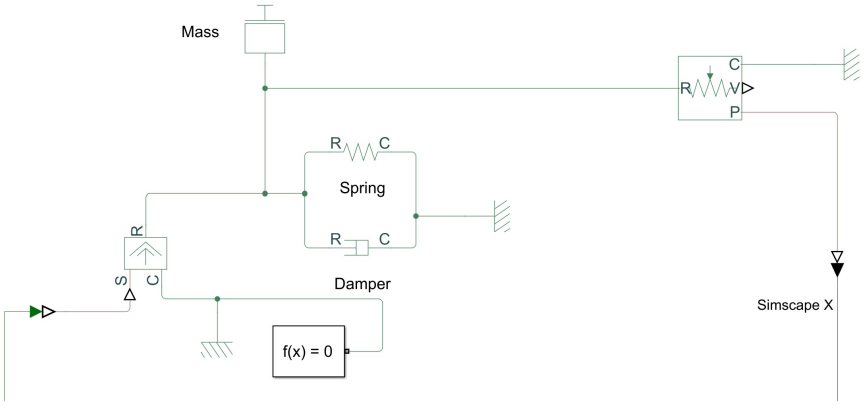

Figure 66: MCK modelled with Simulink

It can be seen from the figure below that the position and velocity of the two models are the same, thus the dynamic behaviour is described in the same way. The trend of the position starts with an horizontal tangent: this is typical of a mechanical system. After this the position curve rapidly reaches the commanded position and overshoots it. Then it stabilizes after a number of oscillation which depend on the mass, damp coefficient and stiffness of the system.

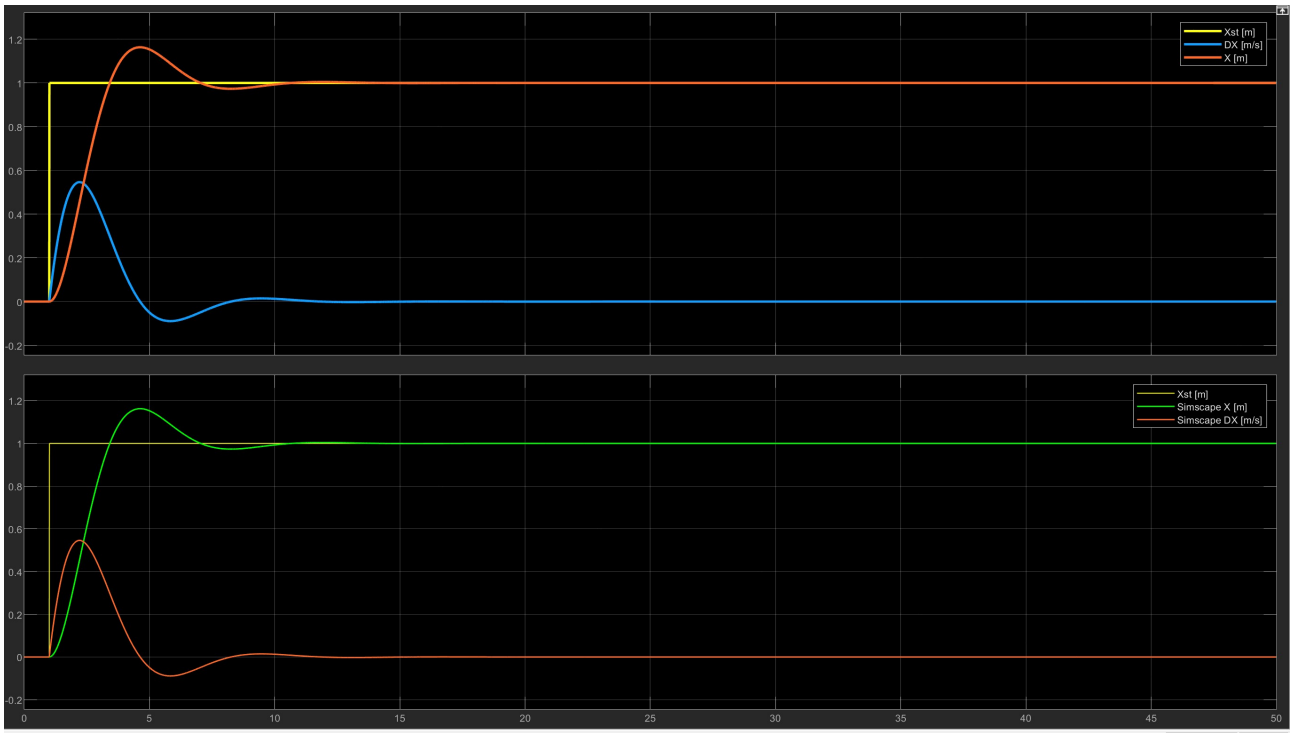

Figure 67: Simulink vs Simscape results

5.2 2 DOF Harmonic Oscillator model: Simulink vs Simscape

The harmonic oscillator is made of two masses which are connected by an ideal stifness spring (k_{R}) and by an ideal viscous damper (c_{R}), which generate a force that is proportional to the relative movement (x-y) and relative speed ($\dot{x} - \dot{y}$) of the two masses. The first mass is subject to the driving force (F_{M}) while the second mass is subject to an external force (F_{R}). The entire system is subject to an absolute damper (c_{A}).

This system can be a simple rapresentation of a compliant coupled mechanical actuation. The compliance is between the actuator and the moving element. For example this can be seen as an hydraulic actuator linked to a movable flight surface through a non infinite stifness rod.

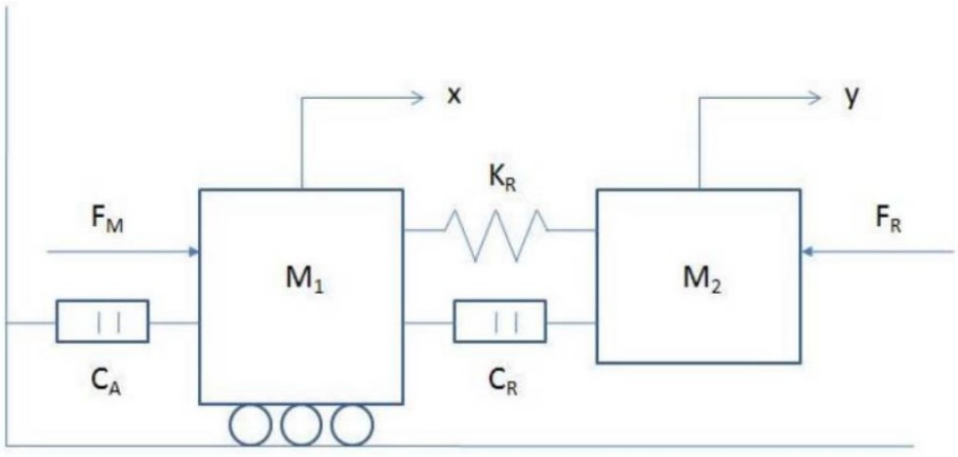

Figure 68: 2-DOF Harmonic Oscillator

The system dynamic response is described by the 2 position d.o.f x and y which are the gravity center of the first mass and the second mass respectively. The driving force is proportional to the error between the comanded position and the controlled variable y through a gain G_{M}. The equations that describe the system dynamics are the following:

$$F_{\mathrm{M}} = G_{\mathrm{M}} \cdot (cmd - y)$$

$$M_1 \cdot \ddot{x} = F_{\mathrm{M}} - c_{\mathrm{A}} \cdot \dot{x} - k_{\mathrm{R}} \cdot (x - y) - c_{\mathrm{R}} \cdot (\dot{x} - \dot{y})$$

$$M_2 \cdot \ddot{y} = -F_{\mathrm{R}} + k_{\mathrm{R}} \cdot (x - y) + c_{\mathrm{R}} \cdot (\dot{x} - \dot{y})$$

The reaction force (F_{R}) has a different behaviour on the two masses: it behaves as a driving force for M_2 and as a resistance force for M_1.

Below it can be seen the 2 DOF harmonic oscillator modelled using the block approach (lower part) and the physical approach through Simscape blocks. As shown for the MCK model, it can be seen that the Simscape model is much more simple and more intuitive than the Simulink block approach.

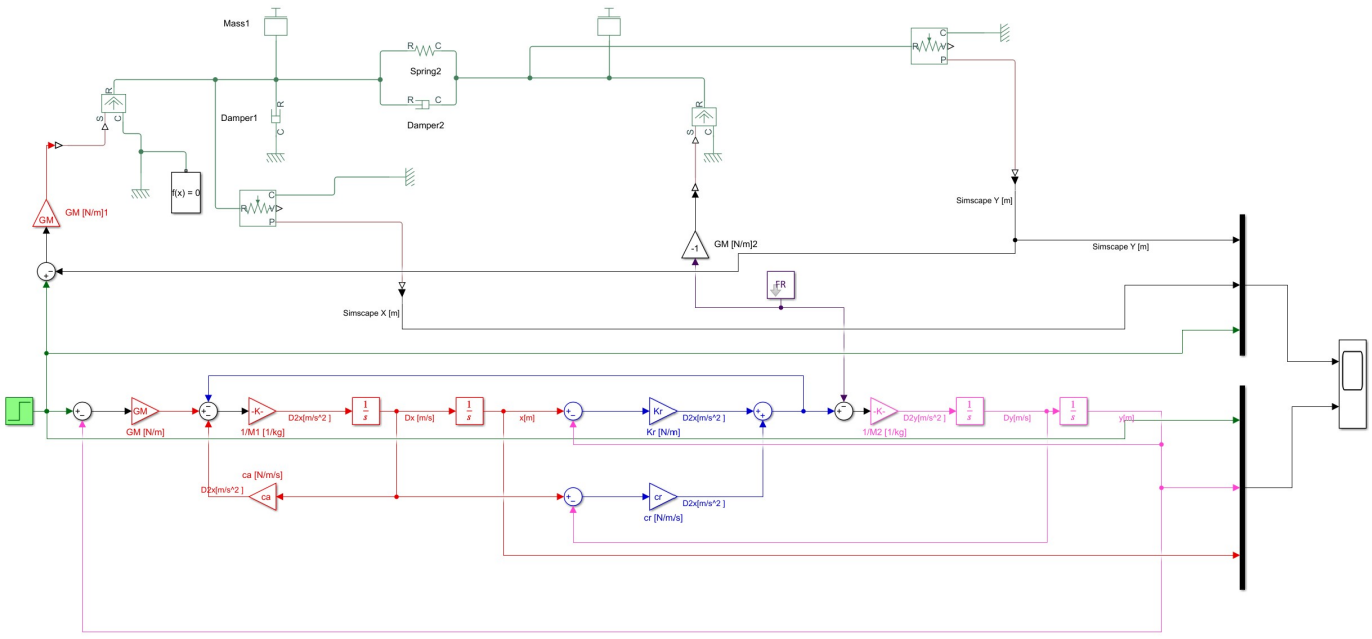

Figure 69: Harmonic Oscillator Simscape vs Simulink

Initially, mass M1 is the first to move because the driving force is directly applied to it. After this the the spring k_{R} is compressed and consequently the mass M2 starts moving. As for the MCK system the two masses start with an horizontal tangent, then overshoot the comanded position stabilizing after a number of oscillations.

After 3 seconds the external force is applied and this time the mass M2 moves before the mass M1 since this force is directly applied on M2. Since in this case a proportional controller is used the static error is not zero: this is done in because an error not equal to zero is necessary to comand the driving force necessary to balance the external force.

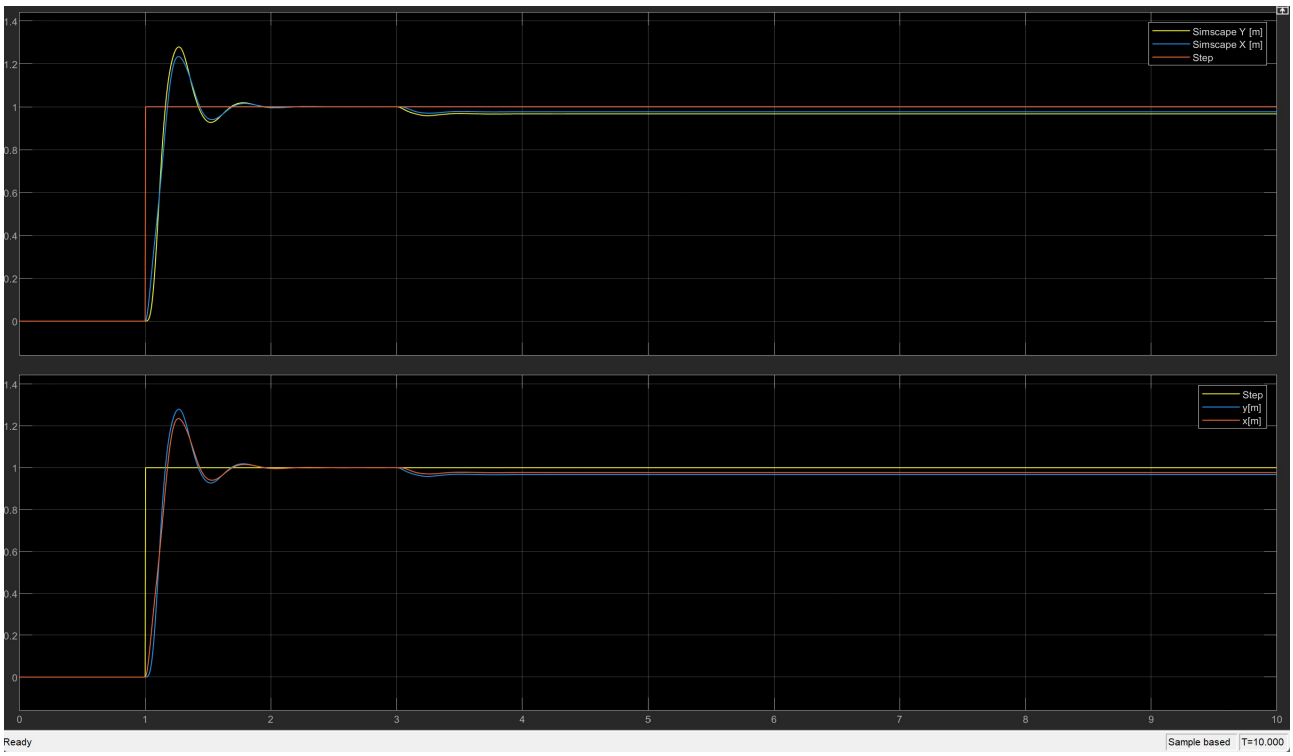

Figure 70: Harmonic Oscillator Simscape vs Simulink

As it can be seen from the figure above, the two models exhibit the same dynamic behaviour meaning that the simscape model can be used to model more complex systems.

6 Friction models: Simulink vs Simscape

In order to correctly model the mechanical part of the actuator, all the non linearities must be taken in account. Firstly, it must be assessed if the friction models used in the Simulink model behaves in the same way as the friction models used in the Simscape environment.

The follwoing MCK model is used to compare the Borello friction model to the Simscape friction model:

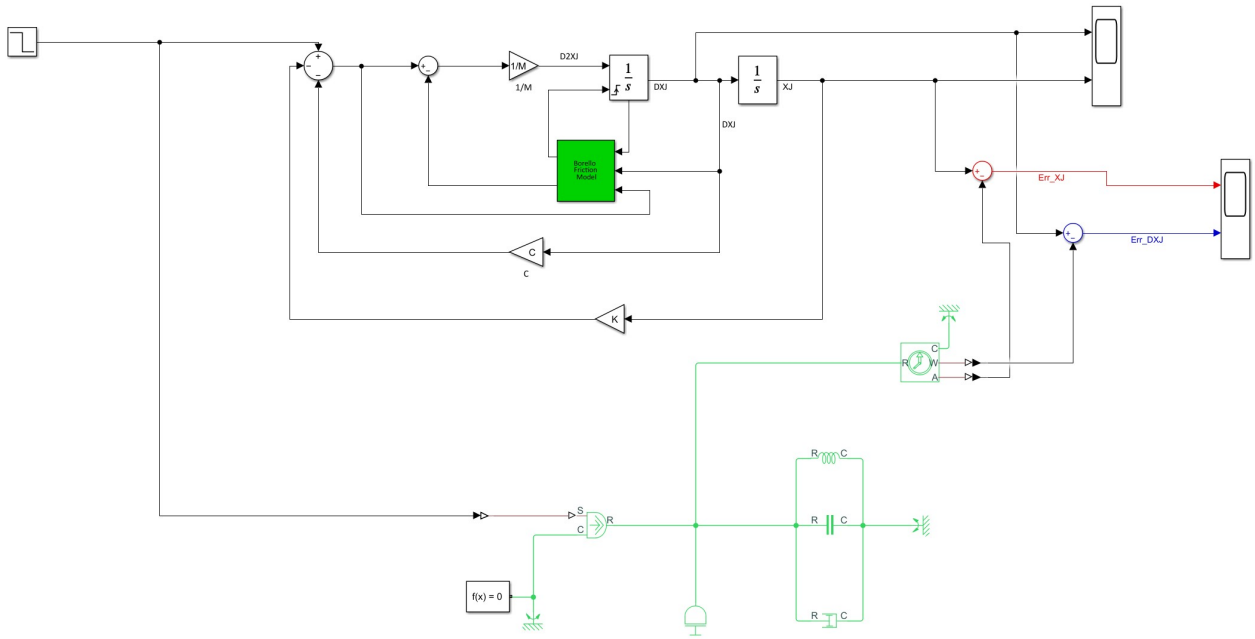

Figure 71: MCK with Borello friction model

with the following Borello friction model which has already been described in section 3.3.5 :

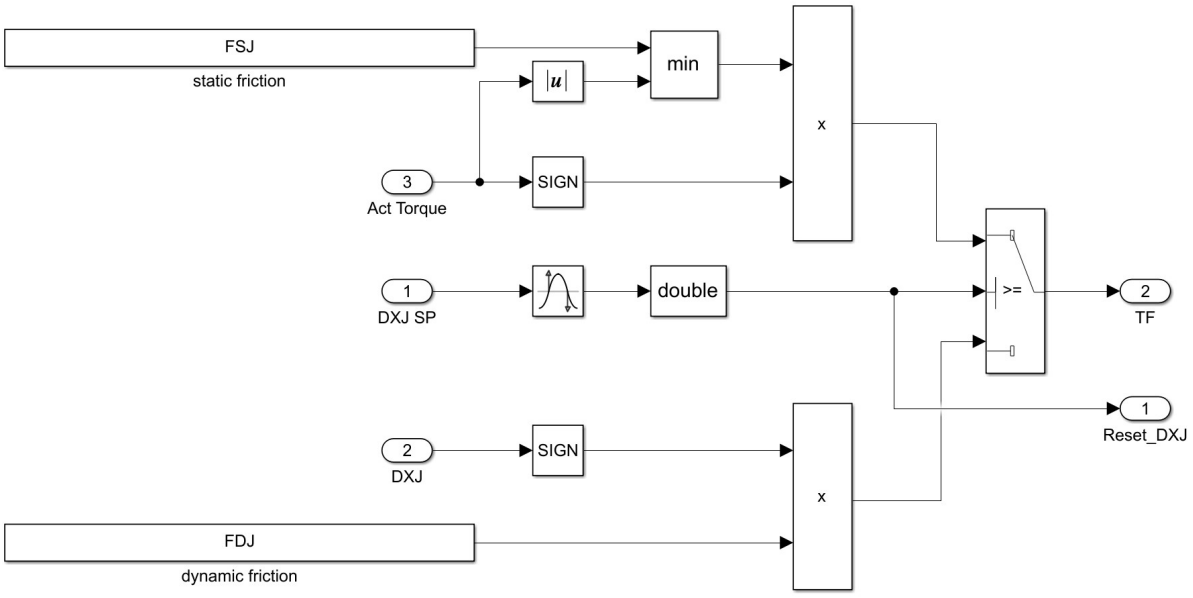

Figure 72: Borello friction model

Two data types were used in order to correctly find the **Breakaway friction velocity**:

- Initially, the following data was used:

Mass	M = 1 Kg
Damper	C = 1 Nm/rad s
Spring	K = 10 Nm/rad
Initial position	X0 = 0
Initial Rotational Torque value	F0 = 10 Nm
Final Rotational Torque value	F1 = -10 Nm
Step Time	Ts = 10 s
Simulation Time	T = 20 s
Static Friction Rotational Force	FSJ = 0.5 Nm
Dynamic Friction Rotational Force	FDJ = 0.25 Nm

With this data the value of Breakaway friction velocity which ensures the minimum error between the Borello friction model and the Simscape friction model is **0.00001201 rad/s**.

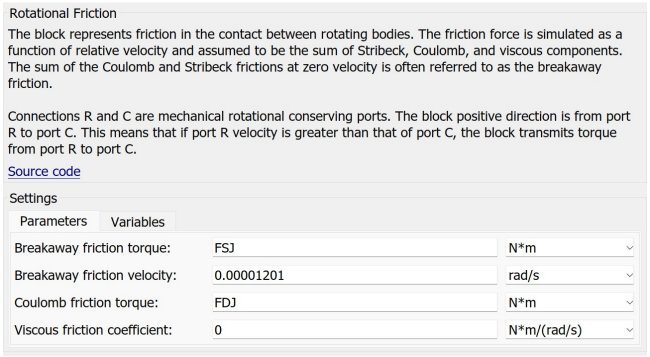

Figure 73: Breakaway friction velocity

It can be seen from the following figures that the error of position and velocity between the Simulink and Simscape model is of an order of magnitude of 10^{-5}.

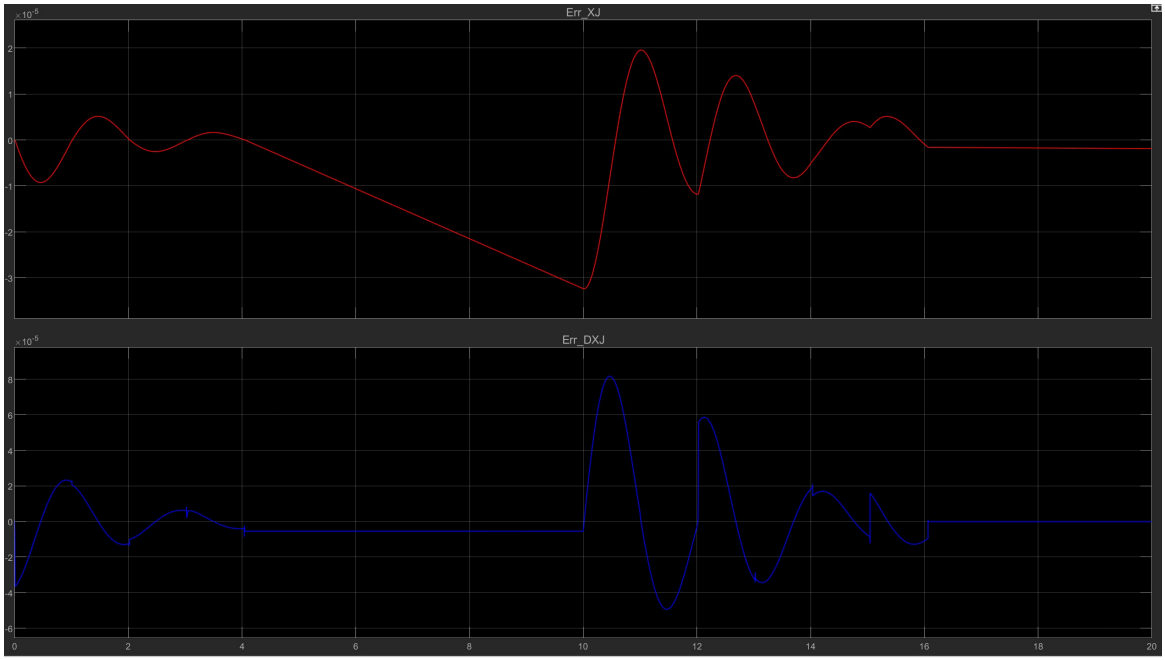

Figure 74: Order of magnitude of the error

- Secondly, the same model with the following data which are those of the motor plus user have been used to identify the optimal Breakaway friction velocity:

Mass	Jm + JU = 2.5e-5 Kg m2
Damper	CM + CU = 1.8563 Nms/rad
Spring	K = 0.01 Nm/rad
Initial position	X0 = 0
Initial Rotational Torque value	F0 = 0.17 Nm
Final Rotational Torque value	F1 = -0.17 Nm
Step Time	Ts = 10 s
Simulation Time	T = 20 s
Static Friction Rotational Force	(FSJM + FSJU)*TMM = 0.1689 Nm
Dynamic Friction Rotational Force	(FDJM + FDJU)*TMM = 0.08445 Nm

Like before, after a number of tests that were necessary in order to obtain the correct Torque value and the stiffness coefficiente of the system, the same optimal value of the Breakaway friction velocity which ensures the smallest error was achieved.

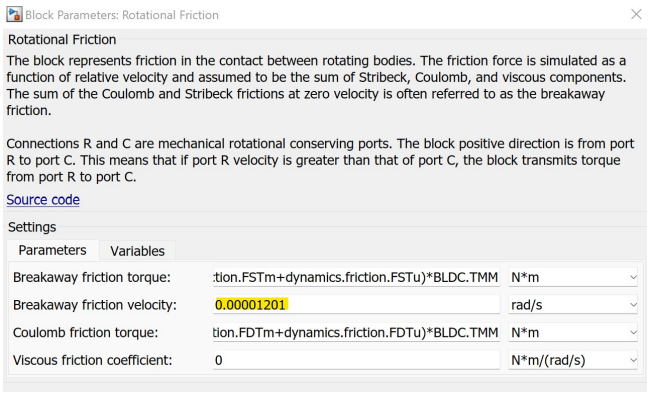

Figure 75: Breakaway friction velocity

This time the error's order of magnitude is between 10^{-5} and 10^{-4}.

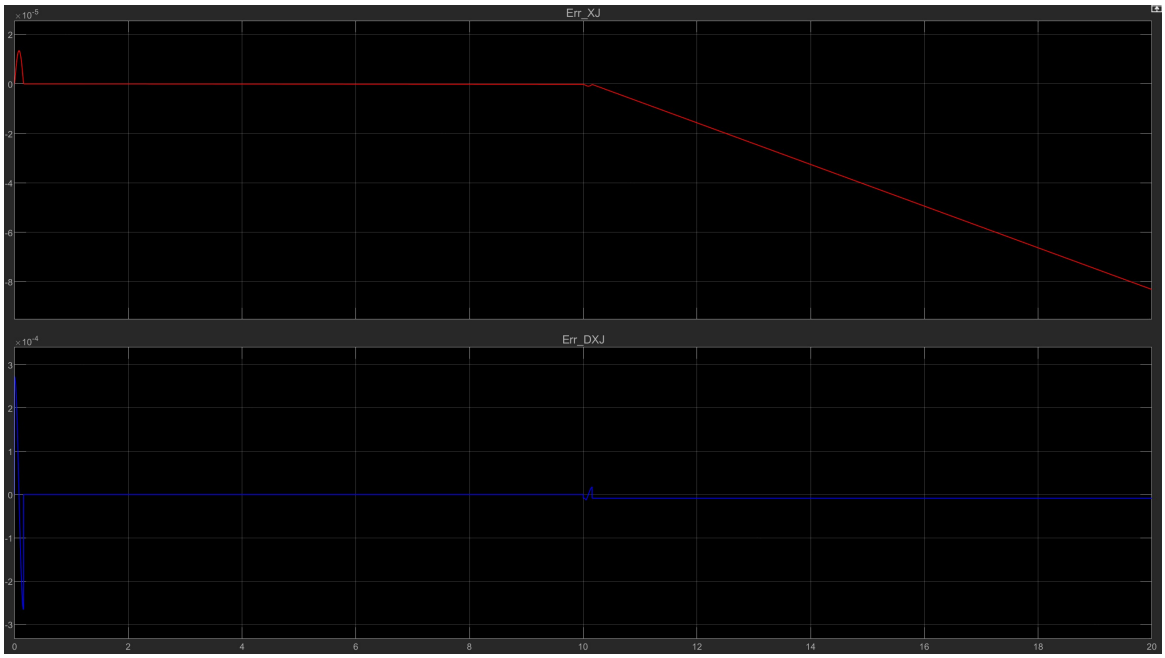

Figure 76: Order of magnitude of the error

Next, the **Hyperviscous saturated friction model** is used on the same MCK system in order to check if the Breakaway friction velocity that was prieviously found can be also used for this model. Two models with the motor and user data are implemented.

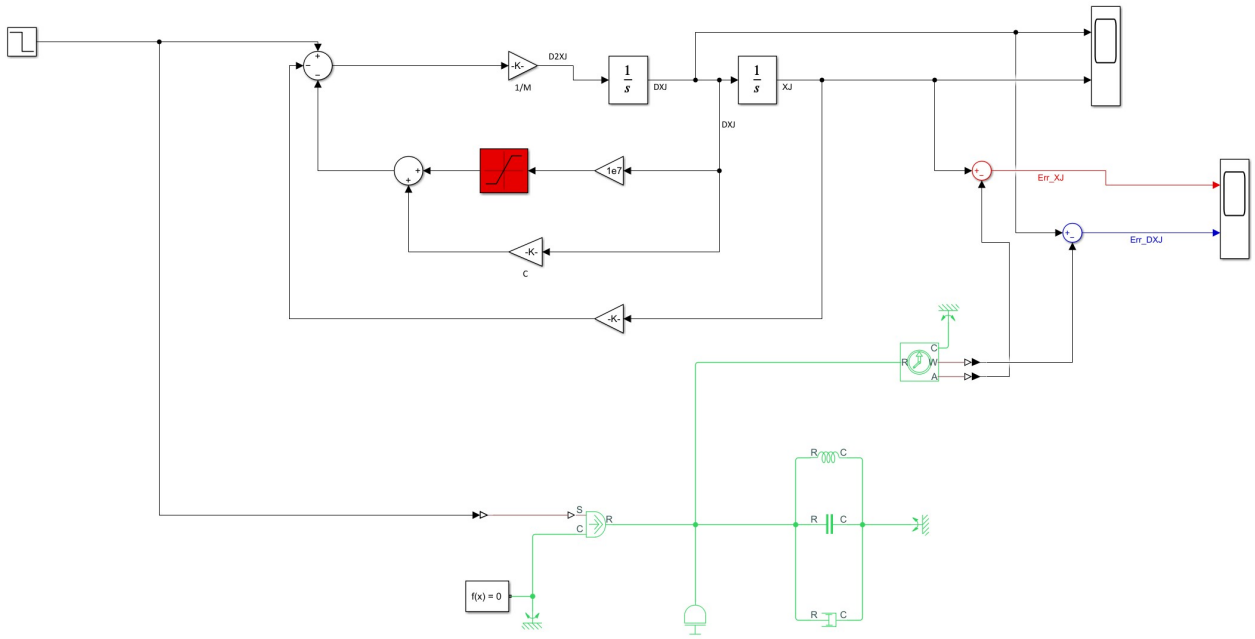

Figure 77: Motor and user Hyperviscous Saturated model

The Hyperviscous saturated friction model is obtained from the Coulombian model by eliminatind the discontinuity in the origin, for null values of the realitive speed v, and aproximating the evolution through a hyperviscous saturated friction model, that is through a viscous coefficient which must be as high as possible but also be compatible with the satibility of the calculation process.

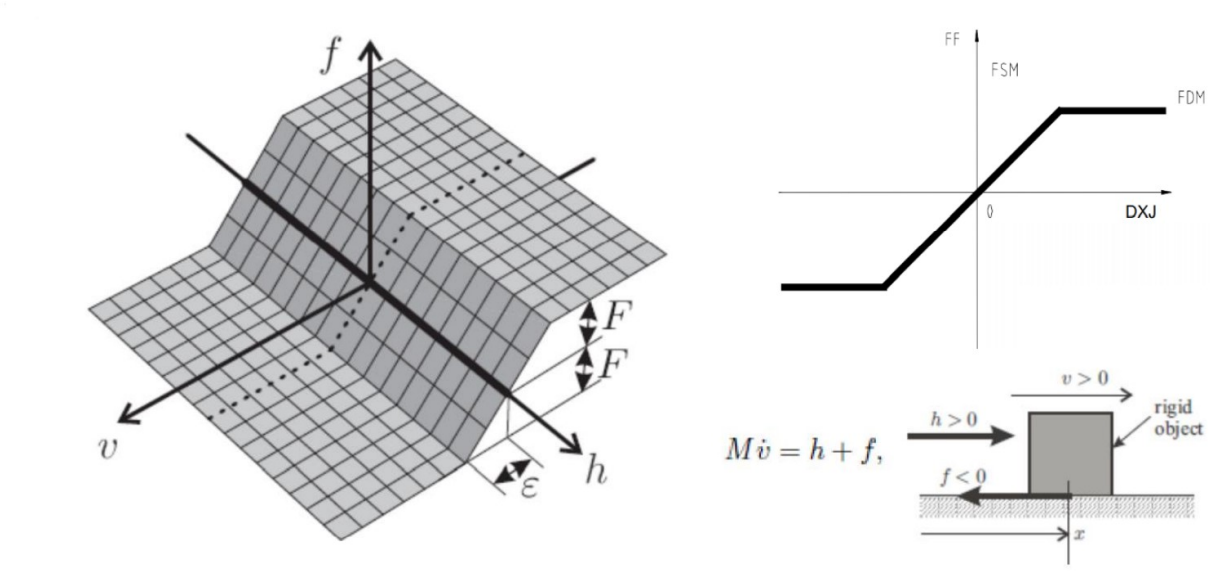

Figure 78: Saturated Hyperviscous friction graphic representation

This way in a limited gap of half amplitude ϵ around the origin of the velocity axis a linearization is accomplished. This linearization, which links the friction force whit the velocity, allows for the removal of the discontinuity. The performance of this model are completely different from those of the Coulombian friction model, in fact, for null velocity, the friction force is also null which means it can't oppose even the smallest external load. This means that the system will move even if a small external force (smaller than the Coulombian friction term) is applied.

This model takes into account the sign of the friction force relative to the speed direction but is unable to correctly differentiate between static and dynamic condition, it is unable to evaluate the halt and maintaing the halt when and external load is applied. It is also unable to evaluate the departure of a still object. The friction force f is obtained in the following manner:

$$f = \begin{cases} F \cdot v/\epsilon \quad if \quad |v| \leq \epsilon \\ sign(v) \cdot F \quad if \quad |v| > \epsilon \end{cases}$$

, where f is the Coulombian friction force, F is the dynamic Coulombian friction force, v is the relative velocity between surfaces and ϵ is the value of v for which f is satured and equal to F.

The following data was used for the motor system:

Mass	Jm = 130e-7 Kg m2
Damper	CM = 9.6e-6 Nms/rad
Spring	K = 0.001 Nm/rad
Initial position	X0 = 0
Initial Rotational Torque value	F0 = 0.07 Nm
Final Rotational Torque value	F1 = -0.07 Nm
Step Time	Ts = 10 s
Simulation Time	T = 20 s
Dynamic Friction Rotational Force	FDTm *TMM = 0.05067 Nm

The value for the Spring stiffness and the Torque value were chosen in such a way that would allow to have a small error. Values of K and F bigger than that would produce error in order of magnitude of 10^4.

As before, the same value Breakaway friction velocity allows for the minimization of the position and speed error between Simulink and Simscape envrionment:

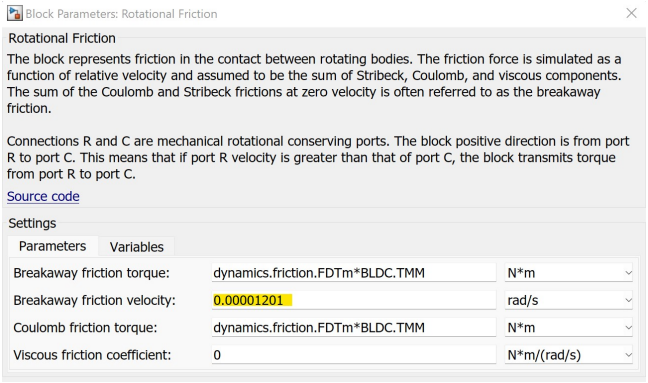

Figure 79: Breakaway friction velocity

This time the order of magnitude of the error is not as small as for the Borello friction model. It is of 10^{-3} for the position and 10^{-2} for the speed, as it can be seen from the figure below.

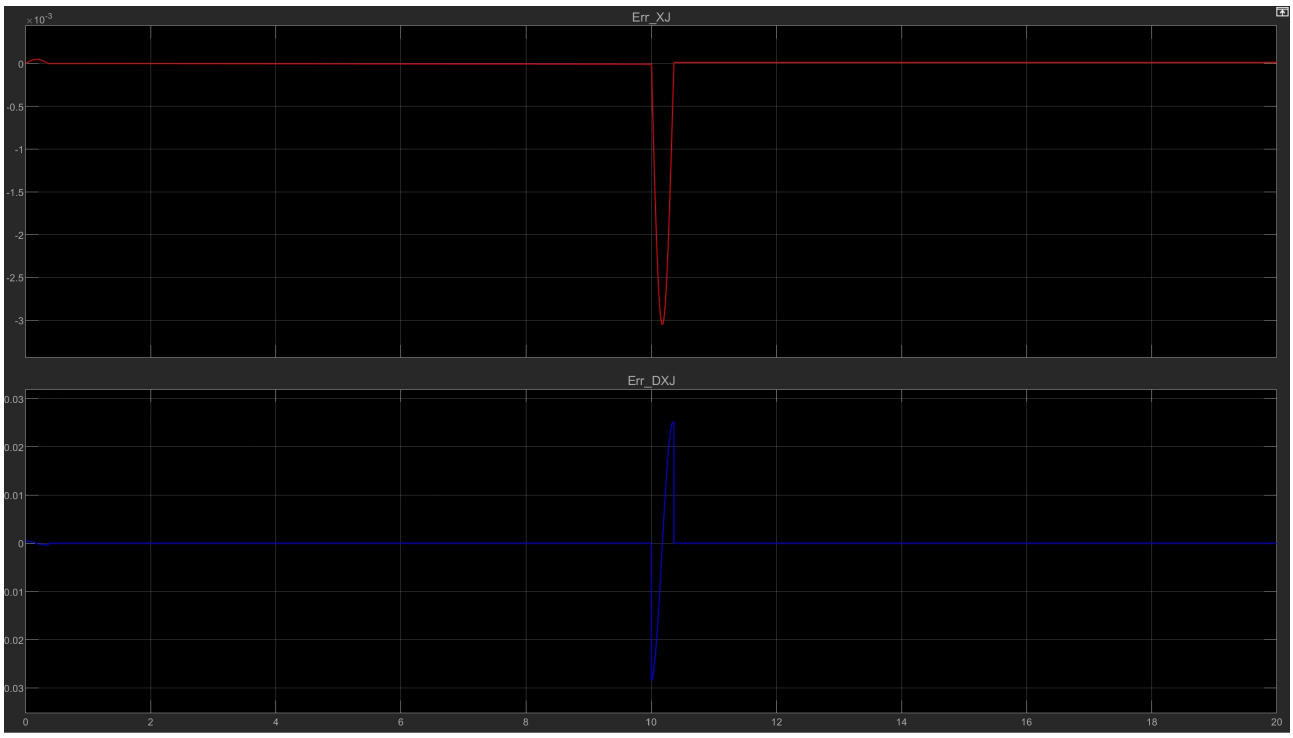

Figure 80: Motor Errors

Now, the data of the user system are going to be used in order to confirm if the value of the Breakaway friction velocity found prieviously can be used for the user:

Mass	Ju = 12e-6 Kg m2
Damper	Cu = 4.507e-6 Nms/rad
Spring	K = 0.001 Nm/rad
Initial position	X0 = 0
Initial Rotational Torque value	F0 = 0.04 Nm
Final Rotational Torque value	F1 = -0.04 Nm
Step Time	Ts = 10 s
Simulation Time	T = 20 s
Dynamic Friction Rotational Force	FDTu *TMM = 0.03378 Nm

As for the motor, the same Breakaway friction velocity has allowed for the minimization of the error between Simulink and Simscape environment. This time a Rotational Torque of 0.04 Nm allowed for an error of 10^{-4} for the position and and error of 10^{-2} for the velocity.

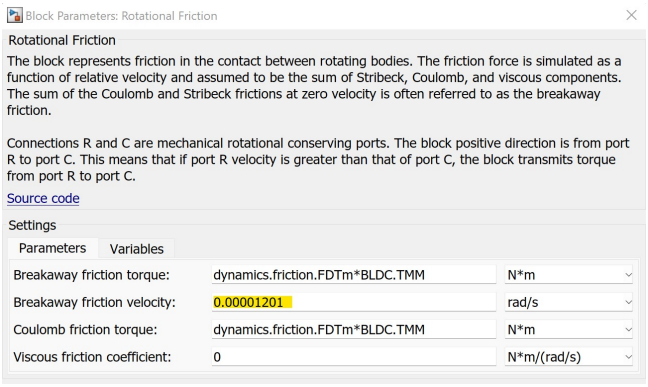

Figure 81: Breakaway friction velocity

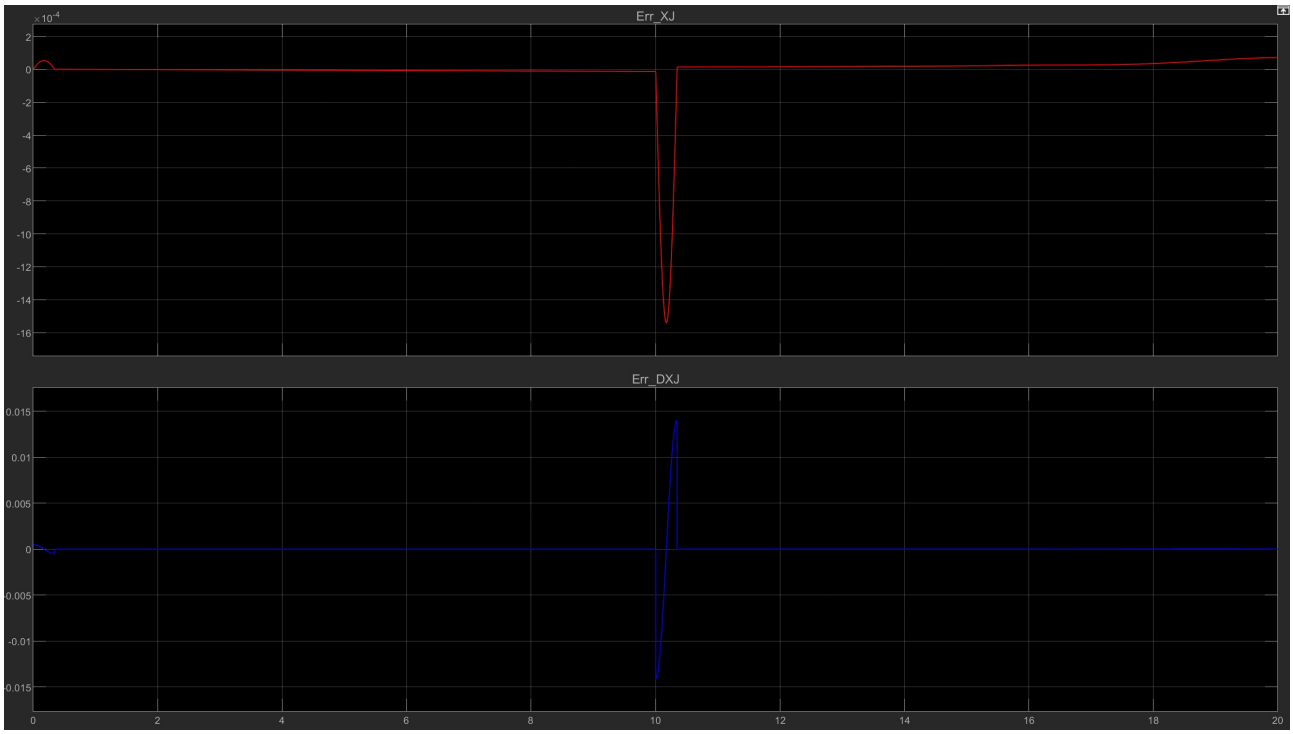

Figure 82: User Errors

7 Backlash: Simscape vs Simulink model

After it was assessed that the Simscape and Simulink friction model behave almost in the same way, the next non linearity which must be introduced is the backlash that is present between the driving gear of the motor and the driven gear of the user. To do this the following 2 D.O.F model was implemented which consists of:

- **The Motor:** it is modelled through a rotational damper, a rotational inertia and a rotational friction;
- **The Mechanical linkage:** this part is modelled through the simple gear, a rotational damper and rotational spring;
- **The User:** like the motor, the user is modelled through a rotational damper, rotational inertia and a rotational friction;

7.1 Only input model

The backlash is introduced through the Simscape Rotational Hard Stop block and is positioned right before the rotational gears. Initially the model included only the input torque as it can be seen from the figure below.

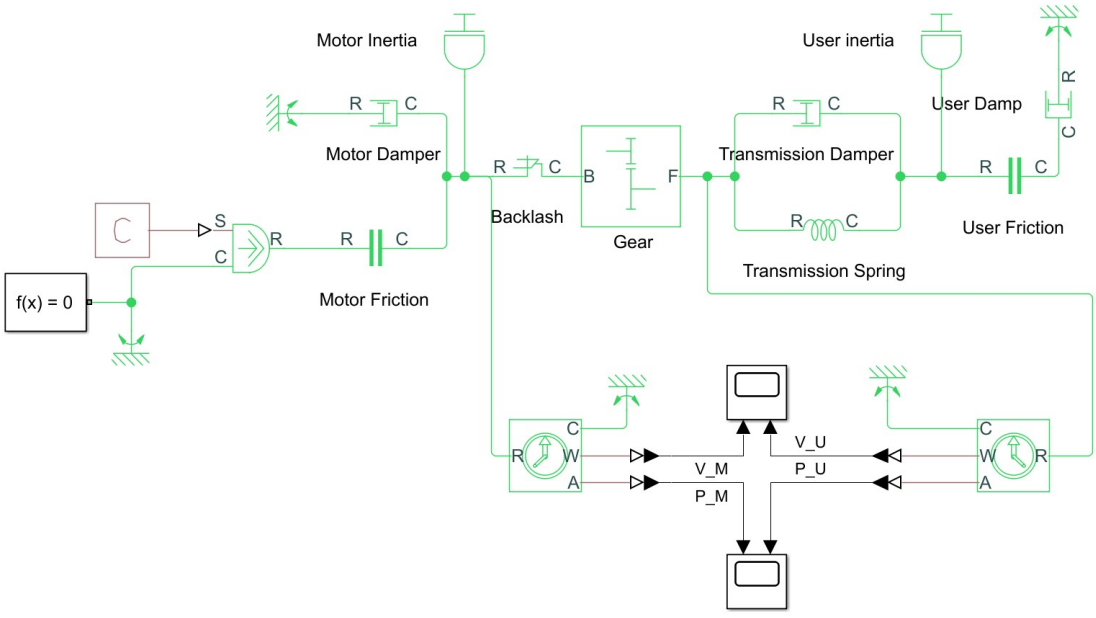

Figure 83: Only input torque mechanical model

The values that are used for the motor and user model are those of the High Fidelity BLDC model.
The first problem arised with the value of the input torque. Initially a torque of magnitude

between 10^0 and 10^1 was used, but the simulation wouldn't converge due to the Motor Rotational Friction block. After this, several decreasing input torque values were tried in order to obtain a solution that has a physical sense. The first value of torque that allowed for reasonable results is of **0.0004 Nm**. This is probably due to the very low inertia of the motor and user and also for the very small value of motor and user damper.
These two last values have caused another problem with the results. The High Fidelity values of 9.54e-6 for the motor damper and of 4.507e-7 for the user damper were leading to meaningless results. So, they were substituted with the same order of magnitude values of 1e-6 for the motor and 1e-7 for the user. No viscosity was considered inside the friction model of the system. Finally, the following values were used:

Motor Mass	Jm = 130e-7 Kg m2
Motor Damper	Cm = 1e-6 Nms/rad
User Mass	Ju = 12e-6 Kg m2
User Damper	Cu = 1e-7 Nms/rad
Transmission Damper	Ct = 5e4 Nms/rad
Transmission Spring	Kt = 0.001 Nm/rad
Rotational Torque value	F0 = 0.0004 Nm
Teeth Ratio	500
Backlash	±1 deg
Motor Dynamic Friction Rotational Force	FDTm *TMM = 0.05067 Nm
Motor Static Friction Rotational Force	FSTm *TMM = 0.1013 Nm
User Dynamic Friction Rotational Force	FDTu *TMM = 0.0338 Nm
User Static Friction Rotational Force	FSTu *TMM = 0.0676 Nm
Motor and User Breakaway Friction velocity	0.00001201
Simulation Time	T = 2 s

The motor and user position and velocity results can be seen in the following diagrams:

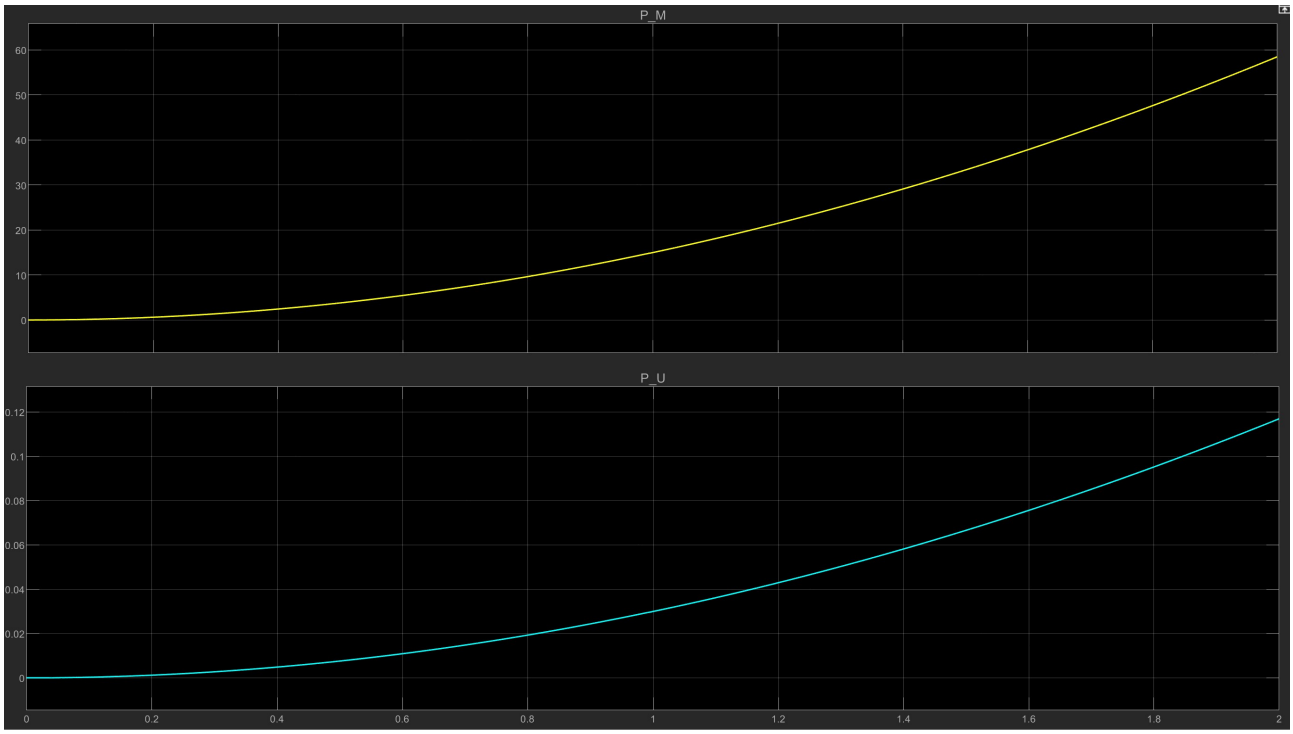

Figure 84: Motor Position (Upper) and User Position (Lower)

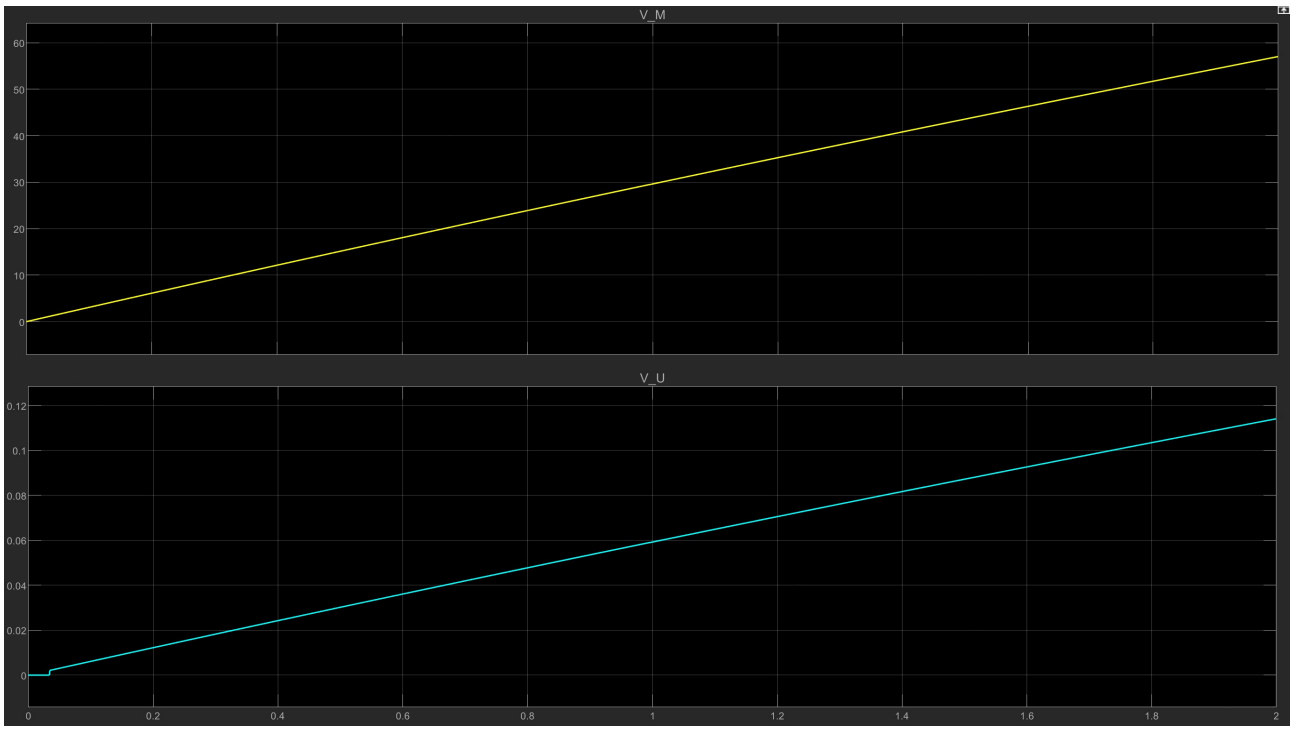

Figure 85: Motor Velocity (Upper) and User Velocity (Lower)

It can be seen from the position and velocity diagrams that initially the motor begins to move and after this the user position varies consistently with the gear transmission ratio and with the motor and user inertia.

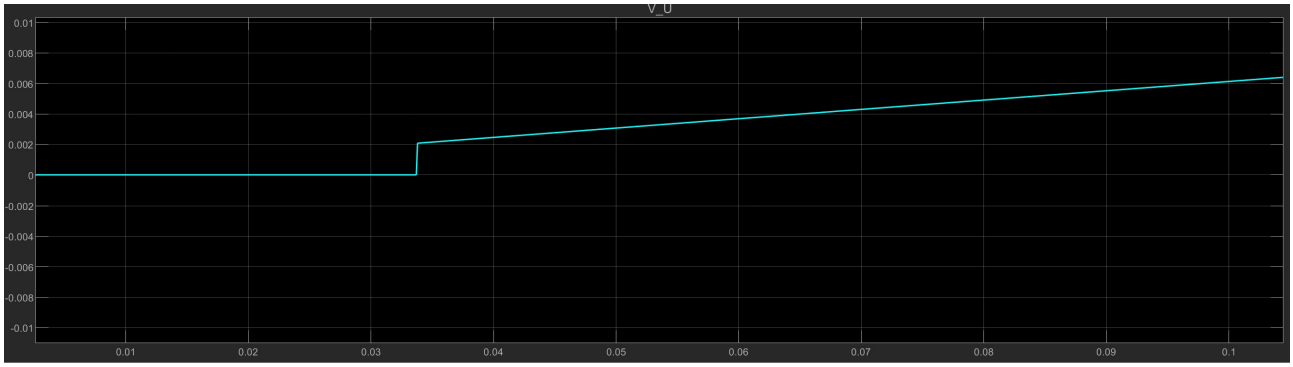

Figure 86: Backlash phenomenon (Velocity)

From fig 86 the backlash phenomenon can be seen from the velocity perspective. From 0 to 0.034 seconds the user velocity doesn't vary and at 0.034 it varies istantaneously from 0 to 0.002 m/s. This is owed to the fact that the backlash introduces a space between the teeth of the gear that must be overcome in order for the user to start moving.

The same thing can also be seen from the position perspective. Altough the motor position is already varying, it can be seen that aproximately until 0.034 s the user position is null. After this the user starts moving according to the it's inertia and the gear transmission ratio.

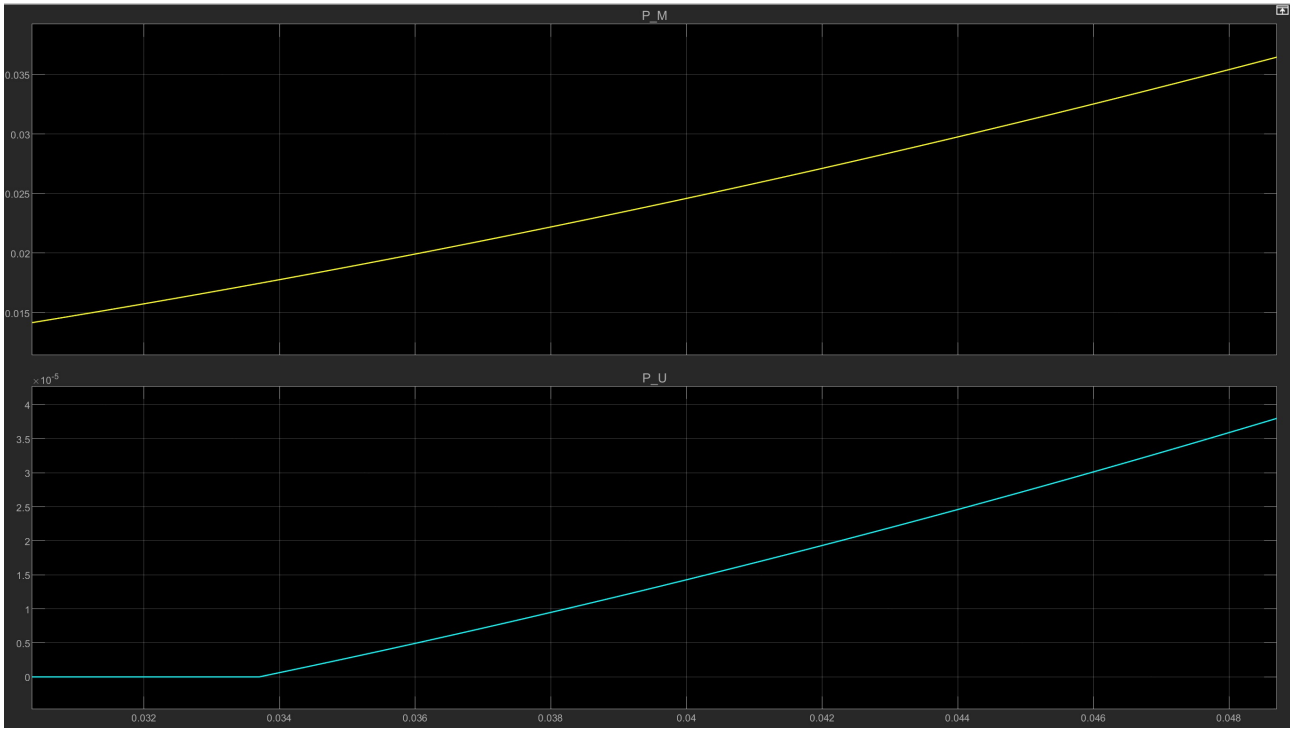

Figure 87: Backlash phenomenon (Position)

Next, the same system was modelled through the Simscape blocks in order to compare it to the Simscape model. The following model was obtained:

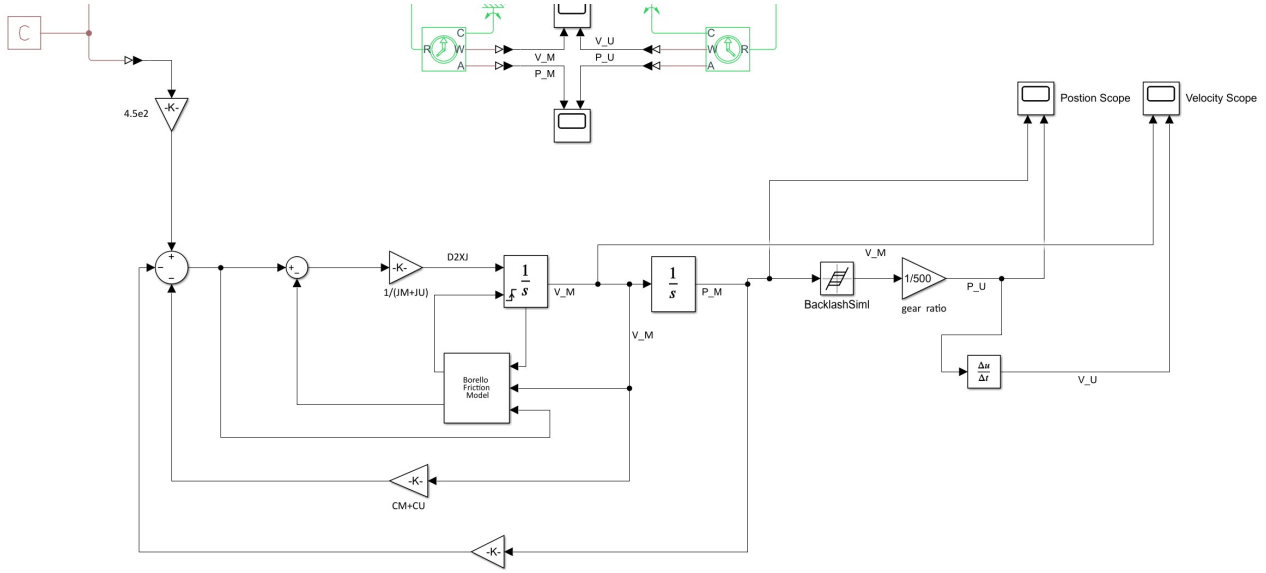

Figure 88: Simulink Backlash model

A few remarks must be made before analising the position and velocity results. As said before, a torque input of 4e-4 was used in order to be able for the Simscape model to work. This input resulted too small for the Simulink model as it produced a null result that is the model is insensitive to the input.

The first value of input that allowed for non null results wa achieved by using a gain of 4.5e2. So an input torque of 0.18 Nm was used for the Simulink model. This difference of system sensitivity to the input may be attributed to the fact that the Simulink model has an inertia and a damping coefficient which is the sum of both motor and user inertia and damping coefficient, while the Simscape model considers each part as a separated component with it's own inertia and damping coefficient.

The following input data was used for the Simulink model:

Mass	Jm + Ju = 2.255e-5 Kg m2
Damper	Cm + Cu = 1.651e-6 Nms/rad
Spring	K = 0.001 Nm/rad
Initial position	X0 = 0
Rotational Torque value	F0 = 0.18 Nm
Teeth Ratio	500
Backlash	±1 deg
Static Friction Rotational Force	(FSJM + FSJU)*TMM = 0.1689 Nm
Dynamic Friction Rotational Force	(FDJM + FDJU)*TMM = 0.08445 Nm
Simulation Time	T = 2 s

The following results were obtained from the Simulink model:

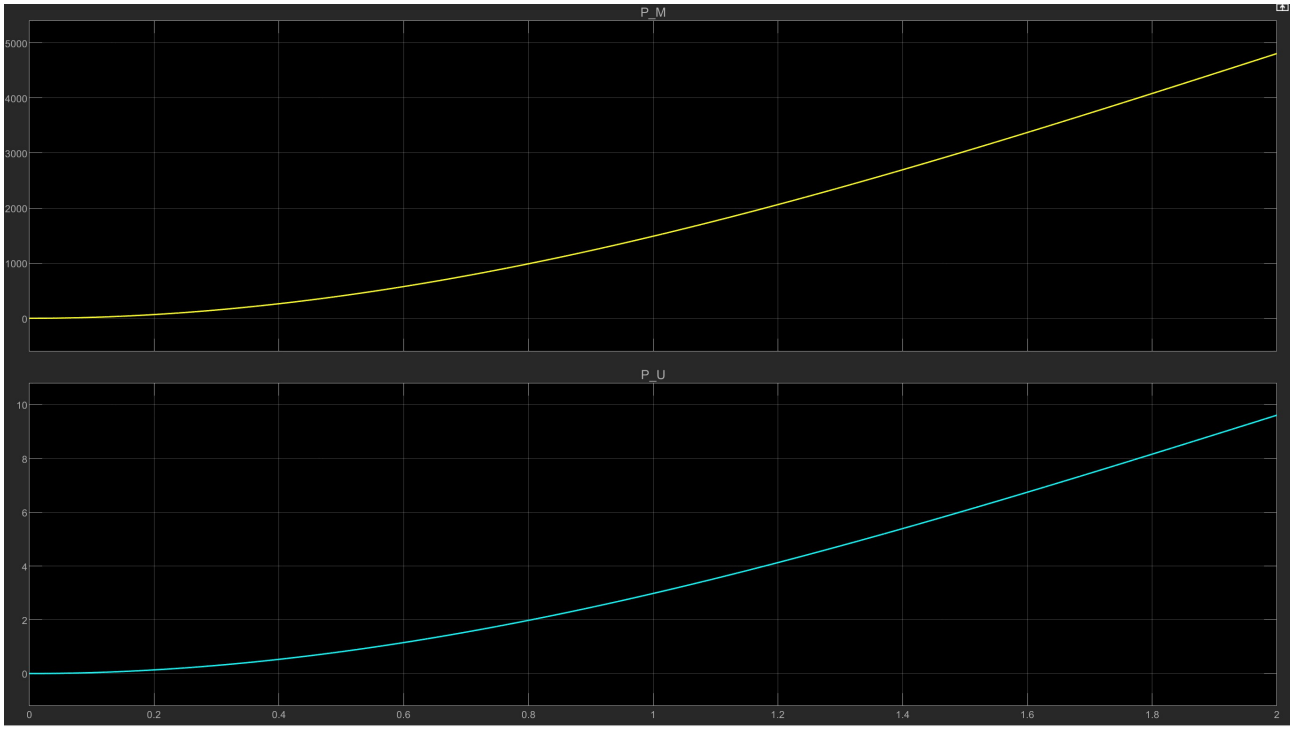

Figure 89: Simulink Backlash model: Position results

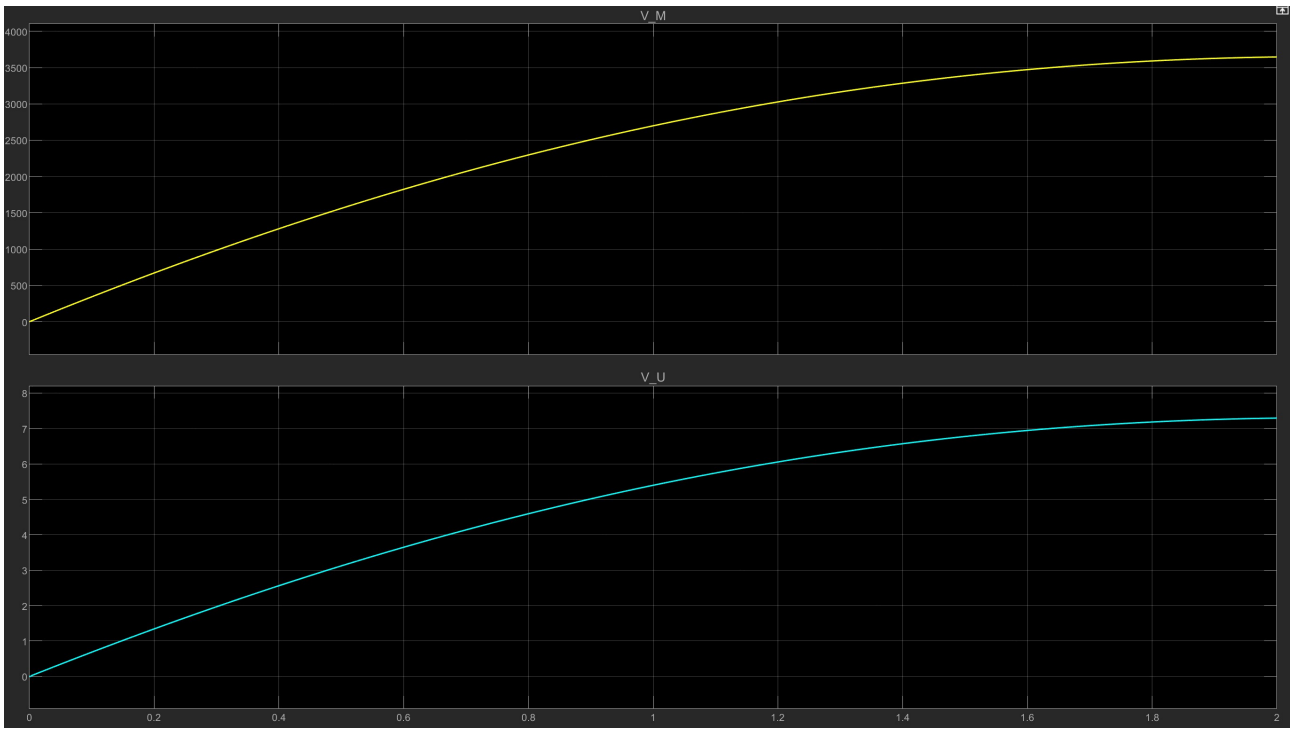

Figure 90: Simulink Backlash model: Velocity results

It can be seen that the trends of Position and Velocity are consistent with those obtained from the Simscape model. A significant difference is the difference in the scale of the diagrams: the Simulink results are 2 to 3 orders of magnitude higher than those of the Simscape results. This is also due to the difference in inertia, damping coefficient and consequently the input torque. Nevertheless, the concavity of the curves and the motor to user ratio values are consistent with the Simscape results.

At first glance it may seem that no backlash is acting on the user, but if we zoom in near on the user velocity diagram, it can be seen that indeed the backlash phenomen is present:

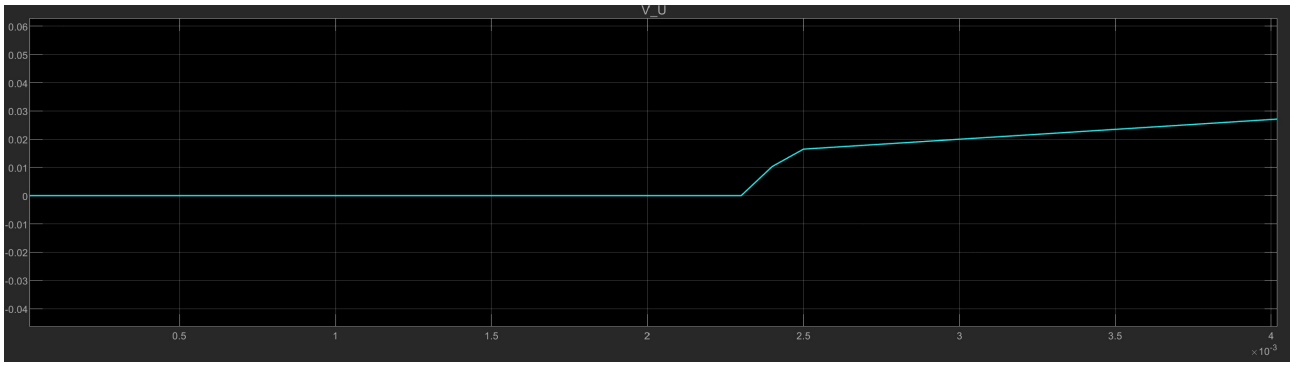

Figure 91: Backlash 1 deg

Differently from the backlash phenomenon in the Simscape model were the velocity had an instantaneously variation from 0 to the moving value, this time the variation is more bland. The a value of 1deg was used for the backlash, and by rising this value it was seen that the trend of the curve starts to be like the one in the Simscape model. If a value of 57.3deg, that is 1 radian, is used for the Backlash the following result is obtained:

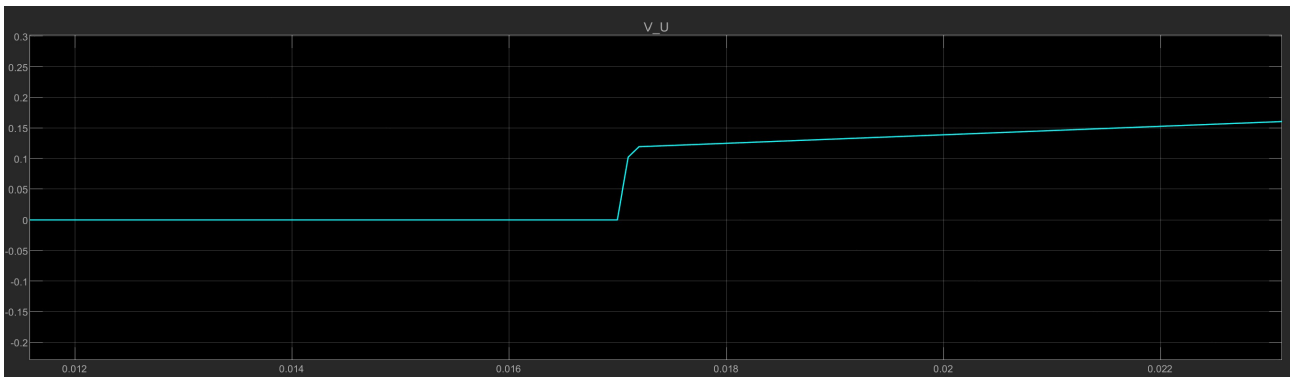

Figure 92: Backlash 57.3 deg

Finally, the backlash phenomenon can also be see from the user position diagram:

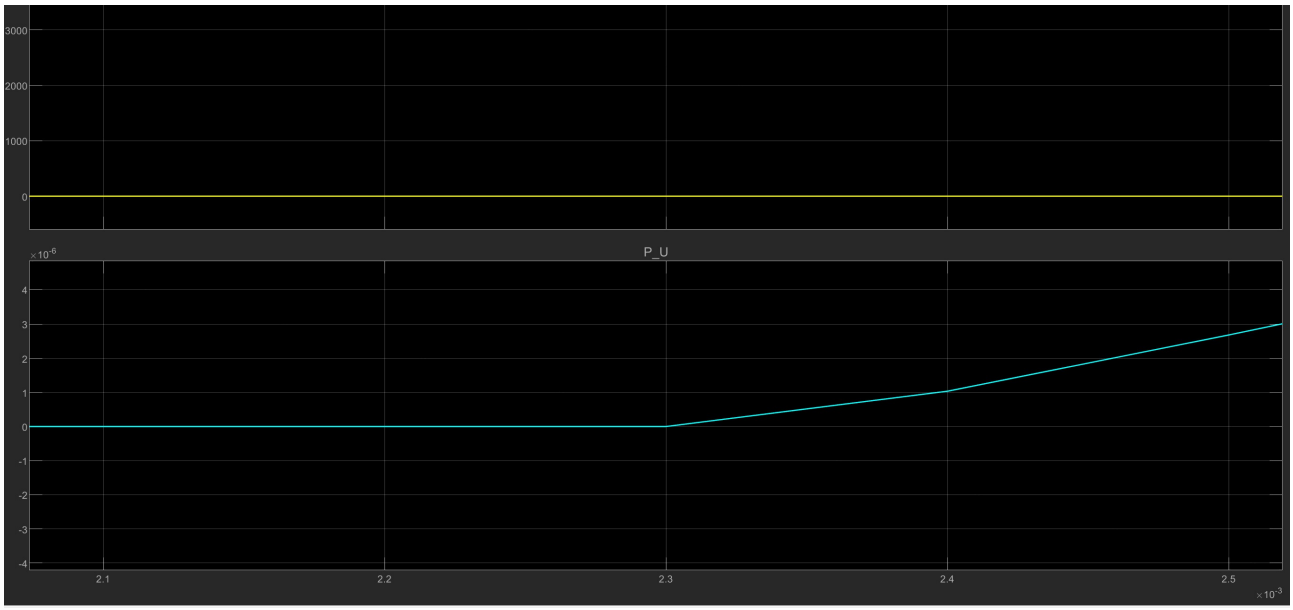

Figure 93: Backlash position

7.2 External load model

In order to approach the more realistic model an external load is applied now to the user. Like before, the Simscape and Simulink model and their results are going to be analyzed.

The Simscape model is the following:

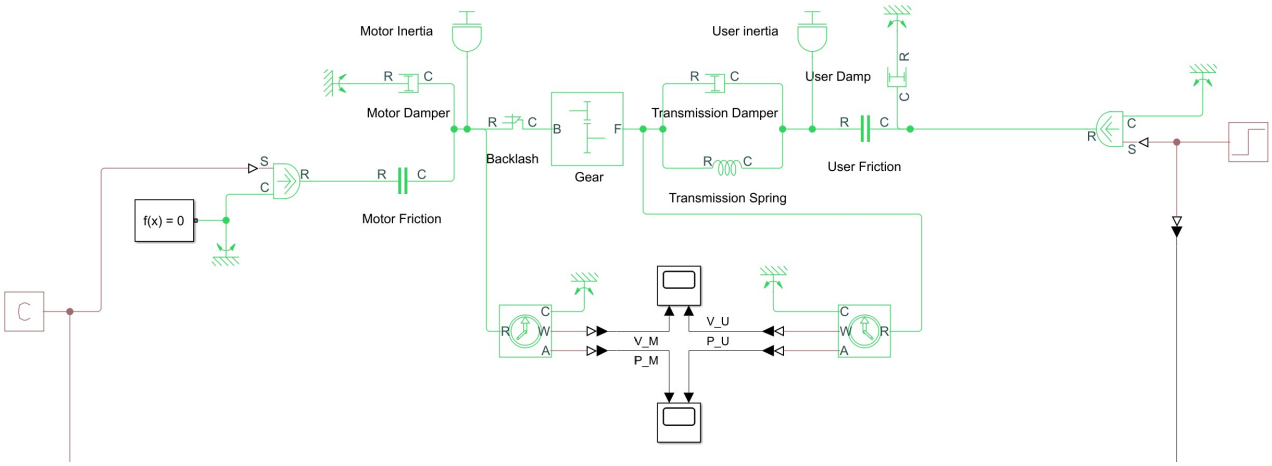

Figure 94: External load Simscape model

Initially, the same data as before has been used for both models. The highest value of external force, that enabled the achievment of sensitive results, is of $8.5 \cdot 10^{-5}$.
The following result, which can be seen from the diagram below, has been obtained. As in the case without the external force, the backlash can be seen, and also a very small impulse representing the external force.

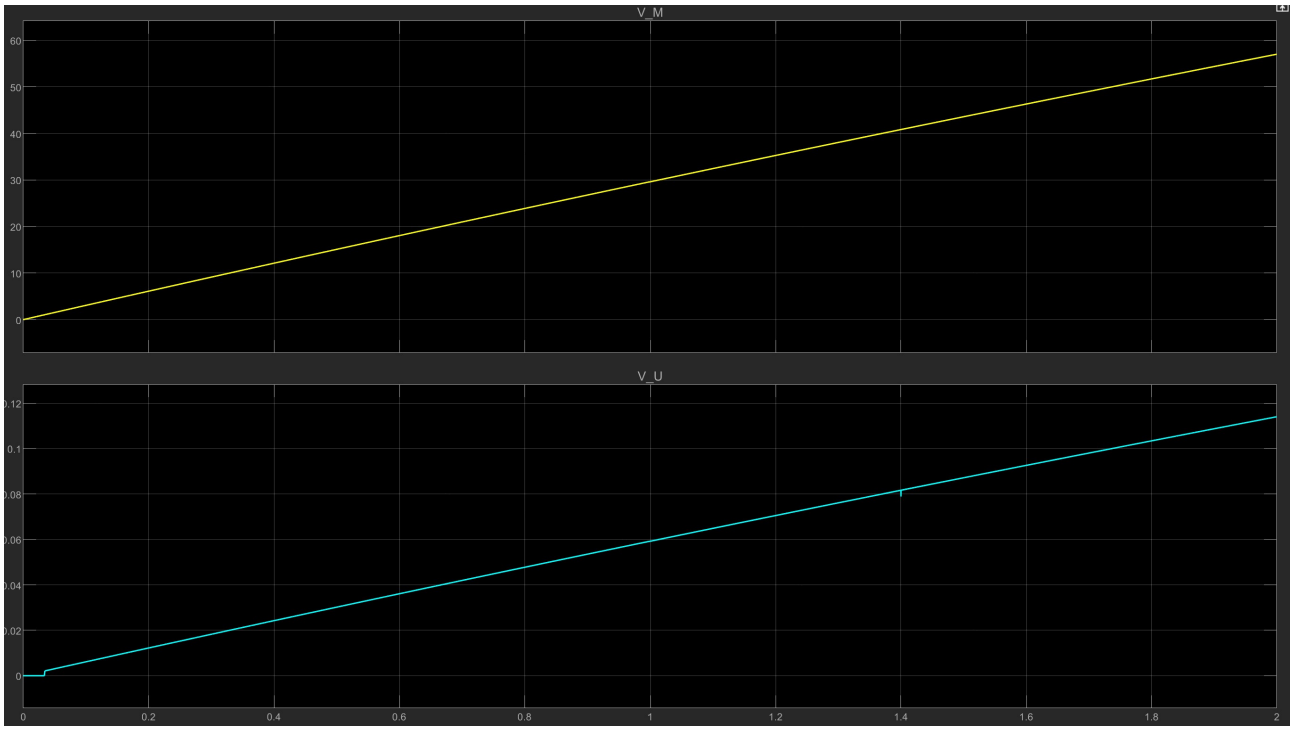

Figure 95: Motor and User Simscape Velocity

By zooming on the area of interest, we can see that the external force affects the system just for a 1/1000 of a second. This is due to the fact that the external force is smaller than the input force. A value bigger than this, would result in a numerical error, not permitting the simulation to converge.

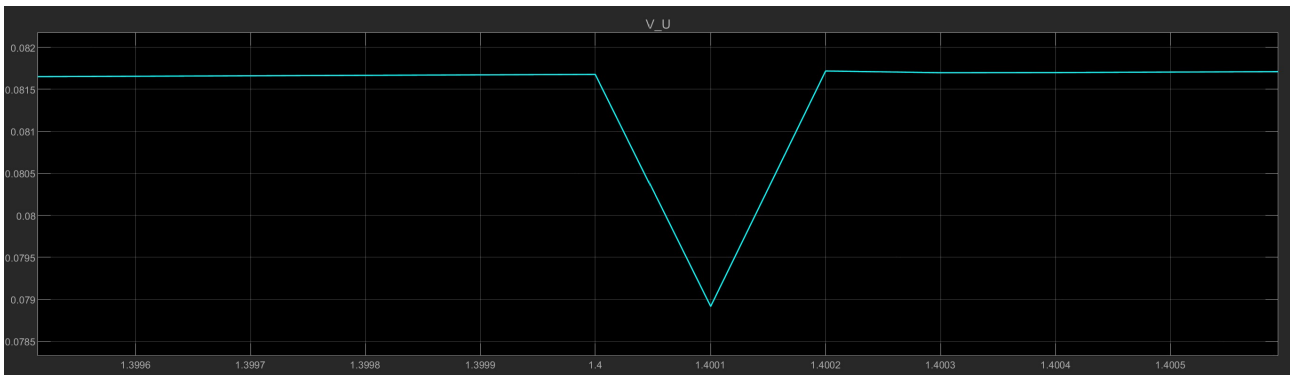

Figure 96: External Force

Another reflecting of the fact that the external force is too small can be seen from the position diagram below, which seems to not be influenced by the presence of the external force.

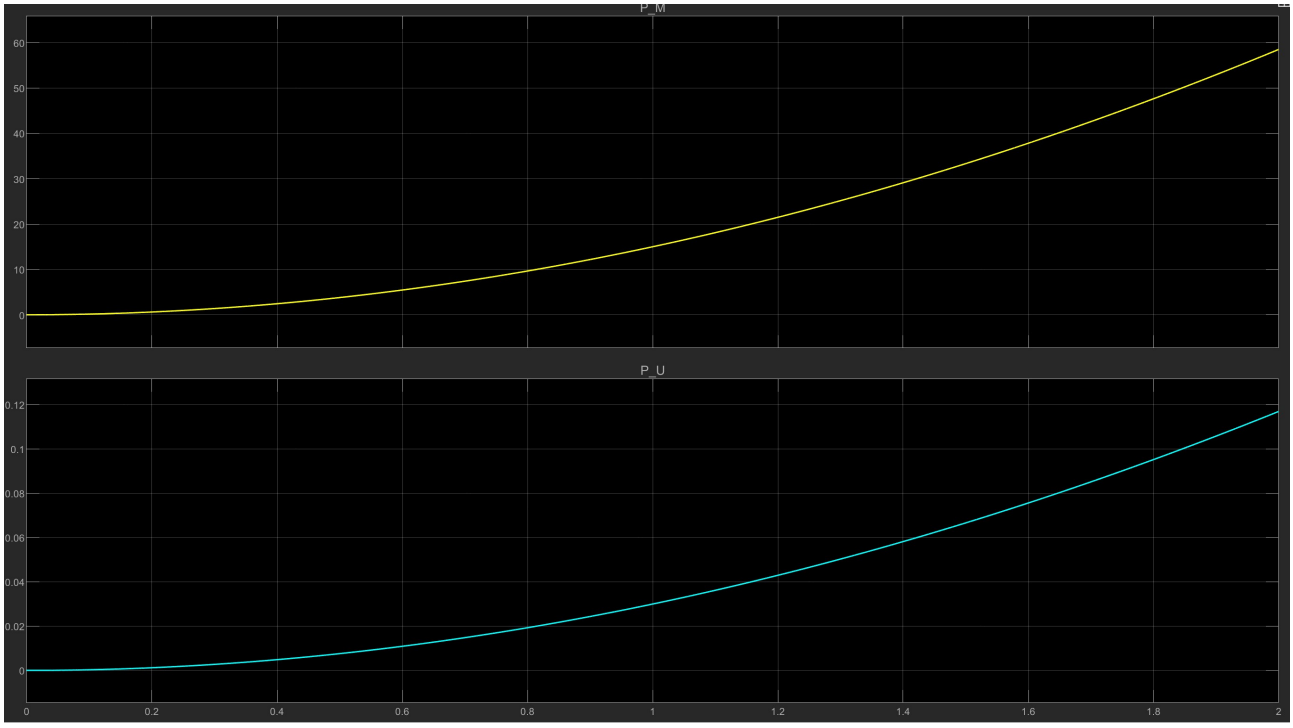

Figure 97: External Force

The Simulink model is identical to the one used before, apart from the addition of the external force. Beside from the gains that are necessary to increase the value of input and external torques, a gear ratio gain has to be included in order to correctly simulate the effect of the external torque. The gain used for the input torque is the same as before, while a gain of $-4.5 \cdot 10^3$ has been used. This gains have been used because the Simscape model is insensitive to the very smal values used for the Simscape model. The model can be seen below:

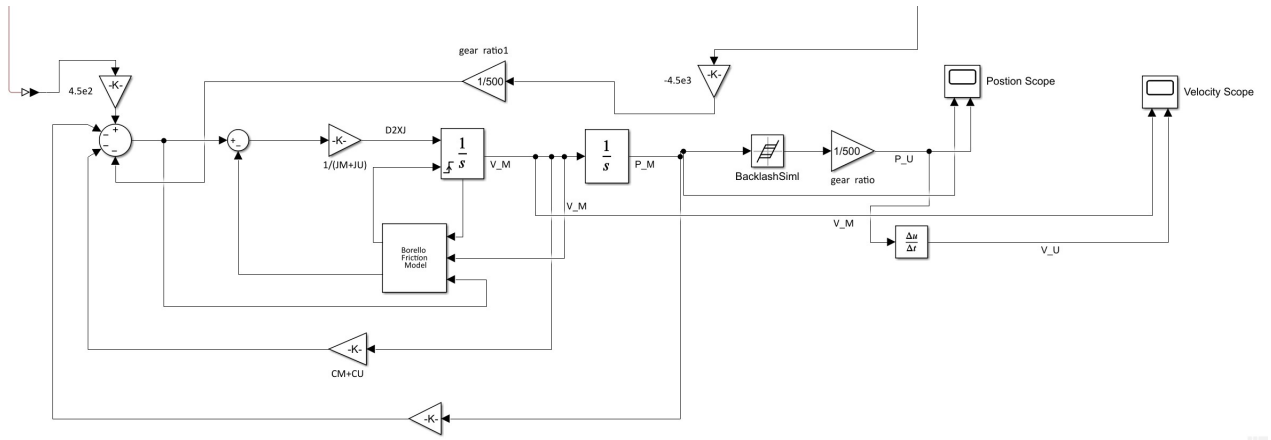

Figure 98: Simulink with External Force Model

Besides the value, which are much higher than those obtained from the Simscape model due to the gains included, it can be seen from the diagram below that the position evolution is very similar to the Simscape one.

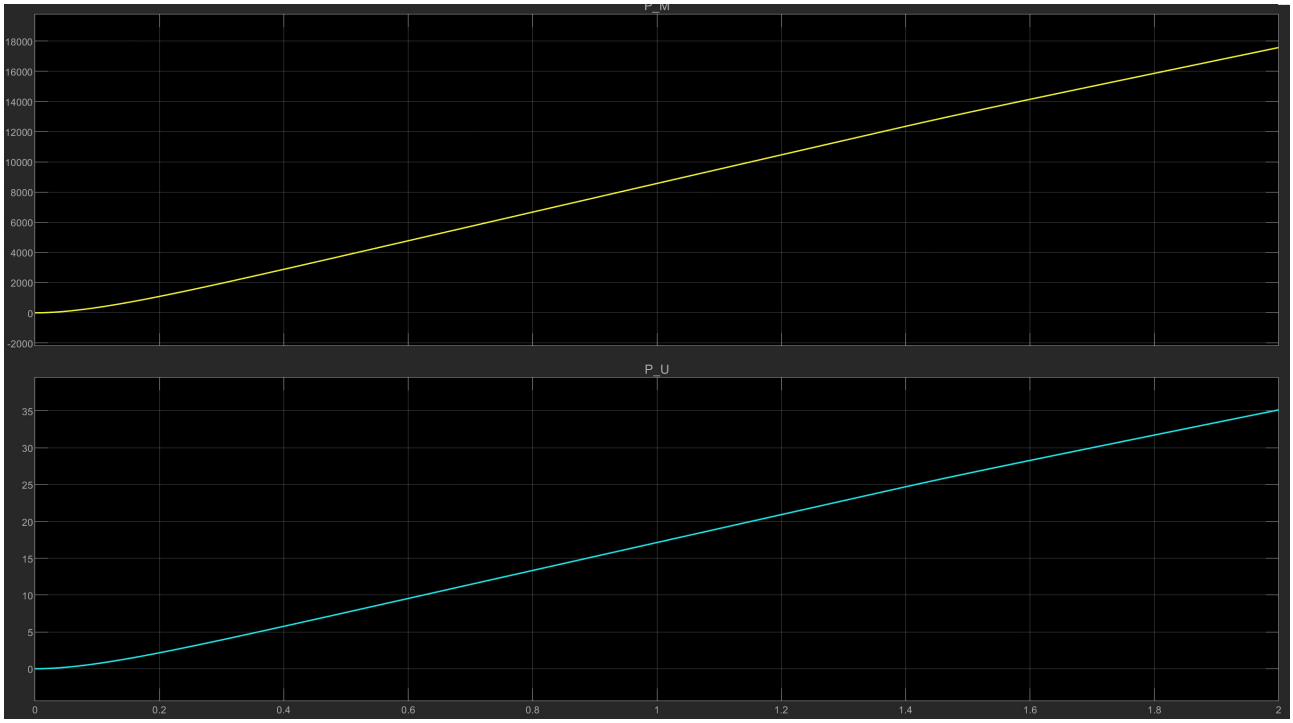

Figure 99: Simulink with External Force Model

This is not the case for the Velocity evolution. In this case the Simscape model has a different progress than the Simscape one. It increases suddenly due to the effect of the input torque, then it settles on an equilibrium state. At 1.4 seconds, when the external torque is applied, the system is deccelerated in order to balance this external force. As it can be seen from the figure below the system settles on a lower velocity than before.

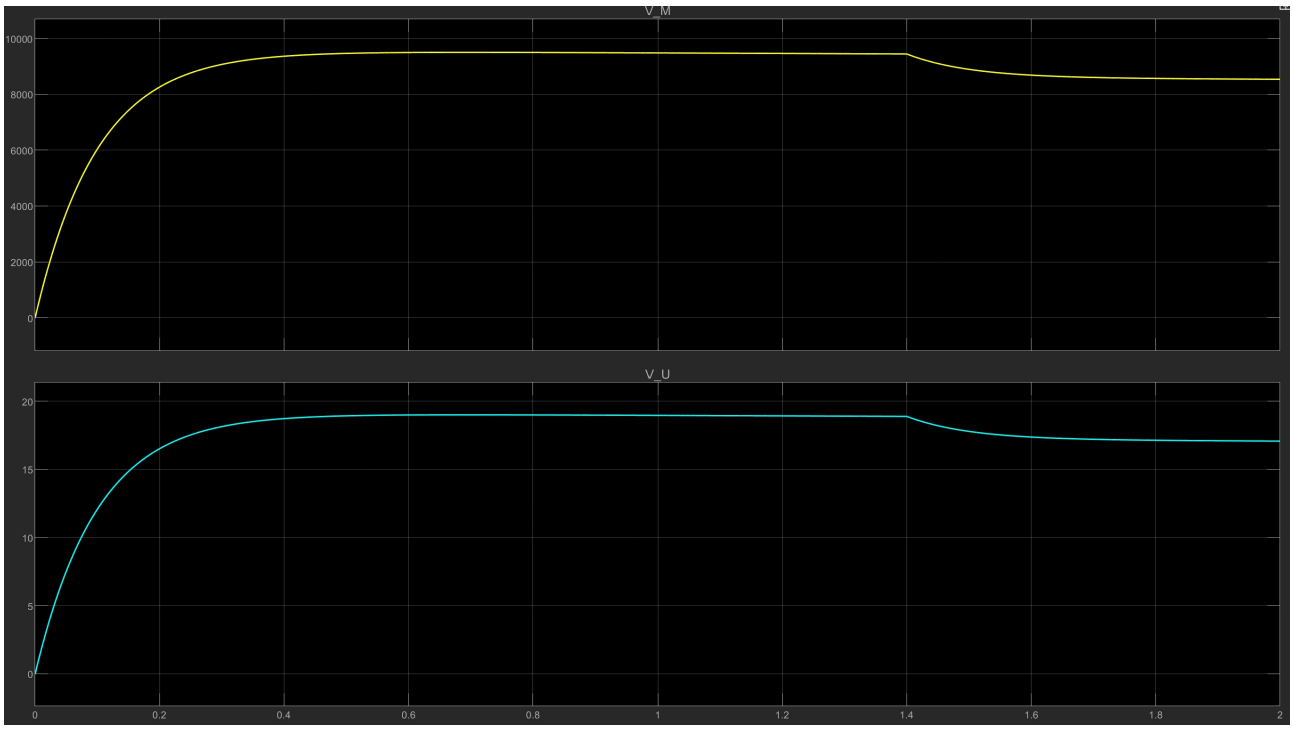

Figure 100: Simulink with External Force Model

The backlash can be seen by zooming on the first moments of the simulation and during the application of the external force as highlighted by the diagrams below:

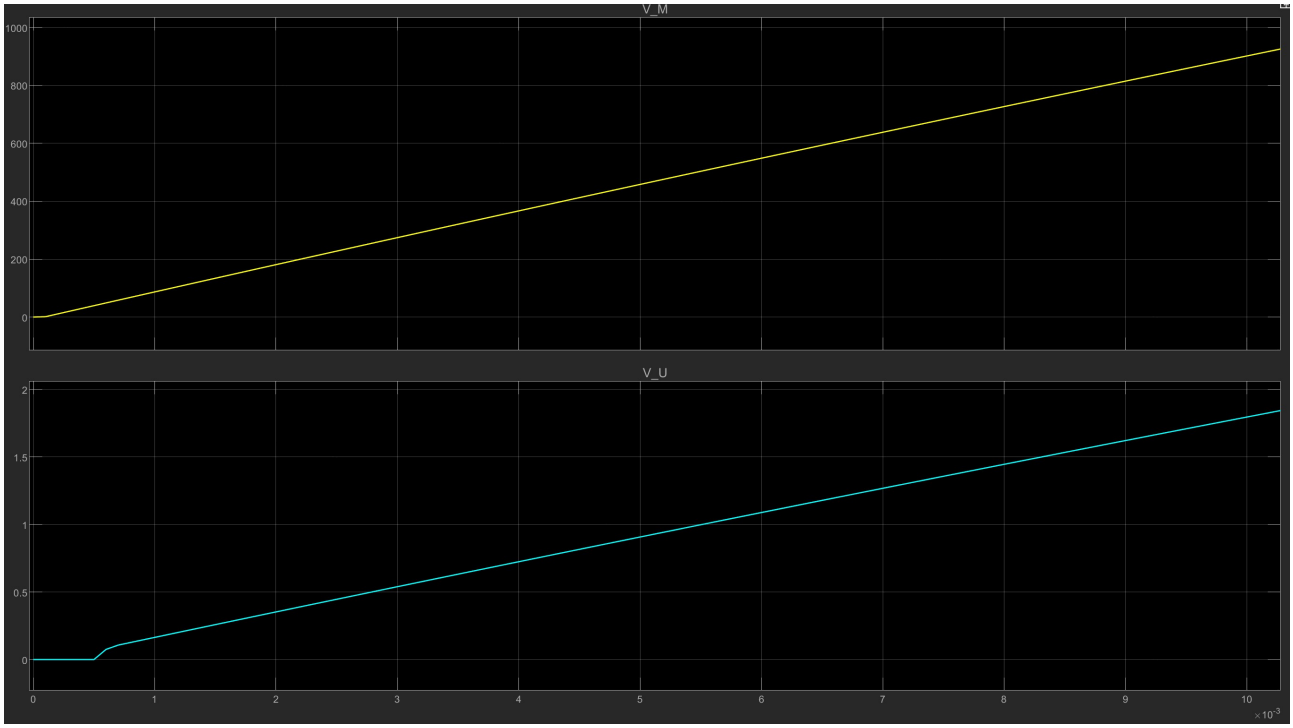

Figure 101: Simulink with External Force Model

Here we can see that the application of the force it's istantaneously felt by the user system, while the motor system's velocity isn't influenced by the backlash.

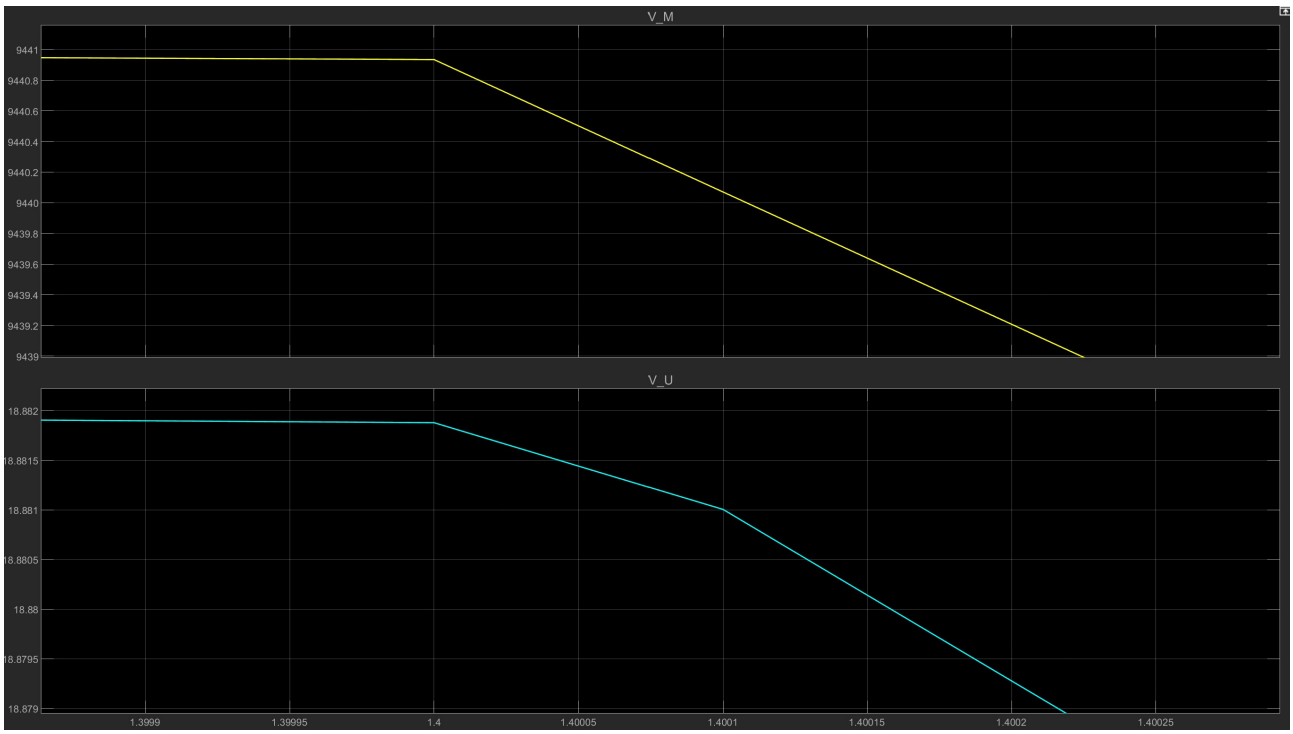

Figure 102: Simulink with External Force Model

7.3 Different model block values analysis

At this point the problem of the differences between the Simscape and Simulink model has to be analyzed in a different way in order to precisely understand which component value influences most the simulation, and if with different values than those of the High Fidelity model, the same results can be obtained from Simscape and Simulink model.
In order to do so and identical model like the ones used in the last paragraph has been used, but with the following values:

Motor Mass	Jm = 0.085 Kg m2
Motor Damper	Cm = 0.03 Nms/rad
User Mass	Ju = 50 Kg m2
User Damper	Cu = 100 Nms/rad
Transmission Damper	Ct = 1e5 Nms/rad
Transmission Spring	Kt = 500 Nm/rad
Rotational Torque value	F0 = 4 Nm
External rotational Torque	Fext = -2500 Nm
Teeth Ratio	100
Backlash	±1 deg
Motor Breakway Friction Torque	5 Nm
Motor Coulomb Friction Torque	5 Nm
Motor Breakway Friction Velocity	0.1 Nm
User Breakway Friction Torque	500 Nm
User Coulomb Friction Torque	500 Nm
User Breakway Friction Velocity	0.1 Nm
Simulation Time	T = 2 s

Also, a gain of 10^3 has been used in order to modulate the input of the Simulink model. Firstly, it can be seen the Velocity of the motor and the user from the Simscape model:

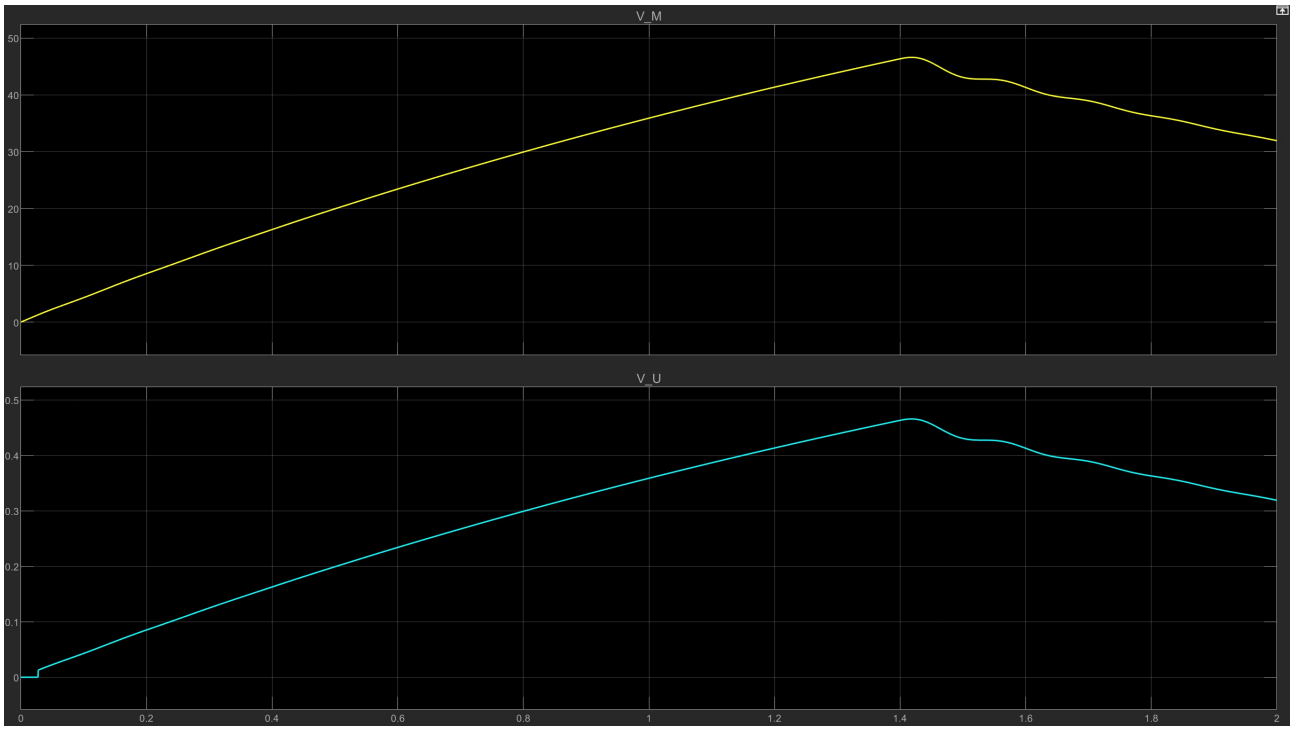

Figure 103: Motor and User Velocity Simscape model

At the instant 1.4s which is when the external load is applied, the system's velocity reduces due to it. Some oscillations can also be observed after the first instants after the application of the load. Like before the backlash can also be noticed in the first instants of the simulation.

As for the position of the motor and user, it can be seen from the below diagrams that initially the system behaves like it behaved when no external load was applied. When the load is applied it can be noticed that the evolution of the curve has a change in concavity, which signifies that the position of the system will settle or eventually diminish.

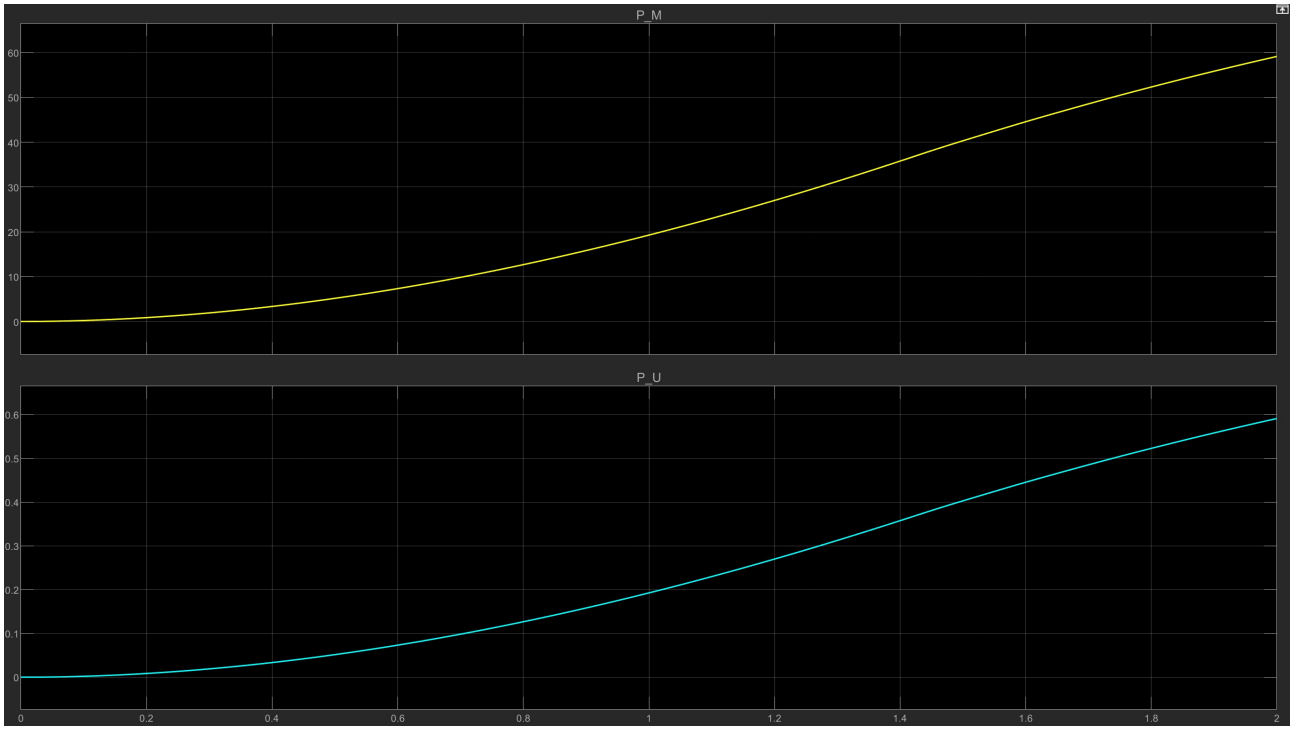

Figure 104: Motor and User Position Simscape model

Next, the Velocity of motor and user Simulink model can be seen. Initially, the system behaves identical to the Simscape model: delayed behaviour on the user due to the backlash of the gear teeth, then an increase in speed.
At the instant of application of the external load, as for the Simscape model, it can be seen that the velocity of the system starts to fall. This time though it has a different evolution than it had in the Simscape model. No oscillation are present, but the system has a steep descent.

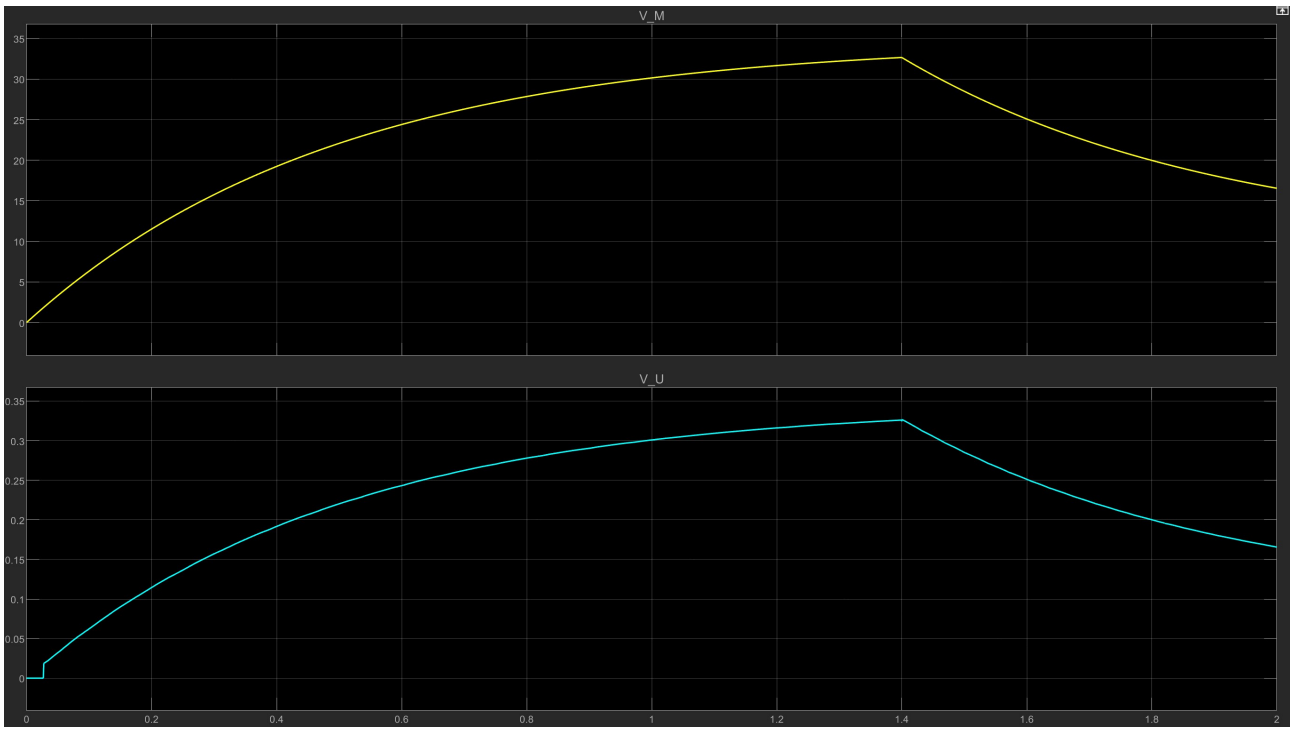

Figure 105: Motor and User Velocity Simulink model

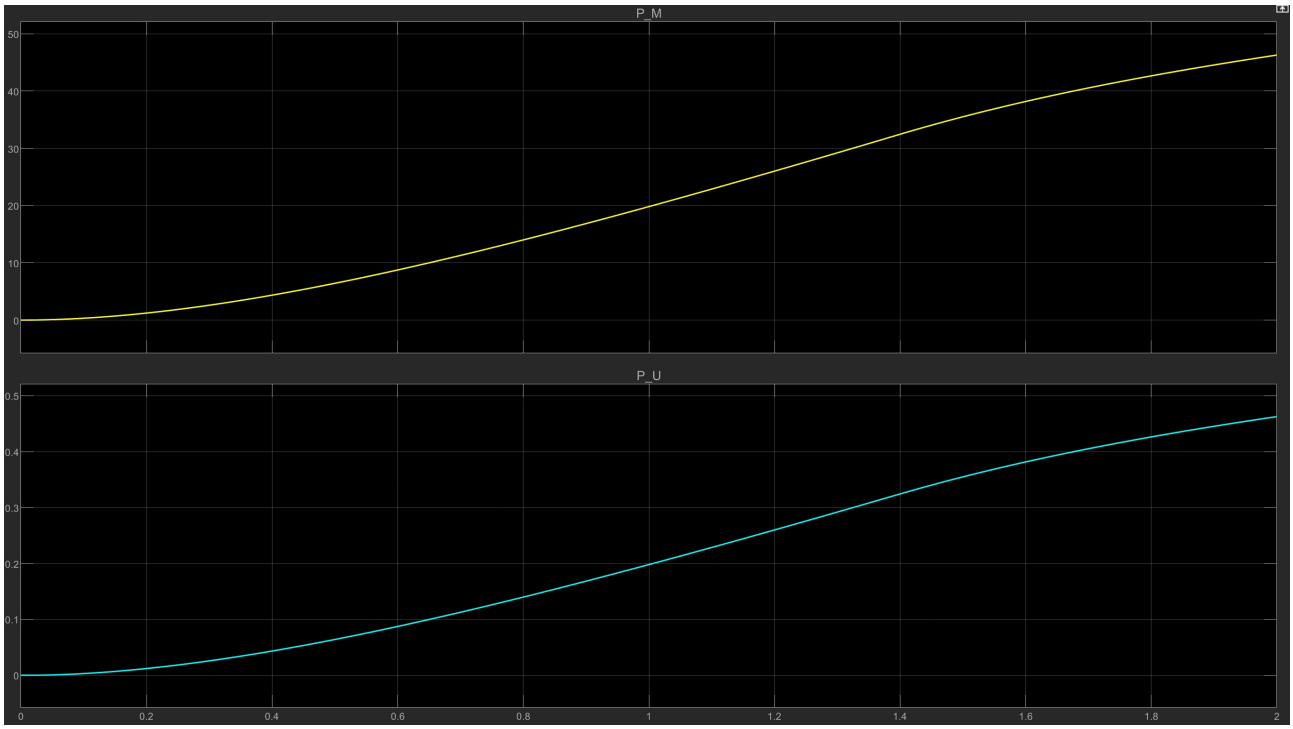

Figure 106: Motor and User Position Simulink model

As for the postition of the motor and user in the Simulink model, they behave in the same way as in the Simscape model.

Next, the same models are used with different type of inputs in order to analyze the behaviour of the system and to better understand which components of the Simscape model influence the final result:

- **Chirp**: the input has an initial frequency of 0.1 Hz, a target time of 10 s and a frequency at target system of 1 Hz. A simulation of 20 sec has been done in order to analyze the behaviour in the first instants but also once the transient has passed. The following diagrams have been obtained:

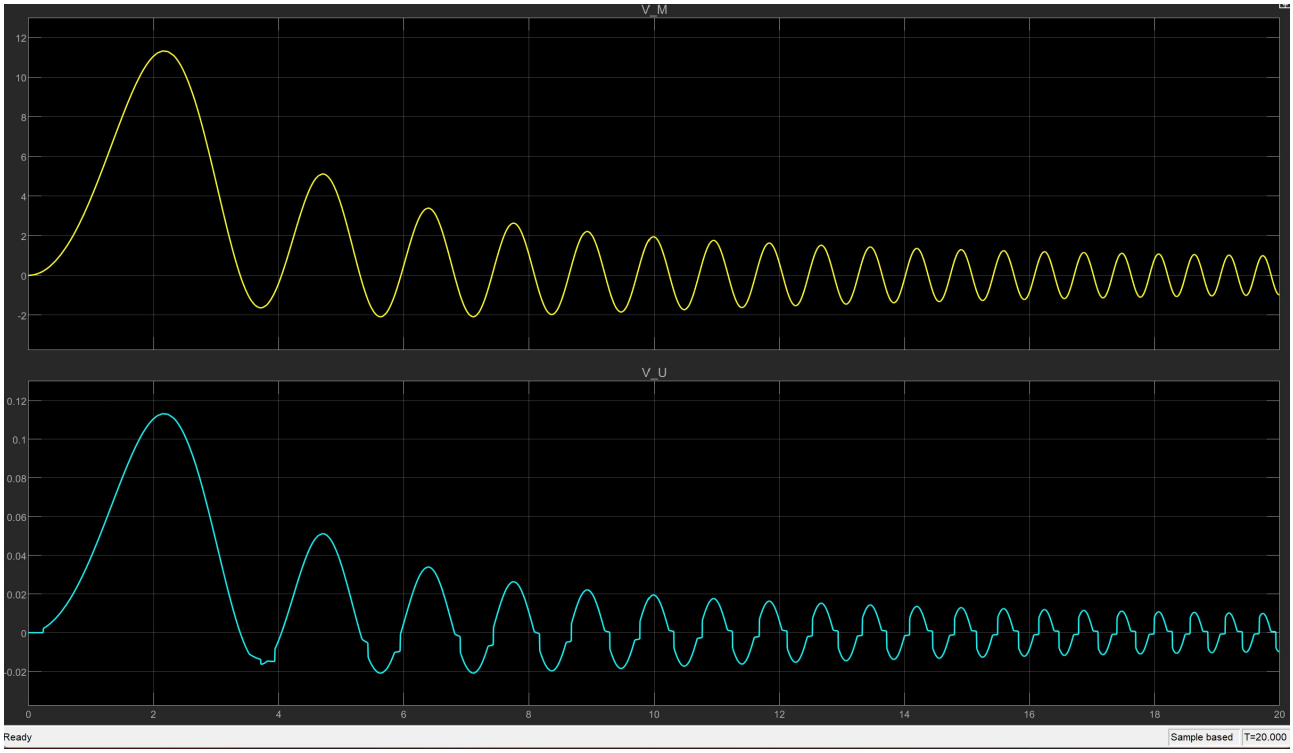

Figure 107: Motor and User Velocity Simscape model

It can be seen from the two diagrams above that the backlash is correctly modeled at the first istants of the simulation, while the first passage through the zero value of the speed, which indicates the brief stopping of the system, is not correctly modeled. All the parameters of the two models are the same except of the rotational damping and rotational spring of the transmission. It has been found, after a trial and error process, that the Simscape model behaves very similar to the Simulink one when the two coefficients are equal to a value of 50.

On the other side, from the Simulink model, it can be seen that even the first zero crossing of the velocity is correctly modeled.

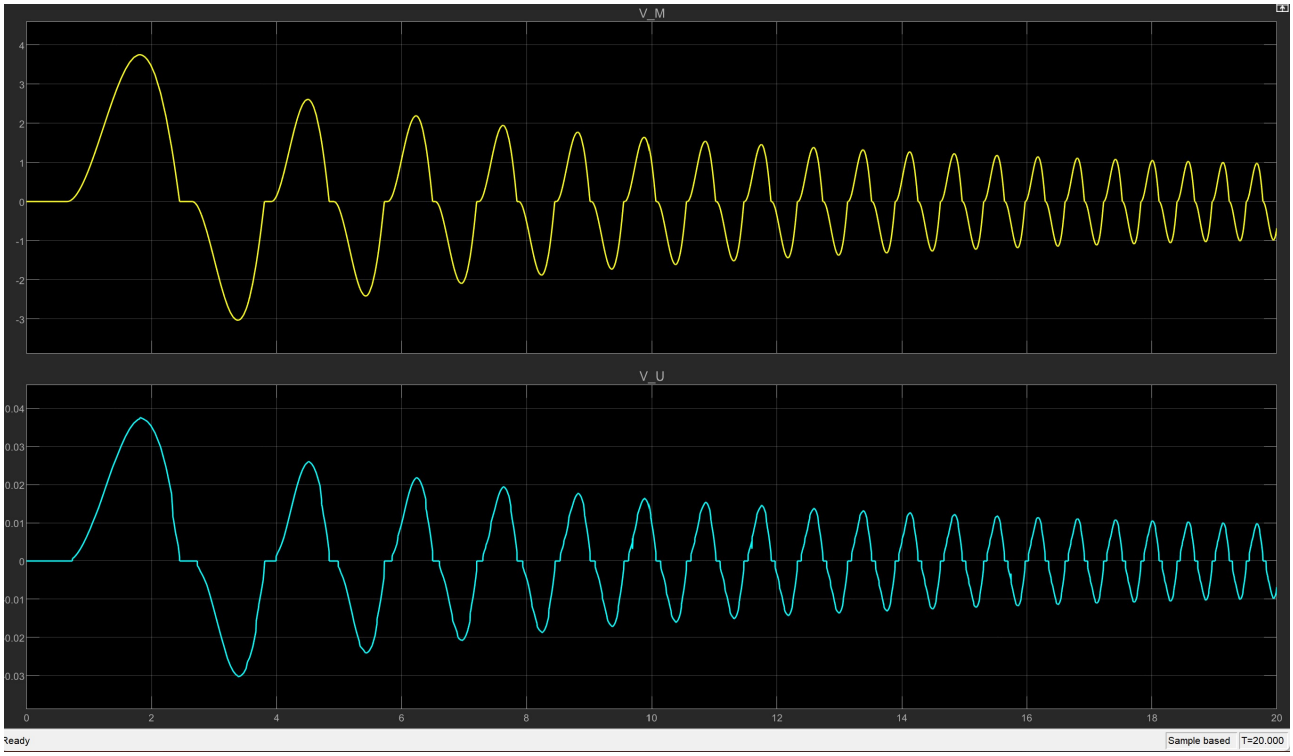

Figure 108: Motor and User Velocity Simulink model

If we zoom on the final instants of the simulation it can be seen that the two systems behave quite identical. The null velocity is still not perfectly overlapped to the zero value, but it differs by a factor of 10^{-3}. In fact the modelling of the backlash is now correctly done by the Simscape model.

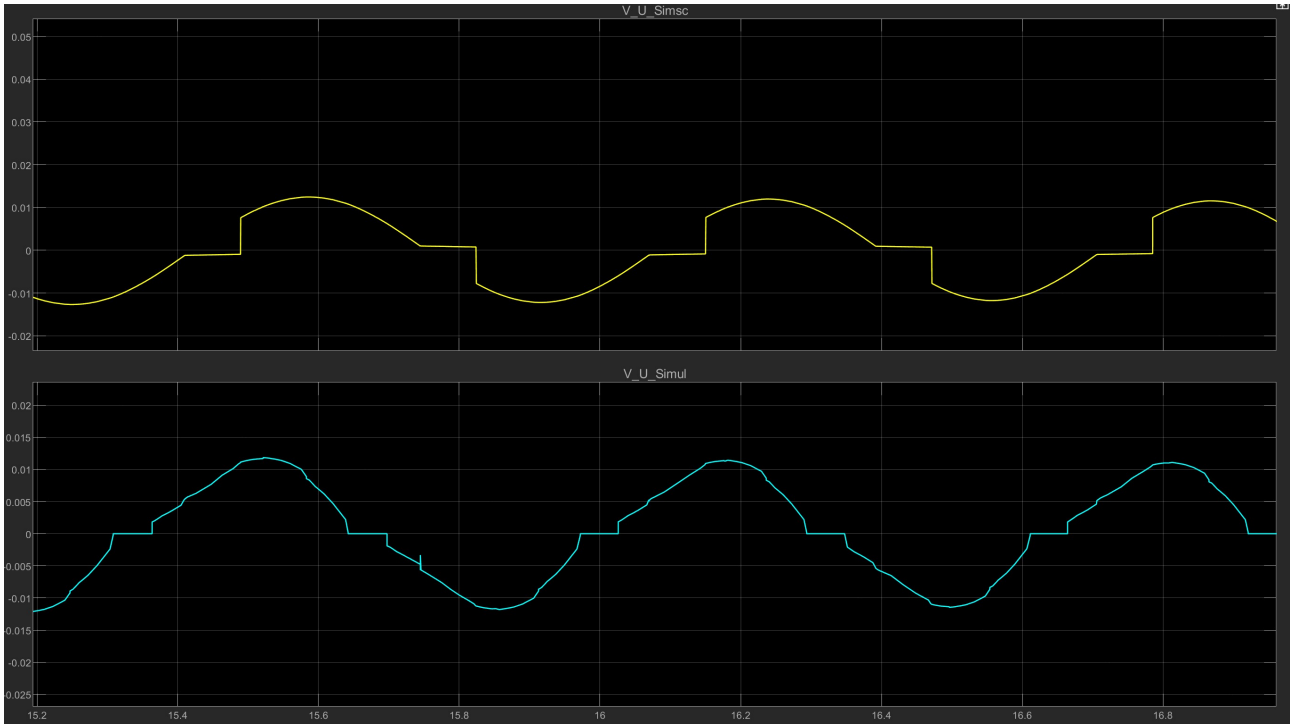

Figure 109: Simscape(upper) and Simulink(lower) user's velocity

As for the position of the two systems, it can be seen in the following diagrams:

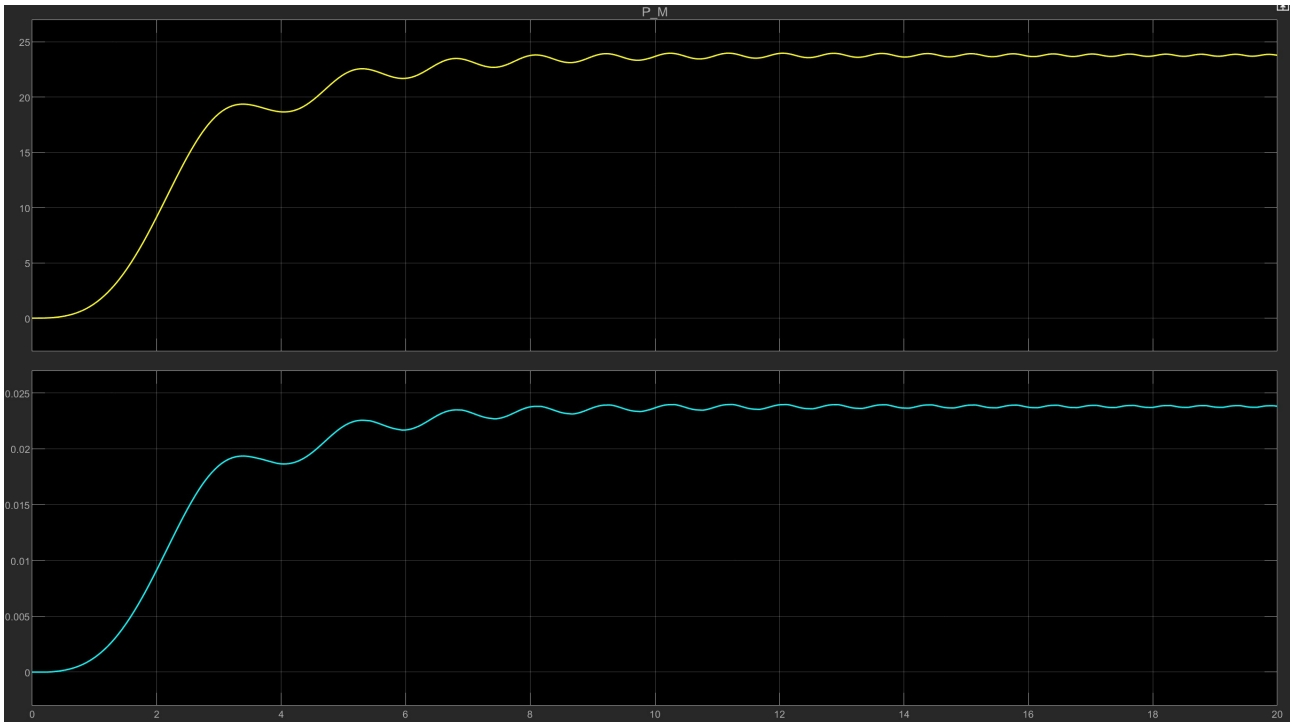

Figure 110: Motor and User Position Simscape model

By analyzing the positions of the Simscape and Simulink models, it can be noticed that they present a different behaviour in the first seconds of the simulation. The Simscape position has an initial rise with an oscillation of a smaller amplitude than that of the Simulink model.

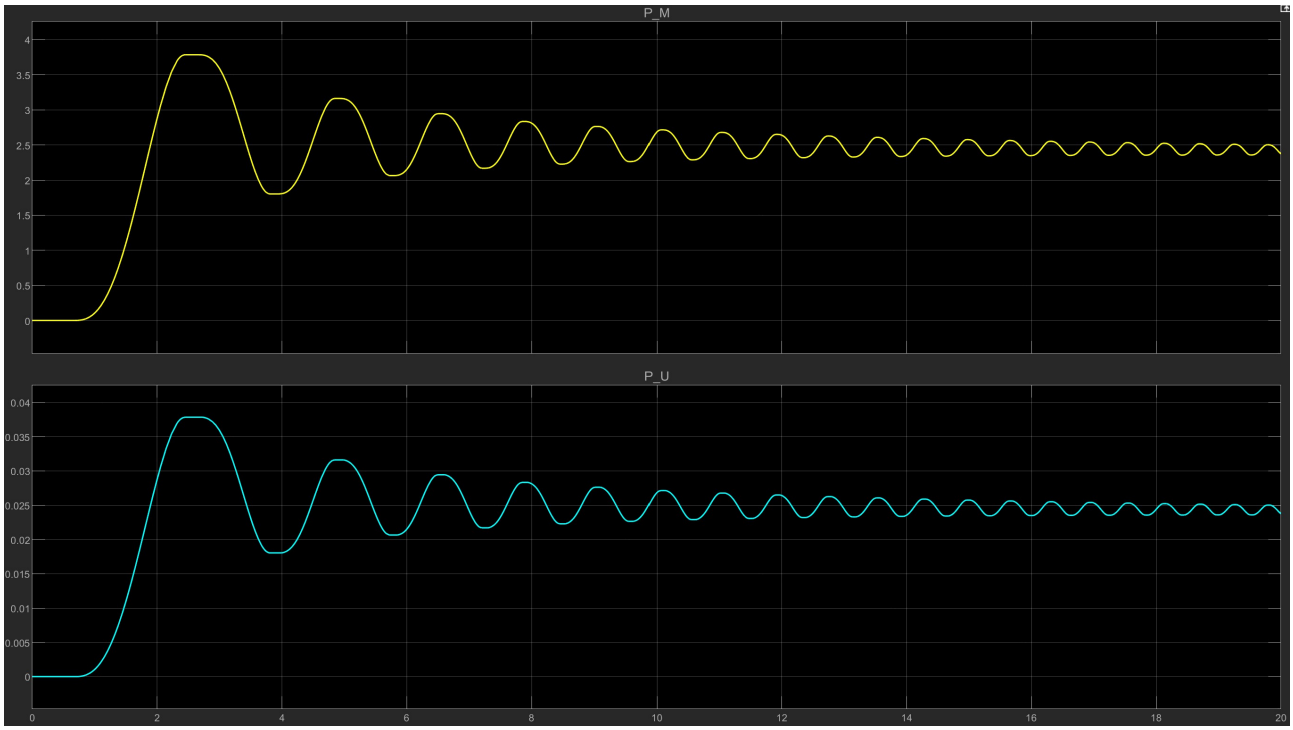

Figure 111: Motor and User Position Simulink model

By zooming on the final instants of the simulation, as for the velocity, the Simscape behaviour becomes very similar to the Simulink one. The position of the two system settles, but slightly on different values.

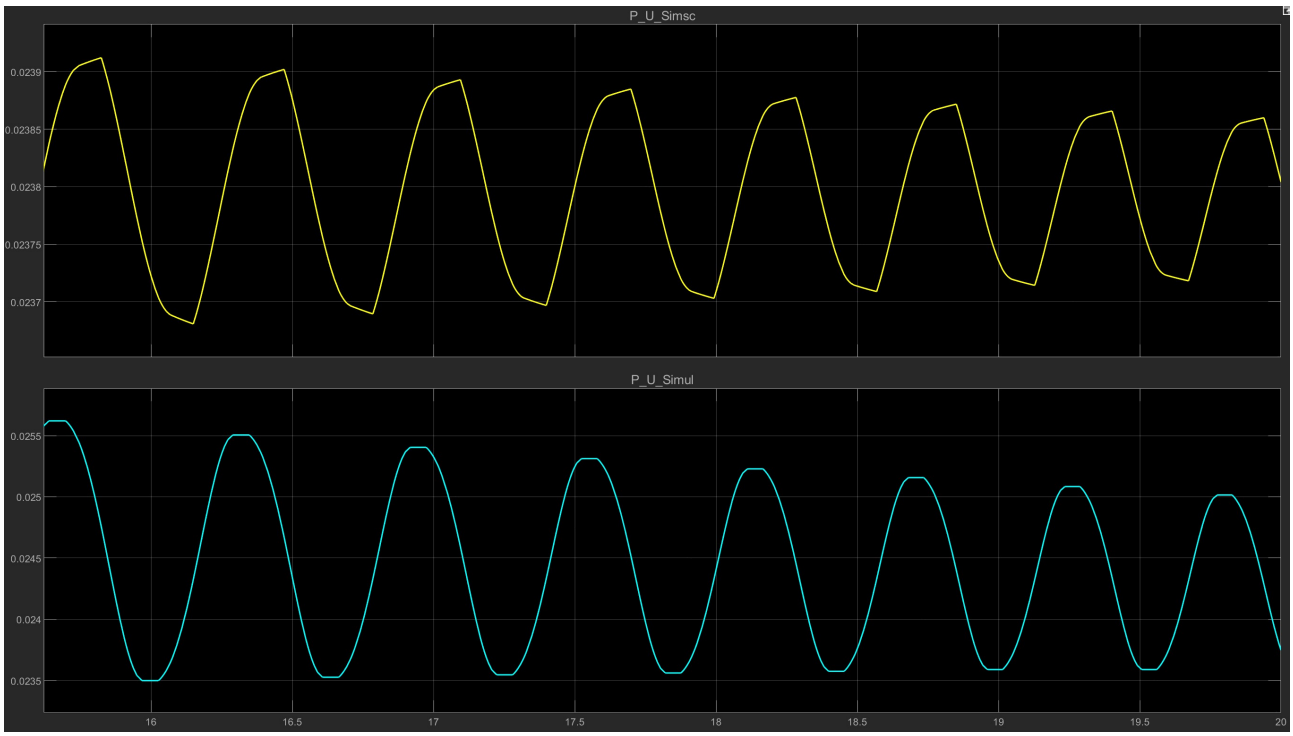

Figure 112: Simscape(upper) and Simulink(lower) user's position

- **Sinusoidal**: the input has an amplitude of 1 and a frequency of 10 rad/sec. From the graphs below we can compare the behaviour of the two systems:

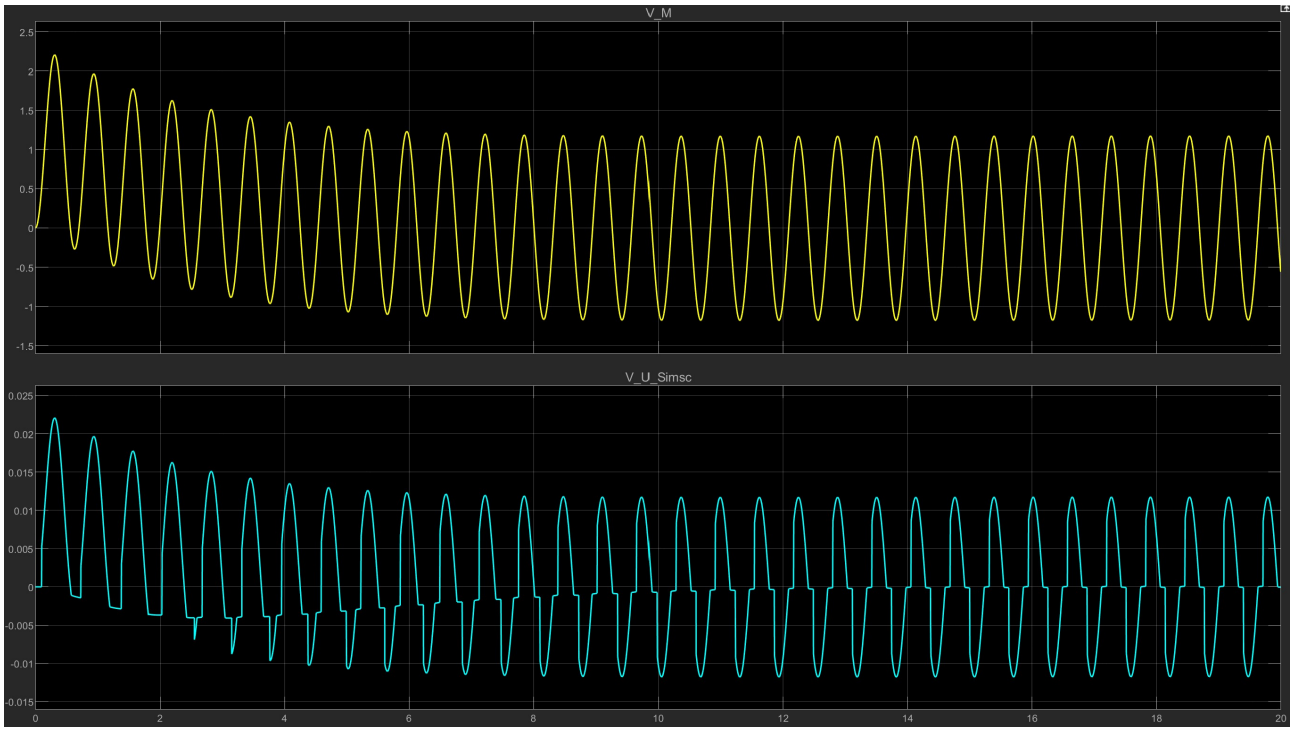

Figure 113: Velocity of motor and user Simscape

Again we can notice that in the first instants of the simulation, the Simscape user's velocity isn't the same as the one of the Simulink model.

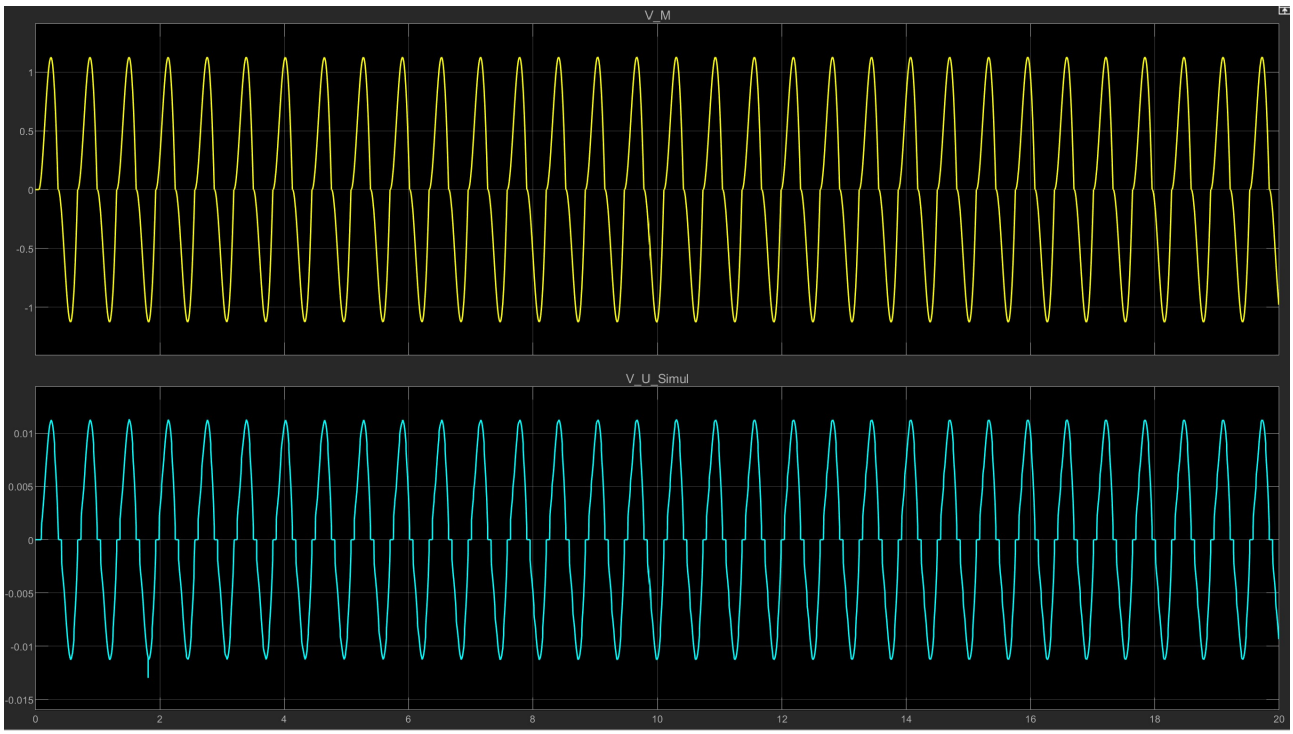

Figure 114: Velocity of motor and user Simulink

By zooming on the on the middle and final instants of the simulation, it can be again seen that the Simscape model's backlash behaves like the Simulink model, and that the two curves are quite completly overlapped.

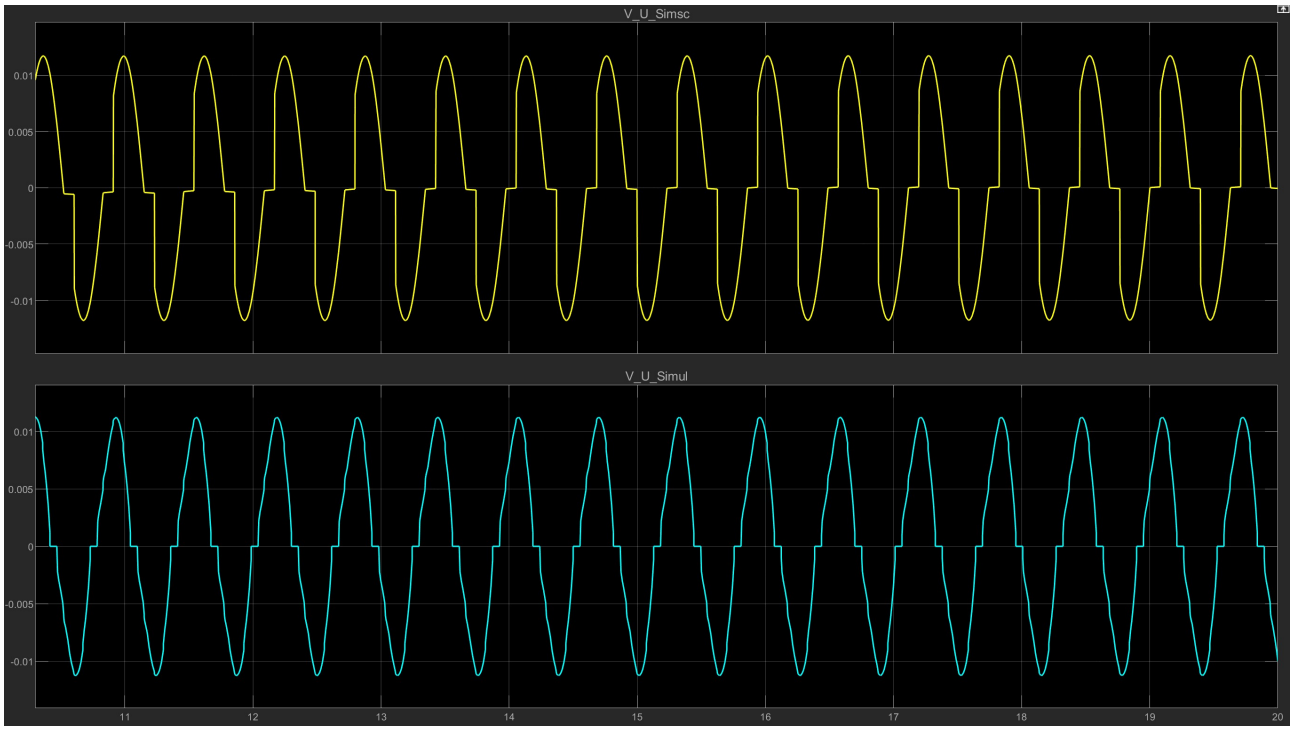

Figure 115: Velocity of user Simscape and Simulink

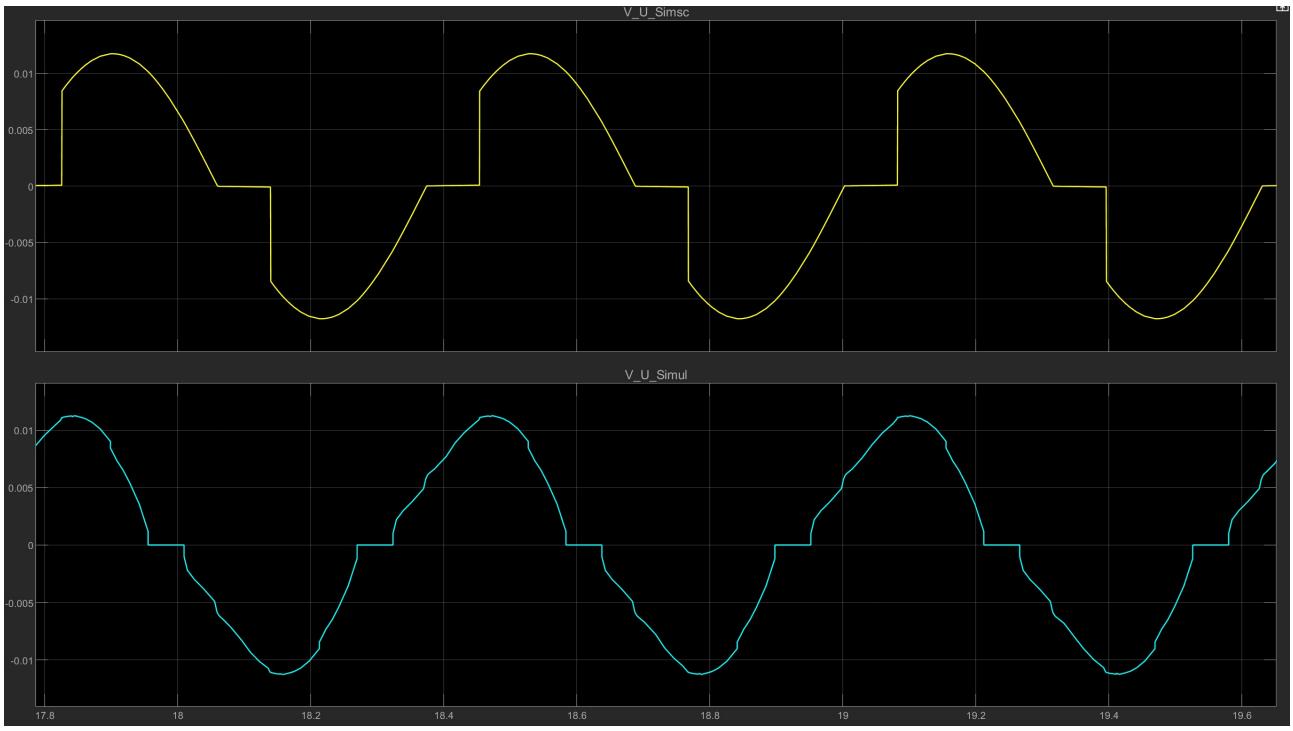

Figure 116: Velocity of user Simscape and Simulink

As for the position, like in the case of the Chirp input, the Simscape model doesn't simulate in the correct way the initial instants. But, as it can be seen from the diagram below, after the transient, the behaviour of the two systems is the same.

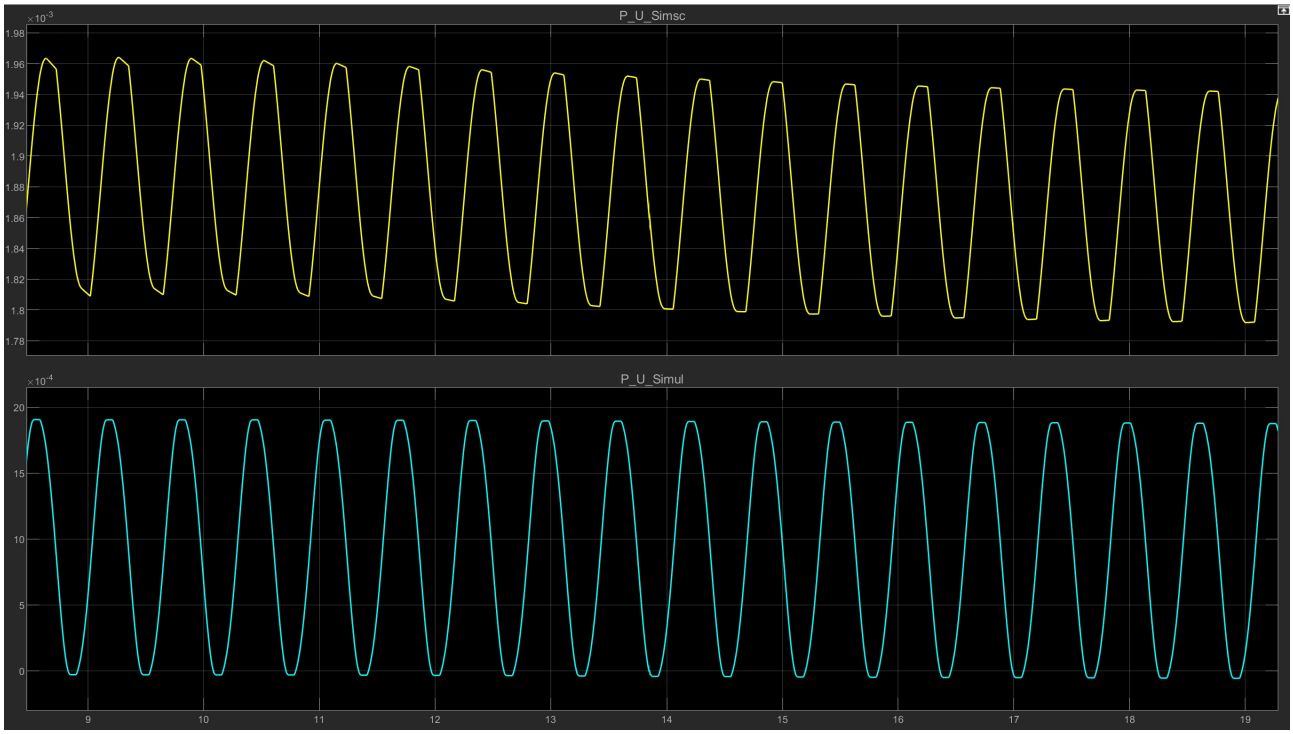

Figure 117: Position of user Simscape and Simulink

From this trial and error simulations the following things can be said:

Firstly, being that the Borrello model cannot be used in the Simscape model, the one used in our simulations makes the system to be very sensitive to inputs higher than a certain value. On the other hand the same input that enables us to obtain some results from the Simscape model, is so small that makes the Simulink model insensitive.

Secondly, the transmission between the motor and user in the Simscape model, is not present in the Simulink model. This certainly plays a part in the differences between the two models.

Lastly but not least, the fact that in the Simulink model the motor and user damping coefficients and the friction coefficients are modelled as one, while in the Simscape they are modelled as individual parts, is the biggest difference that makes the results of the two model to behave differently during the transient. It can already be seen that the the behaviour of the Simscape model is very different form the Simulink one in the first seconds of the simulation.

8 End stop: Simscape vs Simulink model

The two mechanical end strops Xm and -Xm, limit the rotational movement of the system and affect the dynamical behaviour. The presence of the end stop will not affect the dynamical response if the systems movement is contained withing the maximum and minimum values of the end stop. This intoduces additional constraints which are:

1. possibility of movement contained between the values Xm and -Xm;
2. speed of the system must be equal to zero when one of the two end stop is reached;
3. acceleration of the system also must be equal to zero when the end stop is reached;

A Simulink model of a second order dynamical system is being used to study the behaviour of the additional non linearity due to the end stop. The same system has been modeled using the Simscape blocks in order to see if this simple model could prove to give the same results.

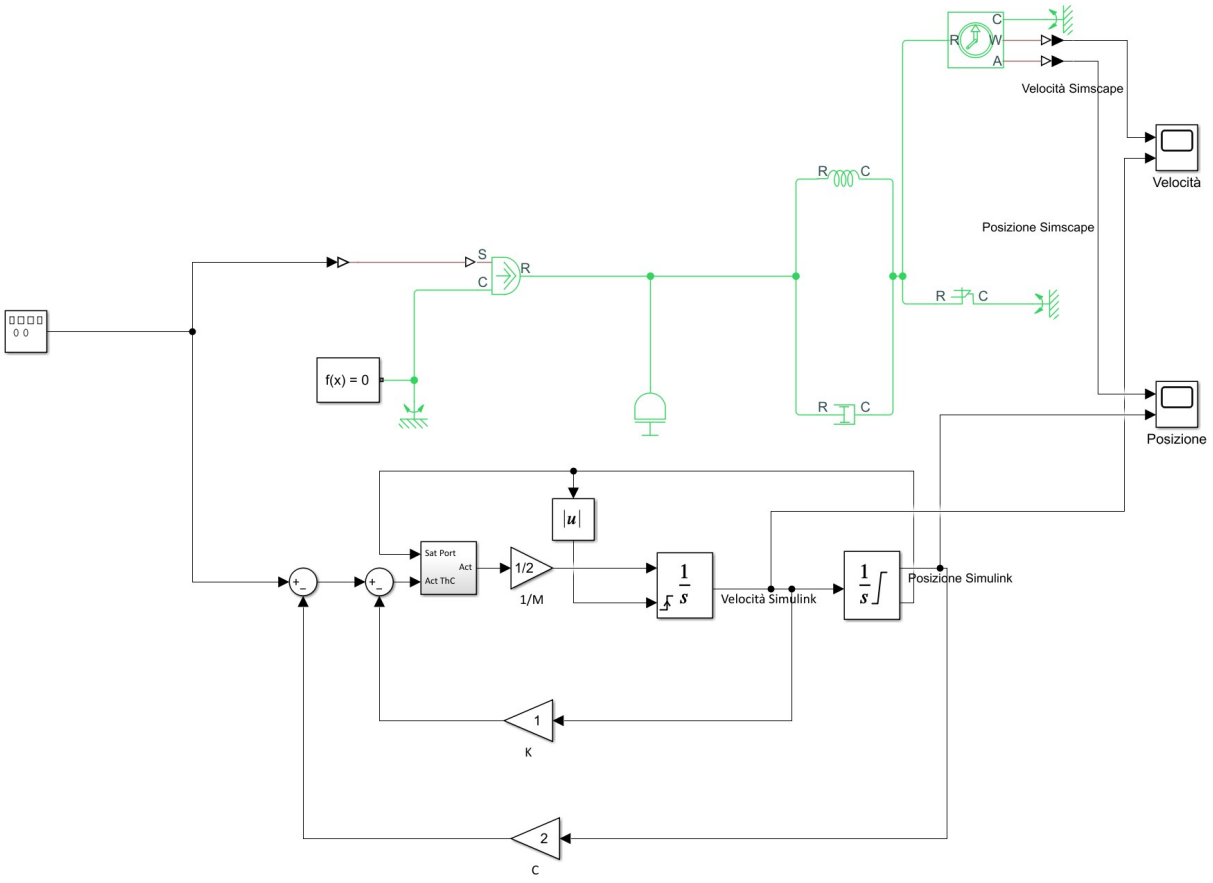

Figure 118: Simscape and Simulink end stop MCK model

Focusing on the Simulink model, it has been proved that by using the mass-damper-spring model with a position integrator that is saturated the behaviour of the system presents a delay that is not real, the speed and acceleration are not equal to zero when the end stop is reached and the system does not take in account the forces of constraint.
To obtain a correct behaviour a speed reset has been used first. This is made by using the saturation port of the position integrator: when the position is equal to the saturation value a number equal to ± 1 which represent the saturated position, or 0 for when the position is not saturated is given to the velocity integrator which then forces the speed to be zero. This is done by the model below

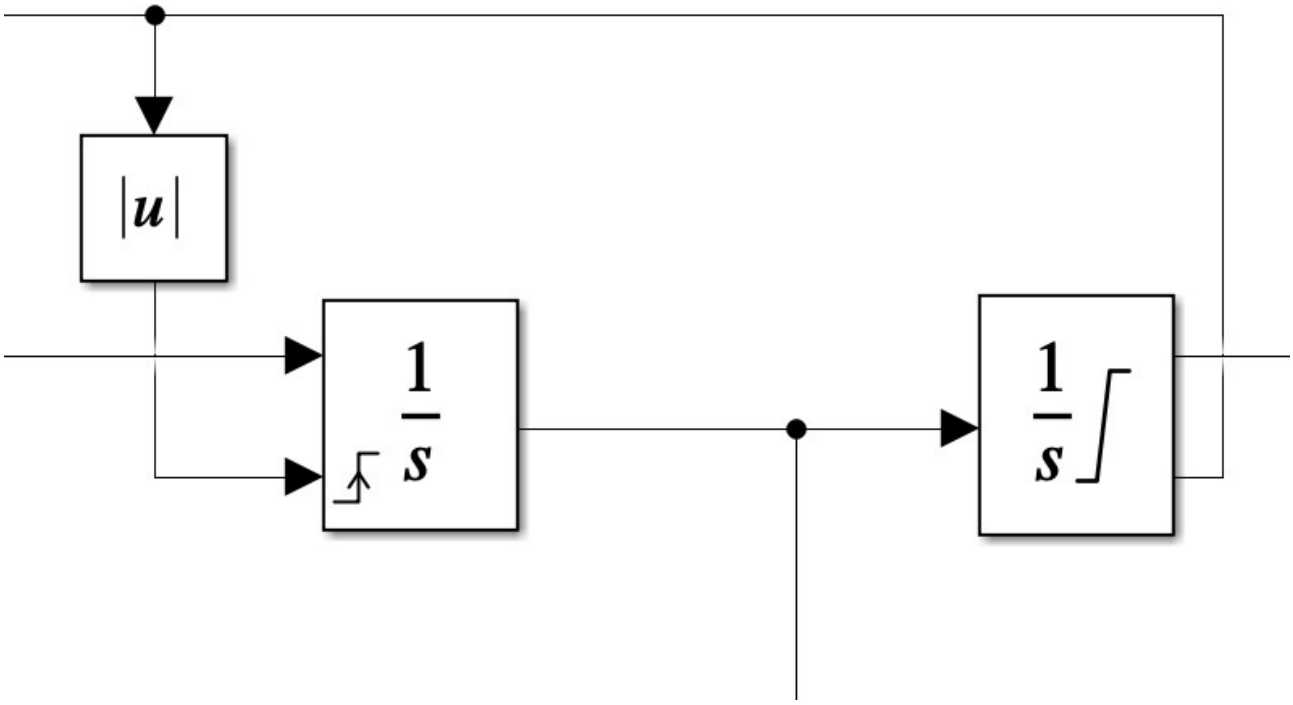

Figure 119: Speed reset

This is not enough to obtain a correct model since after the system reaches the end stop, the speed increases istantly. This is due to the fact that the acceleration is not equal to zero. In order to obtain this the sign of the acceleration is compared to the sign of the saturation port value. If these two are equal in sign it means that the system is at the end strop but is still, so the acceleration given to the integrator is equal to zero. Differently, if the signs are opposite it means that the system is at the end stop but is inverting it's motion, so the value given to the integrator is the calculated acceleration. This is obtained through the model below.

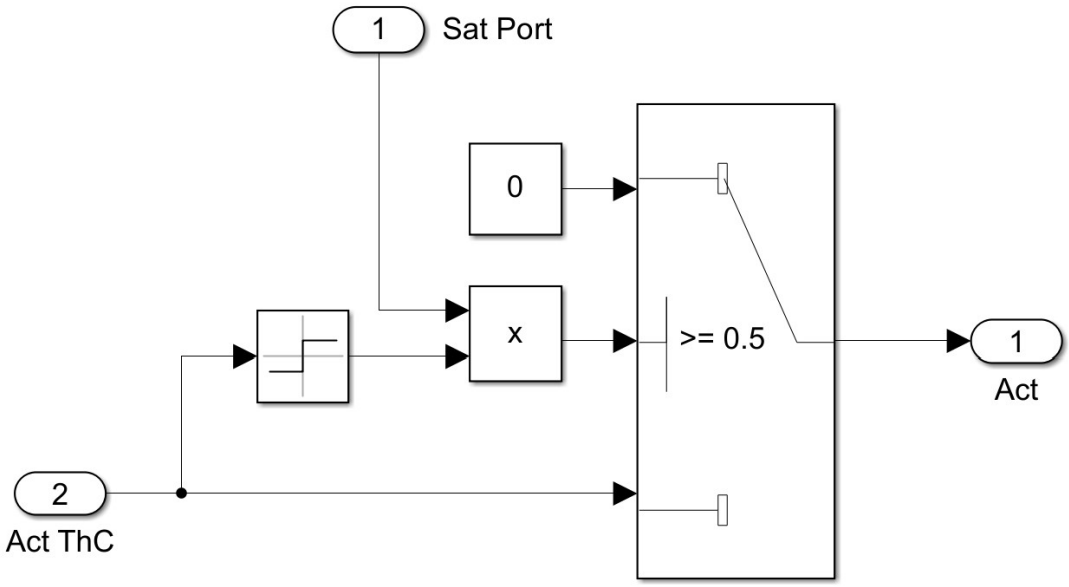

Figure 120: Acceleration reset

The input is a quadratic signal with an amplitude of 100 N and a frequency of 2 rad/sec. The end stop has a value of ± 1 rad. In the figure below the influence of the end stop on the position can be seen. Both the Simulink and the Simscape systems correctly model its behaviour. The value of 1 rad is never excedeed.

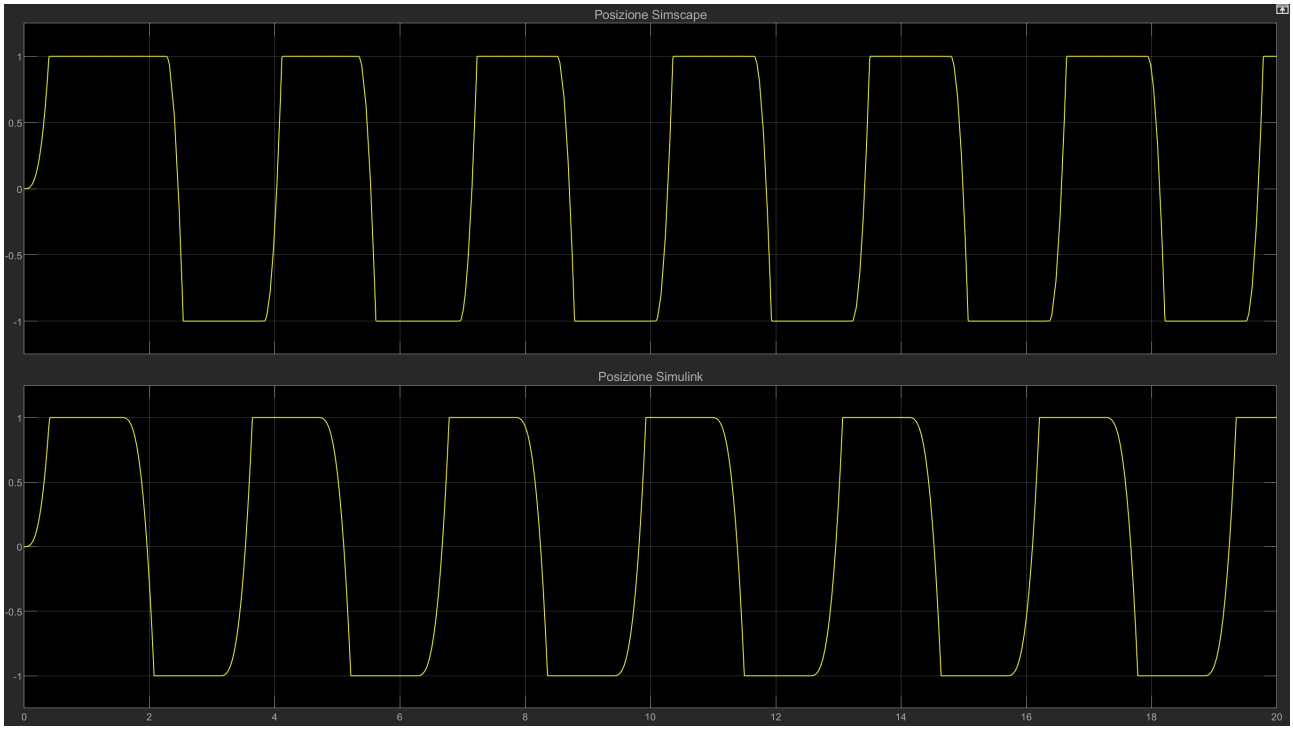

Figure 121: Simscape and Simulink Position

Also the speed is correctly modeled: when the end stop is reached the speed has a null value. The two models seem give identical results from a first view.

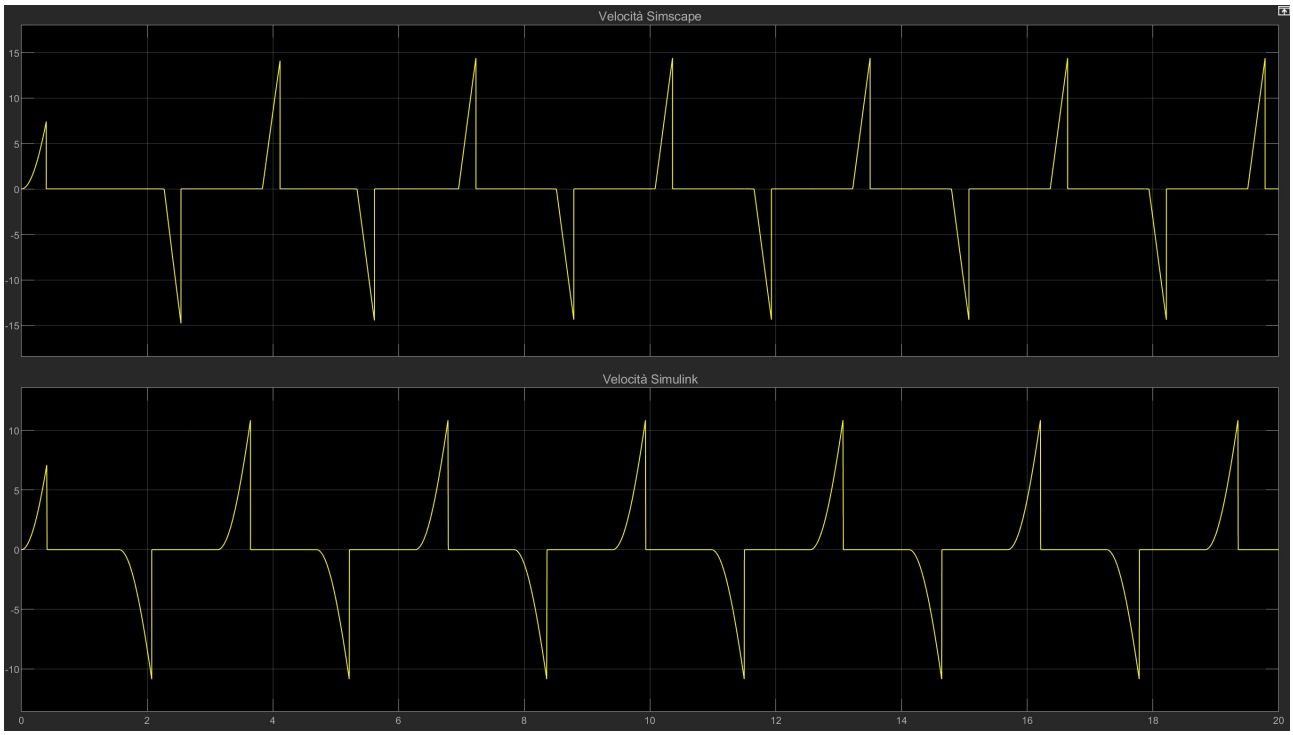

Figure 122: Simscape and Simulink Speed

By zooming on the overlapped diagrams of position(blue) and speed(yellow) the followin remarks can be made: initially the first end stop is modeled in the same way by both systems. From then on, the Simulink system is ahead by half a second with respect to the Simscape model. The maximum speed of the Simscape model is higher than the maximum speed of the Simulink model. When the inversion of motion is made, the velocity diagram of the Simscape starts to increase with a sharp angle, while the Simulink system presents a smoother curve.

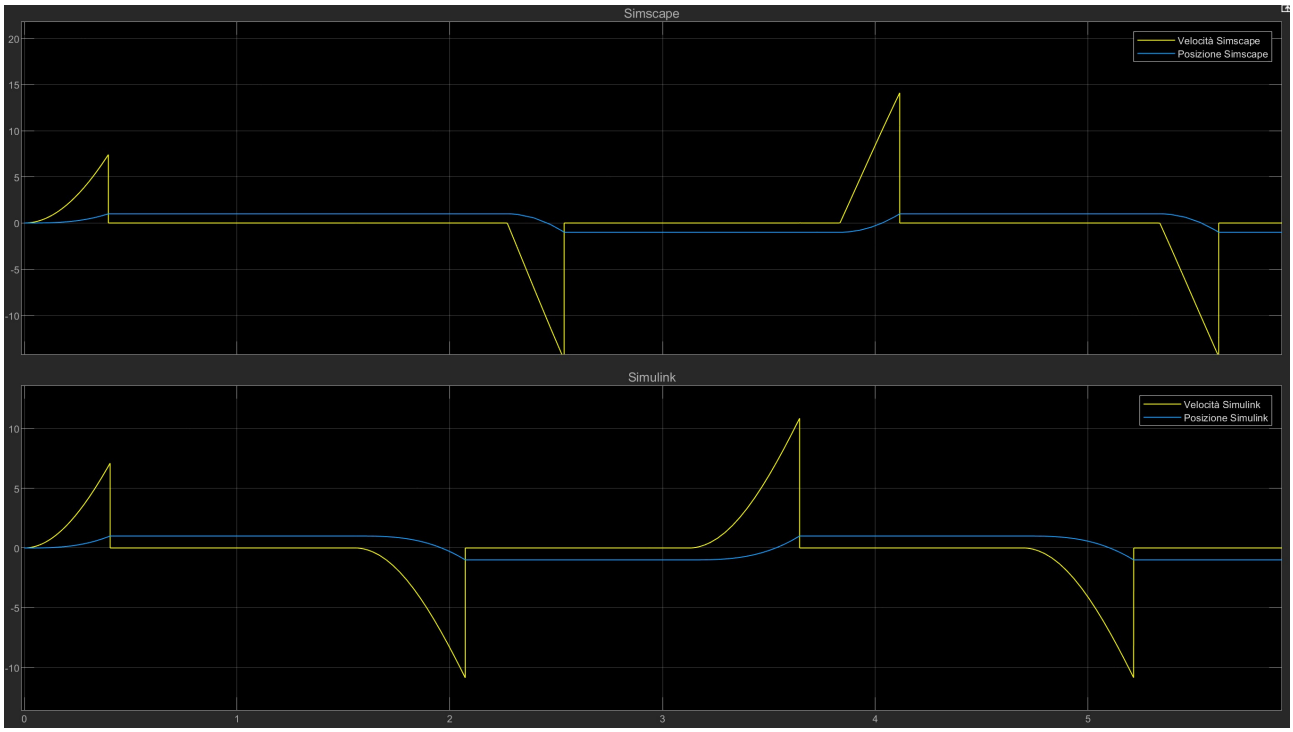

Figure 123: Simscape and Simulink Speed and Position

After proving that the end stop could be modeled through simple mass-spring-damper system, the mechanical actuator model used before is now introduced with the end stop. Below, the two systems can be seen. As seen before, even if the same values are used for both systems, the input that doesn't generate an error for the Simscape model is too small to generate a response in the Simulink model. So a gain is used as an input modulator for the Simulink model. The smallest gain that makes the Simulink system sensitive to the input is that of 115. By doing this we'll achieve two different results from the two systems, at least from a numerical point of view. A sinusoidal input with an amplitude of 5 rad and a frequency of 1 Hz has been used for this simulation.

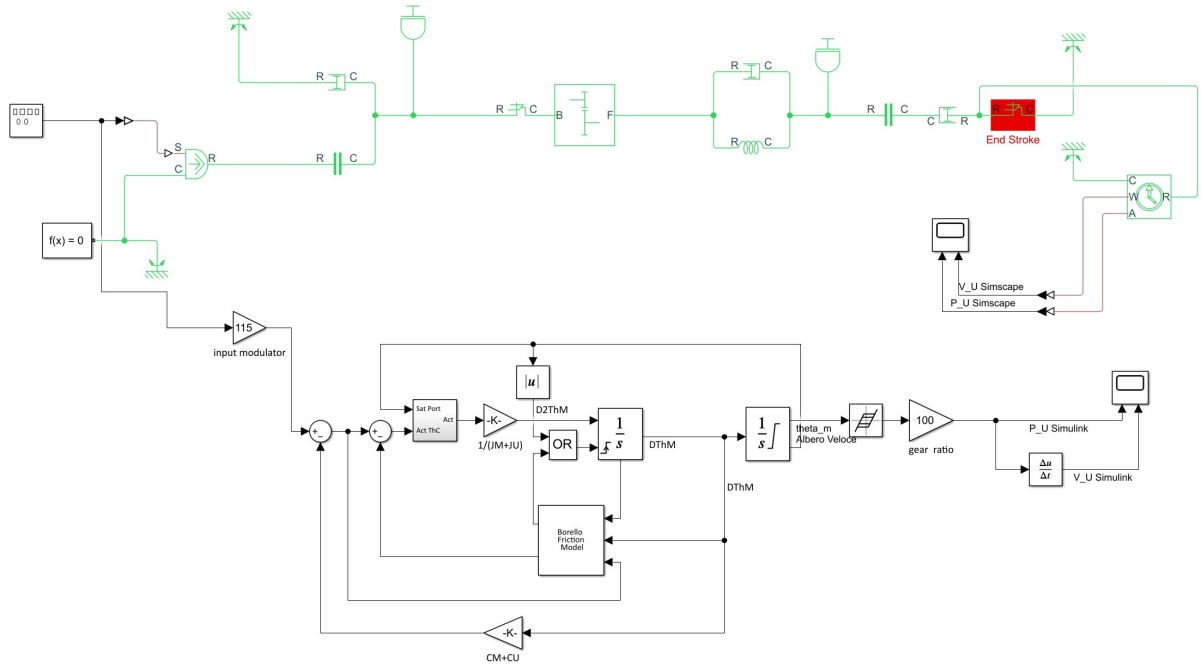

Figure 124: Mechanical Actuator with end stop

In the diagram below the response of the Simscape system to the input can be seen. As before, the position and the velocity are correctly modeled. When the first end stroke is reached the speed will be smaller than in following cases since the system starts from null position.

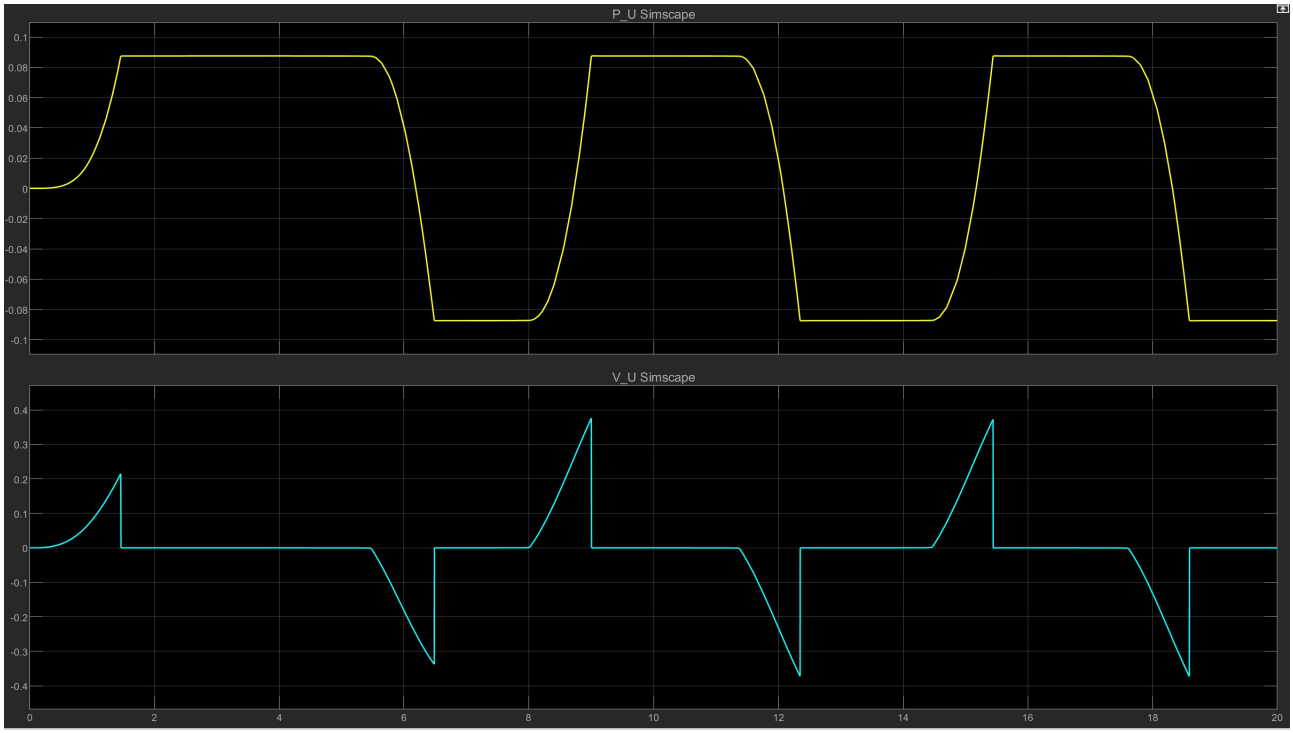

Figure 125: Simscape end stroke response

Quite similiar trends have been obtained from the Simulink model, as the diagram below show. The numerical values are higher than those of the Simscape model, due to the input

gain modulator. Nevertheless, the physical behaviour of the end sop is also correctly modeled by the Simulink system.

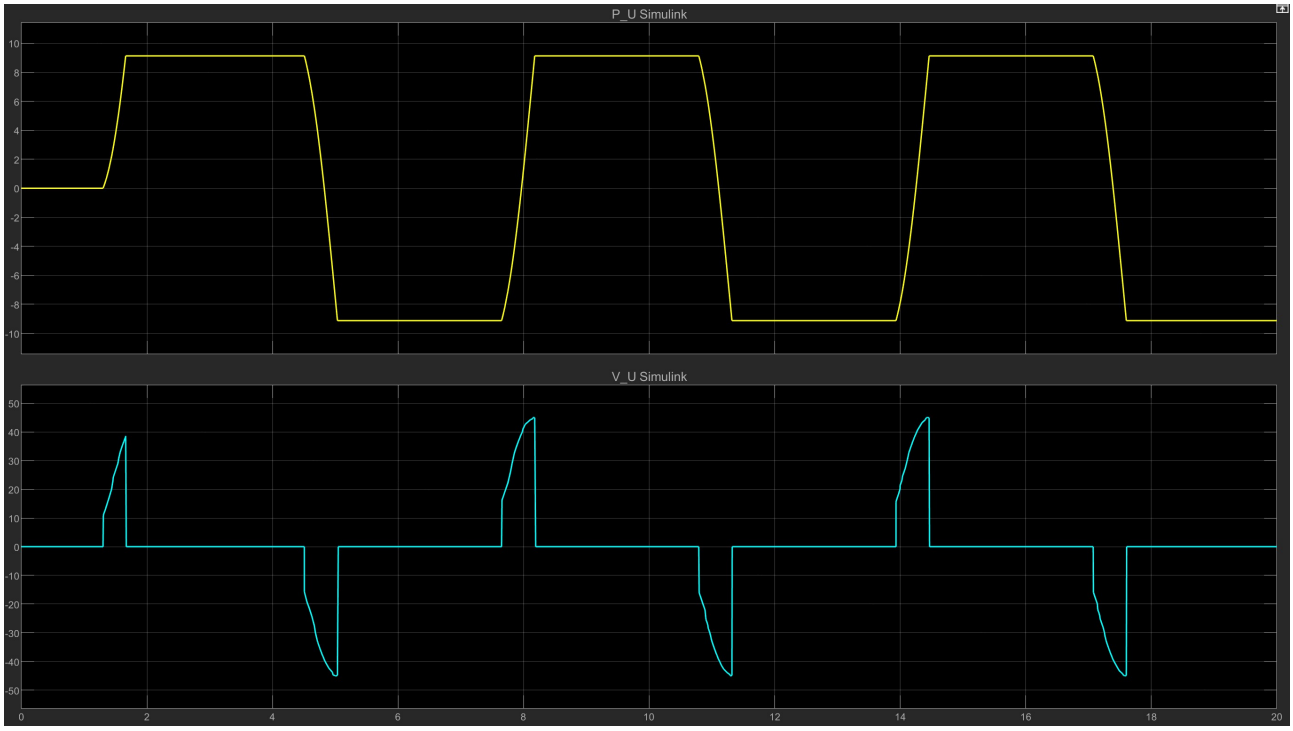

Figure 126: Simscape end stroke response

By superimposing the speed and position of the two systems, it can be better seen that the trends are very similiar regarding the output values and the time.

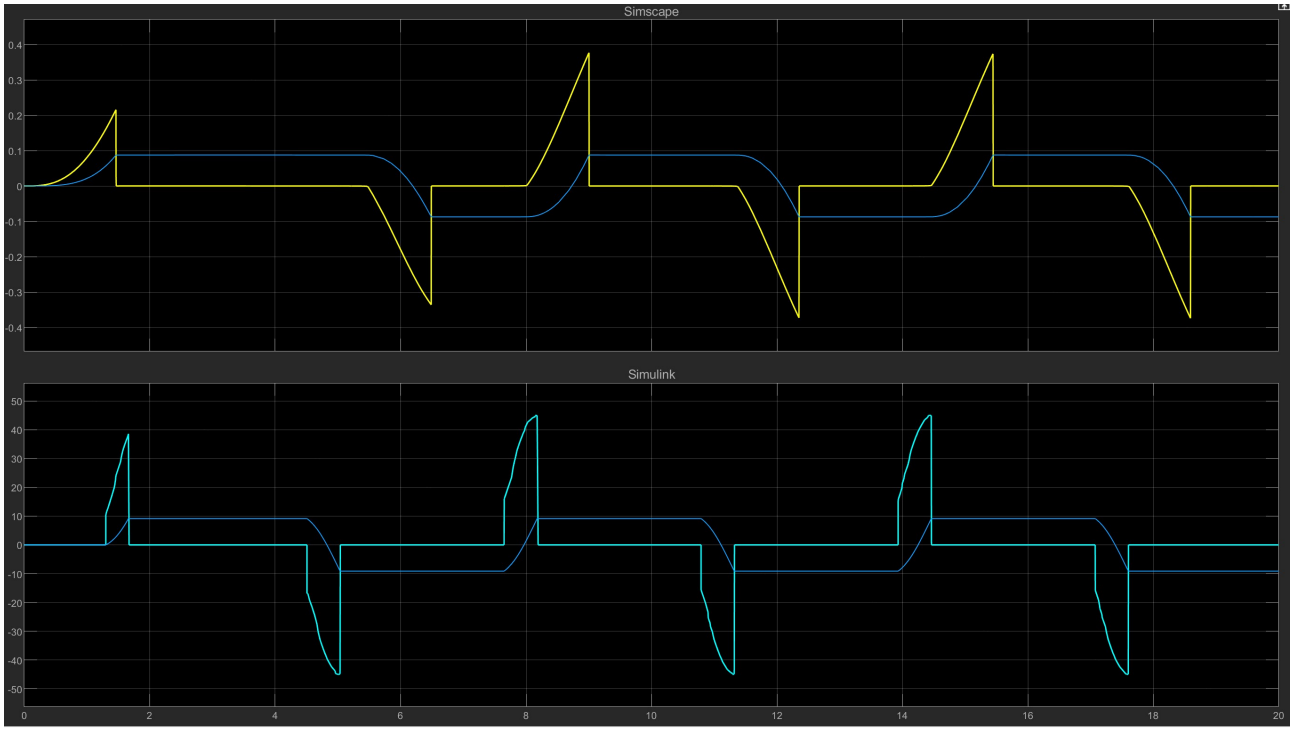

Figure 127: Simscape end stroke response

9 Simscape model with EMA High Fidelity

In order to correctly test the validity of the mechanical actuator developed within the Simscape environment, it is necessary to replace the Simulink mechanical model with the Simscape one inside the BLDC system.
The motor-transmission dynamical model, highlighted in red, is now made of the Simscape and Simulink model, with the outputs linked to the Simscape model in order to evaluate the performance of the mechanical model once it is inside of the whole BLDC system.

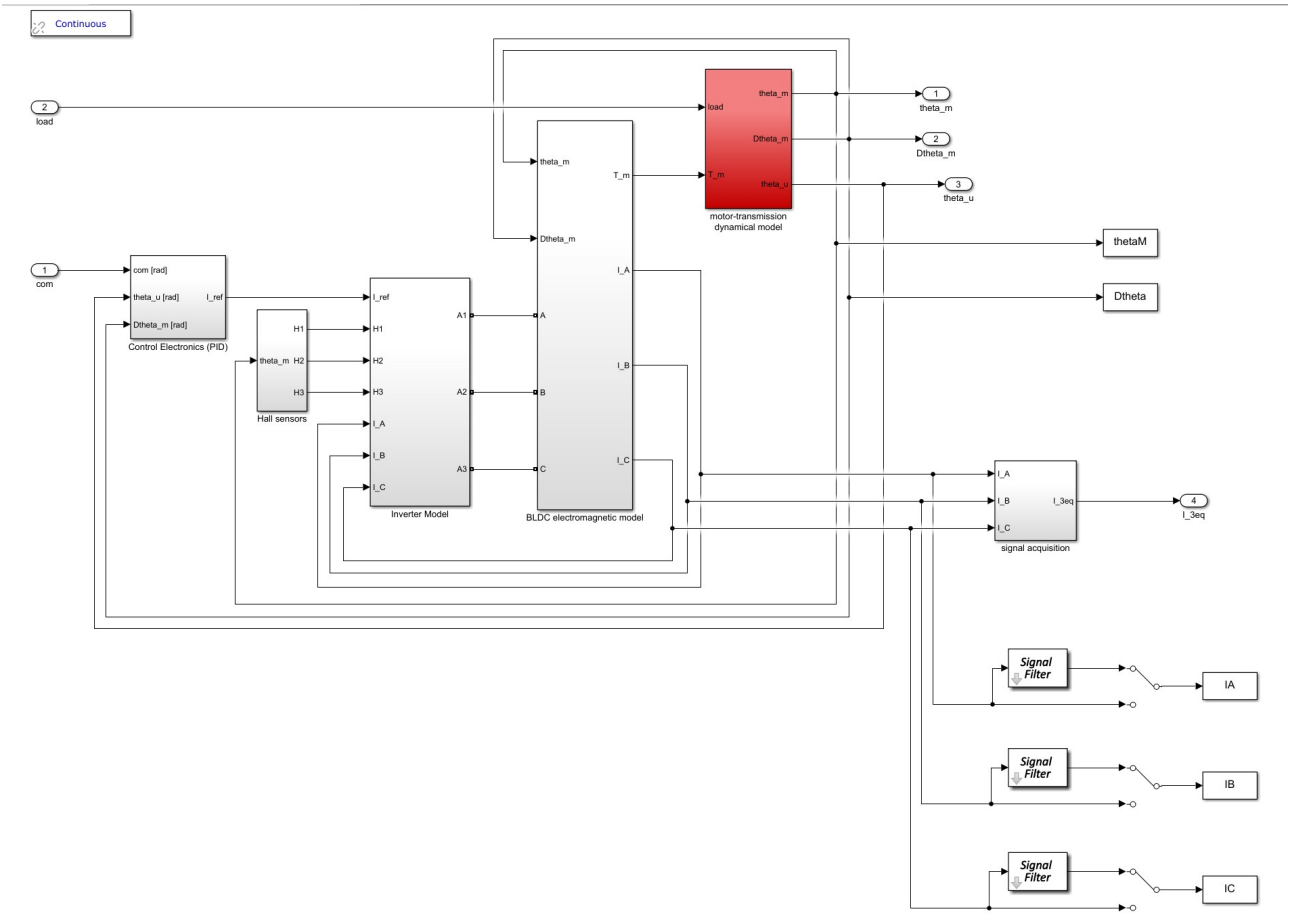

Figure 128: BLDC model

Below the complete motor-transmission model can be seen. It is first necessary to make some clarifications: as stated before, the Simscape model is very sensitive to the value of the input. Values higher than a certain degree make the simulation to terminate. This is due to the rotational friction block of the motor, as evidenced by the image below.

Figure 129: Friction block error due to input value

Having said that, in order to complete the simulation a gain is used which allows for the input signal to be diminished. It has been found that the minimum value of gain that didn't produce an error in the simulation is of 10^{-2}.

The two different outputs, of motor and user, have been highlighted respectively with blue and yellow colour. The values used for the Simscape system are the same as the Simulink one, except for the Rotational Friction Block. In this case by using the values of the Simulink model the simulation could not be carried out since an error would be present. The only value that is different is the Breakway friction velocity. The value obtained previously, so that the Simscape and Simulink model friction response would be the same, was of 10^{-5}. Here a value of 0.1 is being used.
In order to obtain a fairly realistic result, additional gains have been used so to try and obtain a value which is very similar to the Simulink model. The values of gain . The gain values were obtained by a simple proportion in order to obtain a similar value to the Simulink output.

theta m Simsc Gain	1e4
Dtheta u Simsc Gain	44.91
theta u Simsc Gain	222

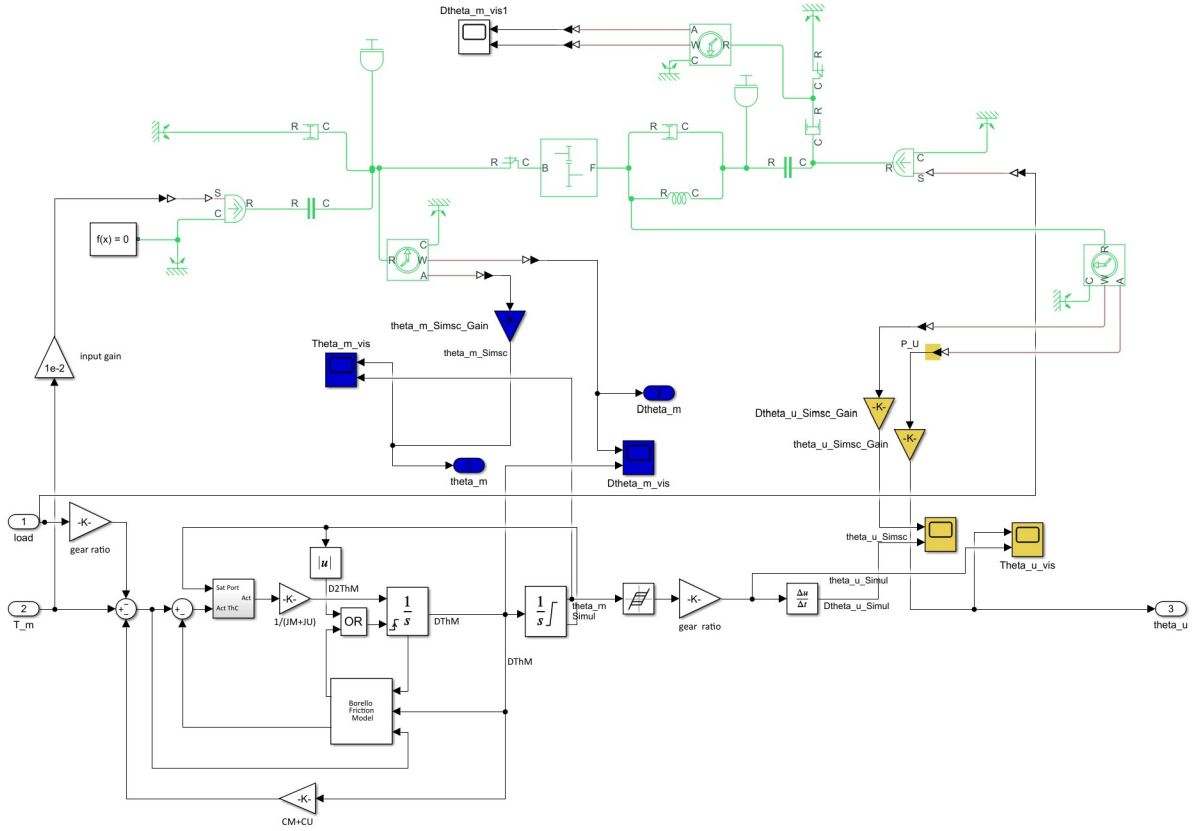

Figure 130: Simscape and Simulink final model

The simulation has been carried out with a sinusoidal input with a half amplitude of 0.1 rad and a frequency of 1 rad/sec. No external load was used.

From the diagram of the user position we can see that the trends and the values are very

similar to each other.

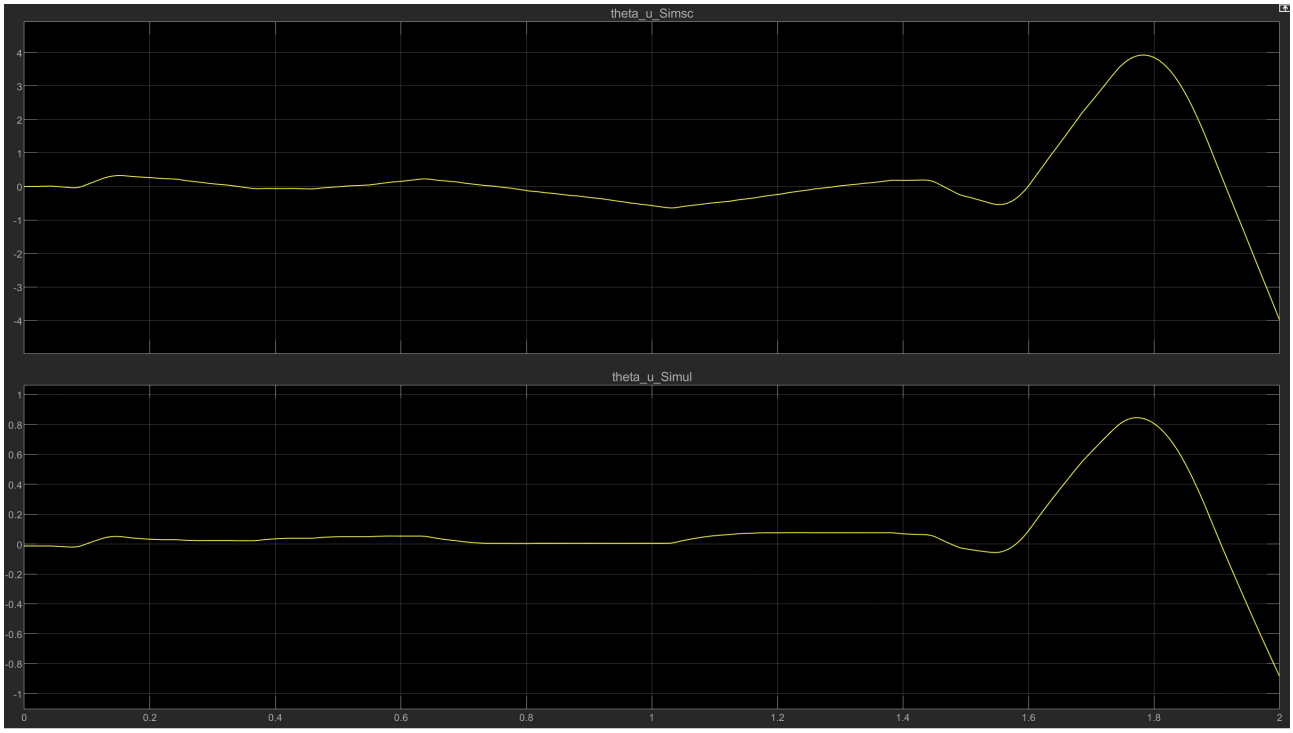

Figure 131: Simscape and Simulink user position

This is also the case for the velocity of the user: the trends and the values of the two curves are consistent with each other.

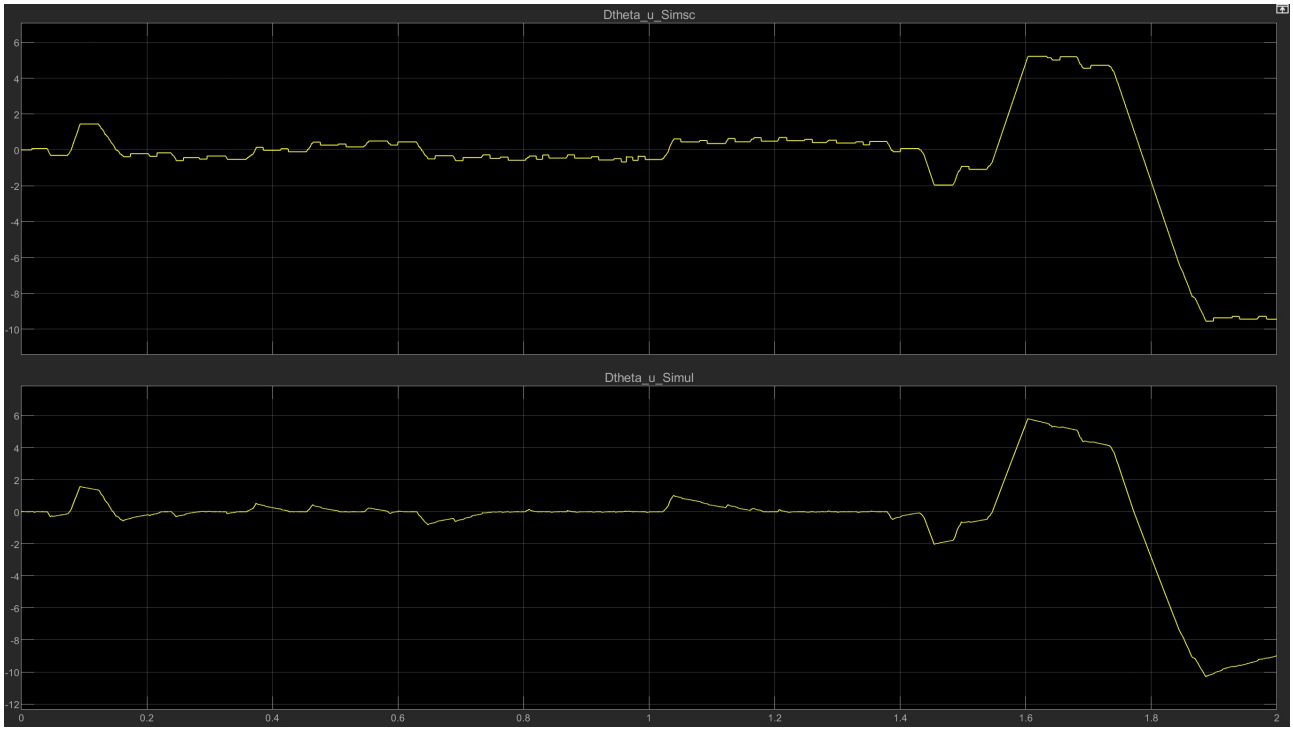

Figure 132: Simscape and Simulink user velocity

Unfortunatelly, this is not the case for the motor's position and velocity. From the two diagrams below it can be seen that two completely different results are obtained by the two systems. The Simulink system gives out a correct result, while from the Simscape one we obtain a result that cannot be analyzed. This is probably due to the frictional model which greatly influences the behaviour of the system.

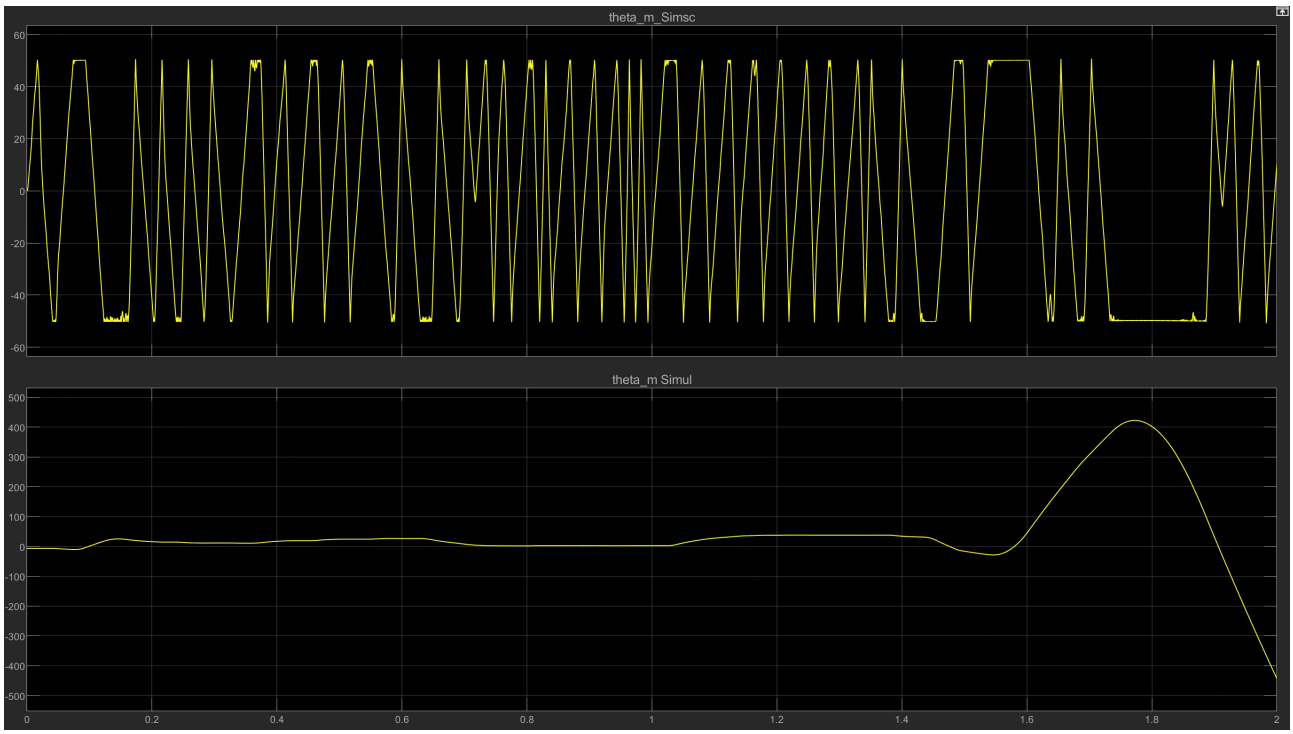

Figure 133: Simscape and Simulink motor position

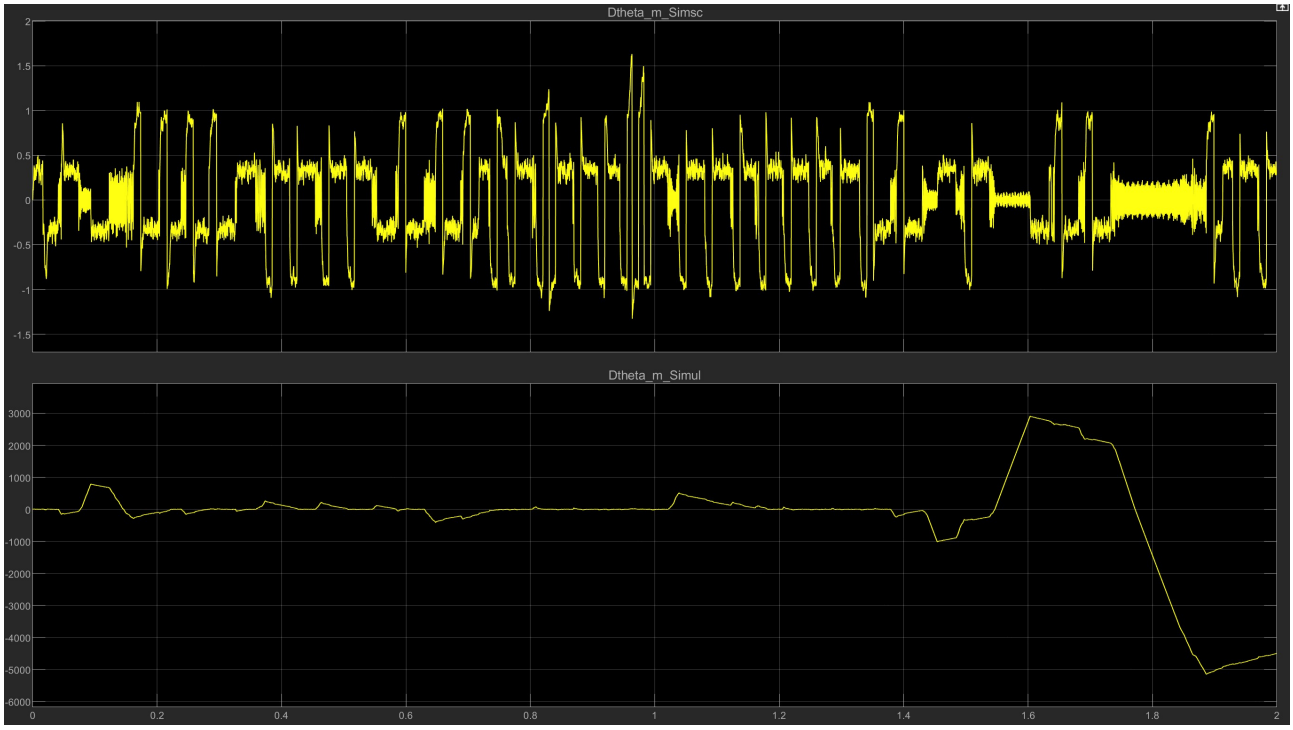

Figure 134: Simscape and Simulink motor velocity

Even if small values of input are used, no correct result is obtain from the motor side of the model. This is an issue that has to be solved in order to obtain a correct model.

Another input was used in order to see the behaviour of the two systems. A ramp with a slope of 10^{-3}. As before, the position and velocity of the motor seem to have a similar behaviour while the motor position and velocity are completly different

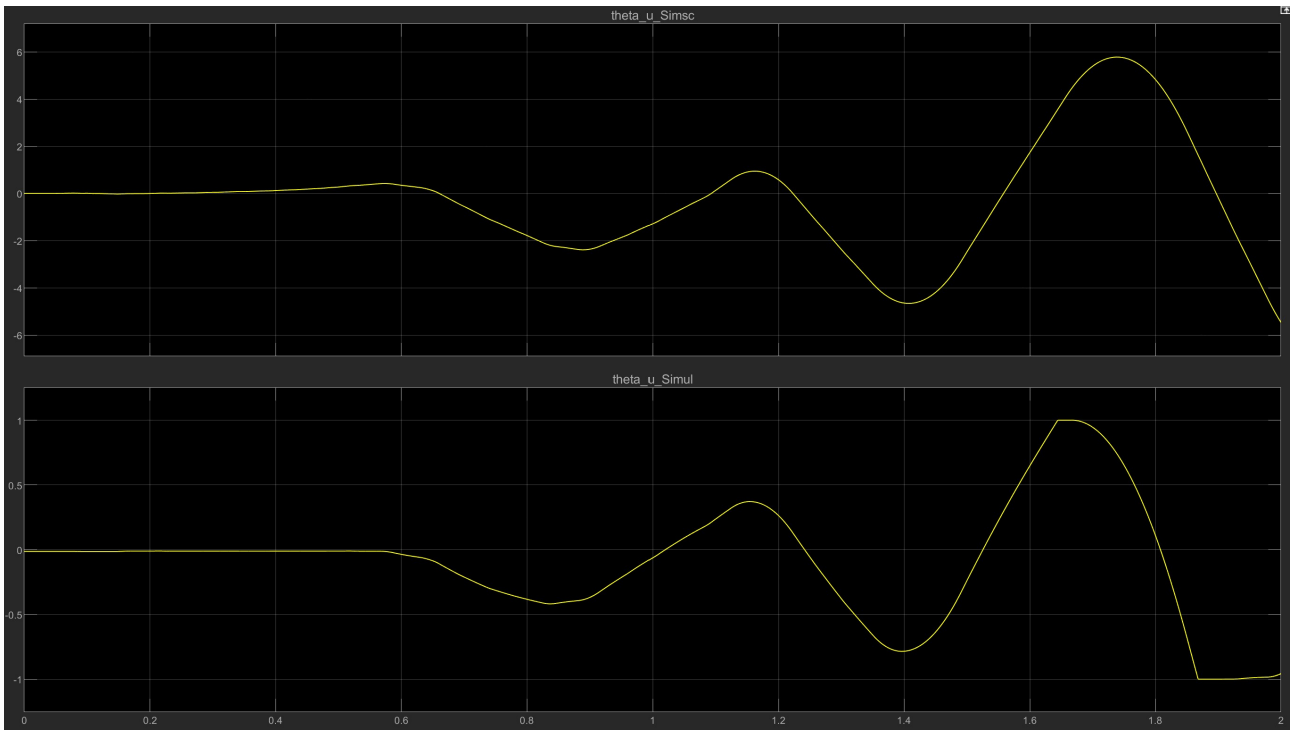

Figure 135: Simscape and Simulink user position

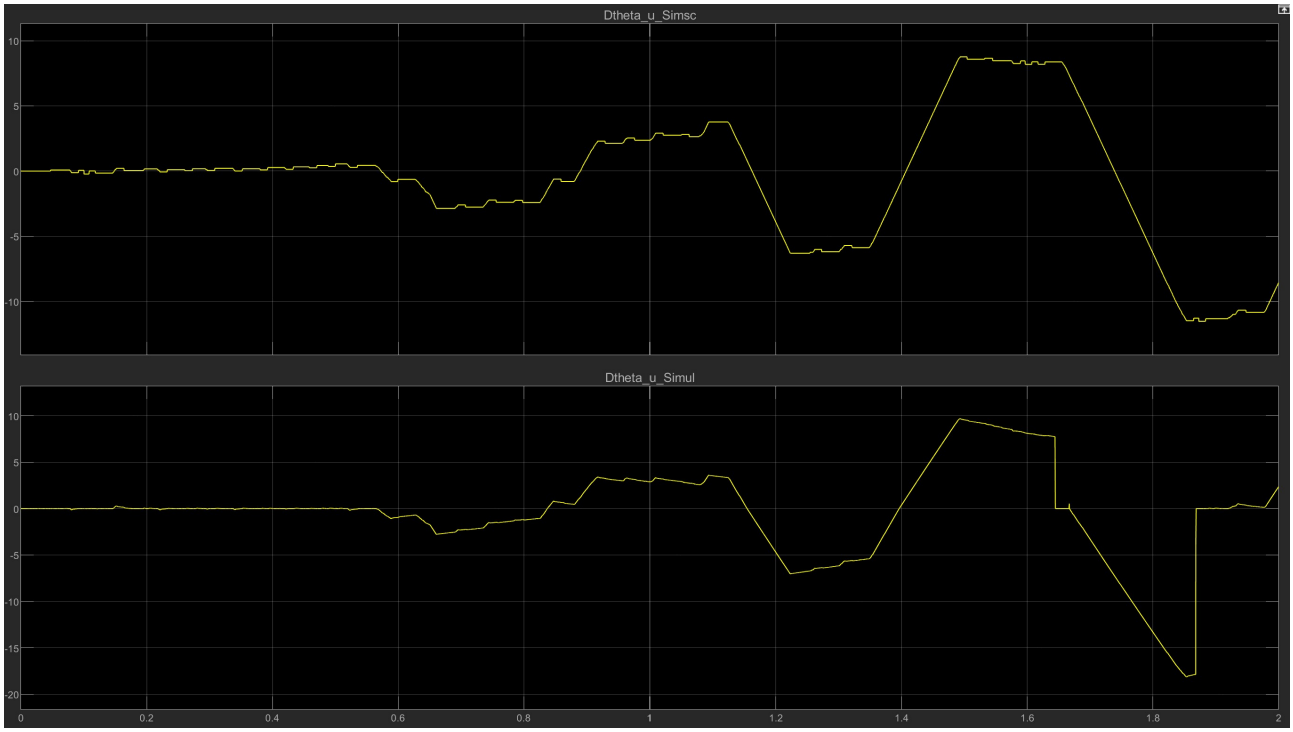

Figure 136: Simscape and Simulink user velocity

10 Final Conclusions

From the results obtained in the last chapter it is clear that the Simscape mechanical model cannot be used in place of the Simulink one at the moment. The main issues which don't allow this are the fact that the motor's position and velocity are not correctly modeled and also, differently from the Simulink model, the simulation time is very high, at least a minute, compared to a few seconds of the Simulink model.

There are a few issues which are the cause of the incorrect behaviour of the Simscape model:

- one of the problems is the fact that there is no friction block in the Simscape environment, that allows the system to behave like the Borrello friction permits. In fact, as was stated before, the other friction models don't correctly allow to simulate the behaviour of mechanical systems, especially when stop and go situation are involved. In order to overcome this problem there are two solutions: to build a custom Simscape block using Matlab logic and formulas in order to obtain the correct behaviour; or else to try and integrate the Simulink Borrello block in the Simscape syste.
- another problem is a consequence of the friction problem: the small dynamic values of the BLDC, both the motor and user, make the Simscape model to be very sensitive to the value of the input. This occurs as an error due to the Frictional Rotational block, which stops the simulation in the first instants.
- the main difference between the two models is the fact that the mechanical motor and user are modeled through a single mass-damper-spring model. While in the Simscape model the two have been separately modeled and a transmission between them was introduced. This greatly affects the behaviour of the two systems, since in principle in the case of the Simscape model, we have two dynamical systems linked through a transmission, while in on the other side we have a single dynamical system.

The study began with the comparison of a simple mass-spring-damper. After it was proved that the Simscape and Simulink models gave the same rsults, an Harmonic oscillator was developed, which also gave satisfying results. This allowed for the development of the final mechanical model of the actuator without the presence of the non linearities.

From the point of view of the various non linearities that have been studied in this work, the following can be said:
Initially the friction was studied on it's own by comparing two mass-spring-damper systems. In order to obtain a usable Breakaway Friction Velocity the error between the position and velocity of the two systems was compared. The value of Breakaway Friction Velocity that gave the smallest value of error was of 0.0000121. The error of position was of 10^{-4} while the velocity error was 10^{-2}. The later value is possibly one of the causes of why the final model doesn't behave like the Simulink one.

Then, the second non linearity was studied. This is the Backlash which occurs in the transmission reduction gear system. Initially, when the values of the BLDC were used, only the input would give satisfying results. The behaviour of the backlash was correctly modeled. When

the external load was introduced this was not the case anymore. The system was insensitive to the external load.
When higher values than those of the BLDC were used, it was very interesting to see that also the behaviour of the external load was correctly modeled. Different types of input have been tested, all of them giving a satisfying but not perfect result. The overall behaviour was the same with small diferences in the timing of the non linearity.

Finaly, the end stop non linearity was considered. It has been proved that a simple mass-spring-damper system resulted in the same behaviour between the two systems. Then, the more complex mechanical side of the actuator was also introduced: also here it can be seen that if not for the too small values of the BLDC, when bigger values are used the two systems behave in quite a similar way.
In order to achieve these results, a lot of trial and error was conducted. All the various blocks have been tested in the beginning with each other and then in the complete model. Initially this was done in order to obtain the Breakaway Friction Velocity which provided the smaller value of error. Then, this was also done for the development of the backlash and end stroke models. In this work only the result which as considered most similar to the Simulink model was presented

This said, more can be done in future works in order to obtain a fully High Fidelity mechanical actuator that behaves like it's Simulink counterpart:

As stated above, it is possible that all the issues which have arised in this work may be removed by using the Borrello friction model. The focus of future works may be to try and develop a custom block in the Simscape environment which will behave very similar to the Simulink Borrello friction model.

The mechanical transmission between the motor and user is not present in the Simulink model. In order to have acceptable results, the values of the spring and the damper were equal to 1. In future works this can be studied and it should be seen how the change in values influence the final result.

Another thing that can be done in the future is to introduce the mechanical model developed in this work, in a complete BLDC Simscape model. This way it is possible to correctly compare the two models side by side and to really see which are the blocks that have the biggest influence.

The purpose of this work was to develop a mechanical actuator in the Simscape environment that could replace the Simulink one in the High Fidelity BLDC. This result was only achieved partially, as the user's position and velocity have a similar behaviour. The model which contains the friction, backlash and end stroke non linearity is a solid base that can be used for future works in order to better develop the and overcome the problems stated above.

The Simscape environment has a great potential to be used in the development of numerical models because of it's great simplicity of use. As opposed to Simulink, where the blocks are connected in such ways to represent differential equations, in Simscape the blocks represent the functioning of the real system , so the various blocks may represent real components and may be interlinked in the same way as it's real counterpart. This has the advantage of being

understood and developed much faster due to the resemblance that it shares with it the real system.

References

[1] Paolo Maggiore,*Simulazione e Sperimentazione dei Sistemi Aerospaziali*. Slides and lessons of the course.

[2] Pier Carlo Berri, *Genetic Algorithms for Prognostics of Electromechanical Servomechanism Failures*. Master Degree Thesis, 2016.

[3] Francesco Nudo, *Numerical modeling of servomechanisms: comparison between different development evironments*. Master Degree Thesis, 2020.

[4] Gaetano Quattrocchi, *Development of innovative prognostic methods for EMAs*, Master Degree Thesis, 2019.

[5] Shuvra Das, *Modeling and Simulation of Mechatronics Systems using Simscape*. Morgan and Claypool, 2020.

[6] Manuela Battipede. *Guida e Controllo del Velivolo*. Slides and lessons of the course.

[7] Jian Fu, Jean-Charles Marè, Yongling Fu and Liming Yu *Advanced Modeling and Simulation of Electromechanical Actuator for Flight Control System Based on Two Degrees of Freedom*. Beijing University, 2017.

[8] Jian Fu, Jean-Charles Marè, Yongling Fu. *Modelling and simulation of flight control electromechanical actuators with special focus on model architecting, multidisciplinary effects and power flows*. Beijing University, 2016.

[9] Simscape Documentation. URL: `https://it.mathworks.com/help/physmod/simscape/index.html`.

[10] Moog Aircraft Group. *F-16 Sustainment Services*. Moog Worldwide, 2015.

[11] Michel Todeschi. *Airbus-EMAs for Flight Control Actuation System-An Important Step Achieved in 2011*. Toulouse, 2011.